The role of secreted bacterial metabolites in regulating adipose biology: the effect of the Lab4 consortium of probiotics on adipogenesis

A thesis submitted in partial fulfilment of the requirement of Cardiff University for the degree of Master of Philosophy

Duncan Connor Roberts

2017

Summary

The gut microbiota has come to be viewed as an extrasomatic organ influencing human health. Obesity is a major global public health challenge urgently requiring development of new treatments. Reports of weight gain after faecal microbial transplant have spurred interest in the potential role of the microbiota in obesity in man. Lab4 and Lab4b are commercially available probiotic products that have recently been shown to be associated with decreased weight gain in high-fat diet mice, and have recently been used to investigate *in vitro* adipogenesis. Brown adipose tissue is highly metabolically active, and is inversely associated with BMI. Bacterial metabolites such as lactate have been shown to induce "browning" of adipose tissue.

The effects of Lab4 and Lab4b cell free supernatant were assessed on *in vitro* adipogenesis using the 3T3-L1 cell line and human primary preadipocytes. Transcriptional markers of adipose phenotype were assessed in 3T3-L1 cells maintained in culture media containing cell free supernatant of the constituent strains of the Lab4/Lab4b consortia.

Lab4 and Lab4b were found to significantly reduce lipid accumulation in late adipogenesis in 3T3-L1 cells, though cell morphology suggested paradoxical acceleration of adipogenesis. Reduced lipid accumulation was likely related to a significant reduction in cell viability. Transcriptional markers of adipogenesis were not significantly altered by treatment, nor were markers of adipose phenotype, but transcripts of UCP1 (the functional protein of brown adipose tissue) were significantly higher in non-differentiating cells maintained in cell free supernatant of two *L. acidophilus* strains (p=0.008).

Assessment of effects in human primary preadipocytes were inconclusive due to cytotoxicity, though treatment with Lab4b appears to dramatically alter cellular morphology and increase what appears morphologically to be lipid accumulation in surviving cells.

Further study and more robust data is needed to determine the effects of Lab4/Lab4b and their constituent strains on *in vitro* adipogenesis.

DECLARATION

This work has not been submitted in substance for any other degree or award at this or any other university or place of learning, nor is being submitted concurrently in candidature for any degree or other award.

Signed …… (candidate) Date……

STATEMENT 1

This thesis is being submitted in partial fulfilment of the requirements for the degree of MPhil

Signed …… (candidate) Date……

STATEMENT 2

This thesis is the result of my own independent work/investigation, except where otherwise stated, and the thesis has not been edited by a third party beyond what is permitted by Cardiff University's Policy on the Use of Third Party Editors by Research Degree Students. Other sources are acknowledged by explicit references. The views expressed are my own.

Signed …… (candidate) Date……

STATEMENT 3

I hereby give consent for my thesis, if accepted, to be available online in the University's Open Access repository and for inter-library loan, and for the title and summary to be made available to outside organisations.

Signed …… (candidate) Date……

STATEMENT 4: PREVIOUSLY APPROVED BAR ON ACCESS

I hereby give consent for my thesis, if accepted, to be available online in the University's Open Access repository and for inter-library loans **after expiry of a bar on access previously approved by the Academic Standards & Quality Committee.**

Signed …… (candidate) Date……

Acknowledgments

Preliminary 3T3-L1 cell culture experiments referenced in this work were performed by Erika Galgóczi.

Production of cell free supernatant, enumeration of microorganisms, and all other microbiological aspects of this work were performed at Cultech Ltd, with the kind assistance of Dr. Daryn Michael, Dr. Alison Jack, and Dr. Tom Davies.

Training in molecular biology techniques and assistance in interpreting results was graciously provided by Dr. Lei Zhang, Dr. Mohd Draman, and Professor Marian Ludgate.

This project was supported by KESS 2 and Cultech Ltd. Knowledge Economy Skills Scholarships (KESS 2) is a pan-Wales higher level skills initiative led by Bangor University on behalf of the HE sector in Wales. It is part funded by the Welsh Government's European Social Fund (ESF) convergence programme for West Wales and the Valleys.

I lost my colon getting my first degree, I lost my money getting a second, and I fully intend to lose my mind in pursuit of a doctorate. With thanks to everyone who enabled me.

Table of Contents

List of Abbreviations

ADP – Adenosine Diphosphate

ARP - Acidic Ribophosphoprotein

ATP – Adenosine Triphosphate

BAT – Brown Adipose Tissue

BMI – Body Mass Index

C/EBP – CCAAT/enhancer-binding protein

CFS – Cell Free Supernatant

CITED1 – Cbp/p300-interacting transactivator 1

CFU – Colony Forming Units

CHOP – C/EBP Homologous Protein

CM – Complete Medium

DM – Differentiation Medium

FCS – Foetal Calf Serum

GAPDH – Glyceraldehyde-3-phosphate Dehydrogenase

GPDH – Glycerol-3-phosphate Dehydrogenase

HDAC – Histone Deacetylase

HFD – High Fat Diet

JAK – Janus Kinase

KLF – Krüppel Like Factors

LAB – Lactic Acid Bacteria

MCE – Mitotic Clonal Expansion

MTS – (3-(4,5-dimethylthiazol-2-yl)-5-(3-carboxymethoxyphenyl)-2-(4-sulfophenyl)-2H-tetrazolium)

MTT – 3-(4,5-dimethylthiazol-2-yl)-2,5-diphenyltetrazolium Bromide

MYF5 – Myogenic Factor 5

NCIMB – National Collection of Industrial, Food and Marine Bacteria

ORO – Oil Red O

PBS – Phosphate Buffered Saline

PCR – Polymerase Chain Reaction

PGC1-α – PPARγ coactivator-1α

PPARγ – Peroxisome Proliferator-Activated Receptor γ

qPCR – Quantitative Polymerase Chain Reaction

SCFA – Short Chain Fatty Acids

SREBP – Sterol Regulatory Element Binding Protein

STAT - Signal Transducer and Activator of Transcription

T2DM – Type 2 Diabetes Mellitus

TLR – Toll Like Receptor

TNF-α – Tumour Necrosis Factor Alpha

UCP1 – Uncoupling Protein 1

WAT – White Adipose Tissue

ZIC1 – Zinc in Cerebellum 1

Chapter 1: Introduction

1.1 – Adipose biology

Excess adiposity in man is a risk factor for many disease states, including leading causes of death and disability such as cancers (Coe *et al.,* 2014), cardiovascular disease (particularly associated with visceral adiposity) (Bastien *et al.,* 2014), and type 2 diabetes mellitus (T2DM) (Day and Bailey, 2011). Overweight and obesity (defined by the World Health Organisation as a body mass index (BMI) of ≥ 25 kg/m^2 and ≥ 30 kg/m^2 respectively) (World Health Organization, 2017) can lead to ectopic fat deposition and adverse effects on markers of metabolic health, namely elevated fasting blood glucose, blood pressure, cholesterol, and triglycerides, and reduced high density lipoprotein levels (Snel *et al.,* 2012; Wang and Peng, 2011). These metabolic aberrations are part of an interlinked constellation of symptoms termed the "metabolic syndrome", comprising any of the three clinical features (Kaur, 2014). The burden of disease imposed by obesity resultantly places a significant burden on health resources in the UK. Costs borne by the UK economy due to obesity were estimated in 2007 at £15.8 billion, including £4.2 billion in costs to the NHS (Department of Health, 2011). T2DM is also a significant public health challenge in the UK, and prevention has been a major focus of public health campaigns. Thus, there is an urgent need for new treatments and public health interventions to address overweight and obesity.

Adipose Tissue

Adipose tissue is a fibrous, loose matrix of adipocyte cells serving multiple mechanical and metabolic functions. Foremost adipose tissue is specialised for energy storage; however, it is also involved in insulation and mechanical protection of vital organs, secretion of hormones (usually ectopically in states of excess adiposity) (Trayhurn and Beattie, 2001), and temperature regulation in neonates (Gilsanz *et al.*, 2013). Fat mass is maintained by the coordinated processes of lipolysis, lipogenesis, and adipogenesis, facilitating the storage of energy in triglyceride form and its

subsequent mobilisation according to metabolic demand (Rutkowski *et al*., 2015). While it was once thought that adipose tissue was a metabolically inert store of energy in the form of triglycerides, there is now an appreciation that adipose tissue can be seen as an endocrine organ (Coelho *et al.,* 2013). Adipose tissue can exhibit secretory capabilities, expressing "adipokine" hormones, notably leptin and adiponectin. However, in states of excess adiposity, these tissues can also ectopically secrete cytokines such as tumour necrosis factor alpha (TNF-α) and interleukin 6 (Kwon and Pessin, 2013). TNF-α has been implicated in the development of obesity related insulin resistance. In obesity, a persistent level of low grade inflammation is often present, resulting in chronically elevated levels of circulating TNF-α (Nieto-Vazquez *et al.,* 2008). TNF-α impairs glucose uptake both in muscle tissue and adipose tissue, inhibiting insulin signalling by activating the inhibitor κB kinase complex, resulting in serine phosphorylation of insulin receptor substrate proteins (Gao *et al*., 2002). As a result, adipose depots have the potential to influence glucose metabolism not only within their own tissues, but systemically. Reduction in the size or adverse metabolic activity of adipose tissue may therefore positively impact metabolic disease, or prevent its development.

Adipose tissues are not phenotypically homogenous. Adipose tissue is often characterised into three distinct groupings; white adipose tissue (WAT), brown adipose tissue (BAT), and an intermediate "beige" phenotype, also interchangeably called induced brown adipose tissue or "brite" (brown-in-white) (Harms and Seale, 2013). BAT is highly metabolically active and exhibits thermogenic capacity. This is functionally important in maintaining body temperature in neonates, and thus is located in anatomically distinct sites associated with vasculature and critical organs (Sacks and Symonds, 2013). The mitochondria of BAT cells express uncoupling protein 1 (UCP1), which upon activation induces permeability in the inner mitochondrial membrane, permitting protons pumped into the intermembrane space to leak back into the mitochondrial matrix (Nedergaard *et al.,* 2001), this process is summarised in Figure 1.1. This results in an uncoupling of oxidative phosphorylation from ATP production; substrates are oxidised but result in a relatively low production of ATP, and energy is dissipated as heat. Uncoupling is of particular interest in the prevention

and treatment of metabolic disorders, and is seen as a potential therapeutic target as “inefficient” mitochondrial function due to induced uncoupling of oxidative phosphorylation leads to increased substrate utilisation without typically consequent levels of ATP.

BAT deposits appear to be inversely correlated with BMI and fat mass (Cypess *et al.,* 2009). In adults with detectable BAT, exposure to mild cold leads to better blood glucose control, higher insulin sensitivity, and greater energy expenditure than control (Chondronikola *et al*., 2014). However, despite a strong mechanistic rationale it is not yet established whether BAT activity is a causative factor in the prevention of such diseases on a population level.

While beige adipose tissue exhibits many similarities to BAT, including expression of UCP1 and multilocular lipid droplet morphology, they also maintain distinguishing characteristics. BAT is thermogenically competent in its basal state, whereas beige adipocytes require activation through cold challenge or β-adrenergic stimulation (Harms and Seale, 2013). Further, brown and white adipocytes in mice develop from different embryonic precursors. BAT derives predominantly from myogenic factor 5 (MYF5) expressing cells, engendering the hypothesis that resultant tissues are metabolically favourable due to a skeletal muscle related lineage (Rowland *et al*., 2015). Conversely, WAT derives predominantly from MYF5 negative cells. At present, whether beige adipocytes arise from mature WAT or are of a distinct lineage remains a matter of debate, though experimental evidence suggests that a majority of beige adipocytes are formed through *de novo* adipogenesis rather than transdifferentiation (Wang *et al*., 2013). Also, despite the dogmatic $MYF5^{+}/^{-}$ model, certain subsets of WAT in mice derive from $MYF5^{+}$ cells (Sanchez-Gurmaches *et al*., 2012). Despite much study, as lineage tracing is the only technique which can definitively define a cell’s developmental origin, such studies have only occurred in mice and it remains unclear whether the proposed MYF5 dichotomy is true in humans.

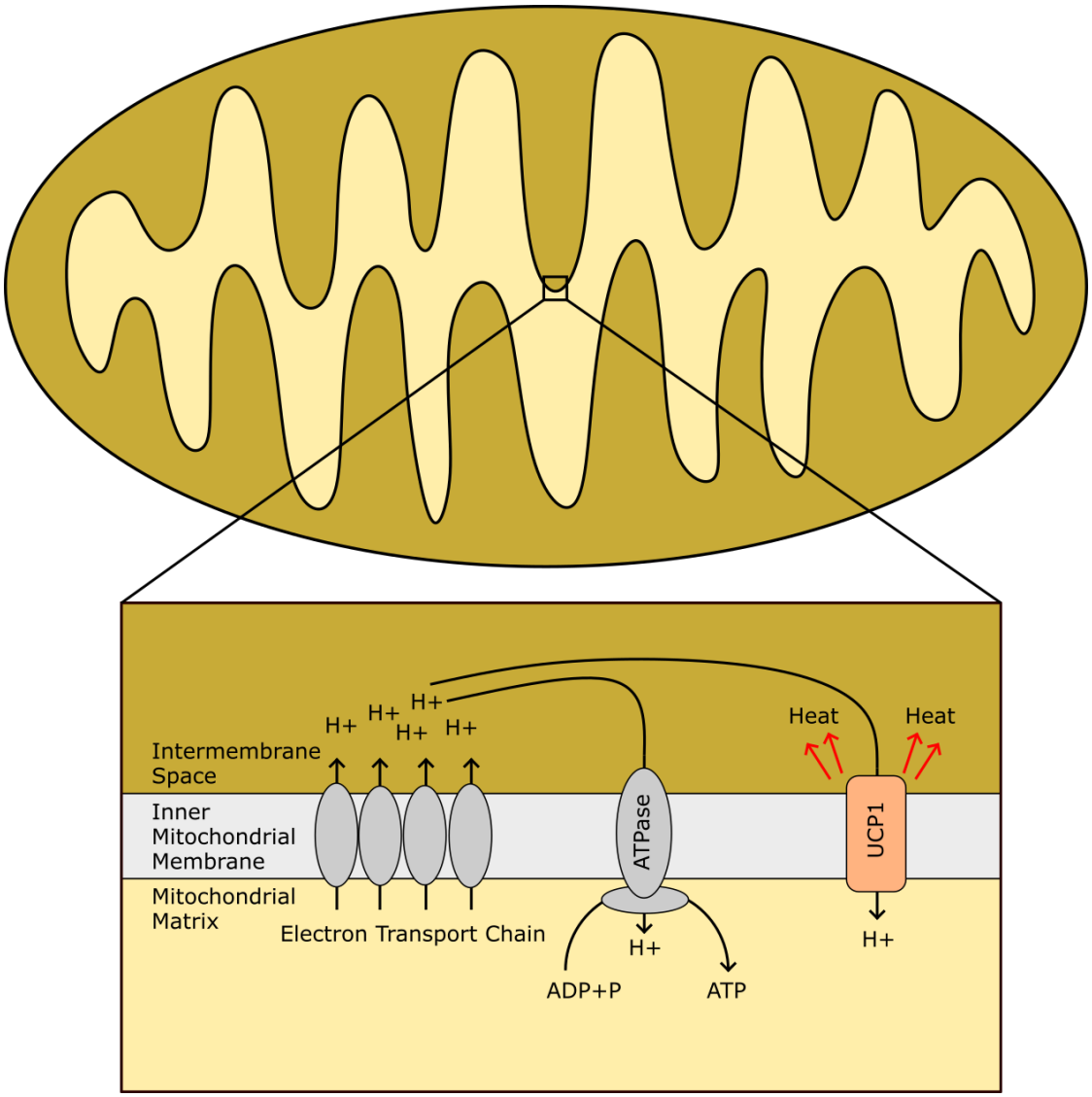

Figure 1.1 – Representative diagram of the location and function of UCP1. Akin to the function of ATP synthase, UCP1 facilitates the re-entry of hydrogen protons into the mitochondrial matrix, however it does so without the concomitant generation of ATP, resulting in high substrate utilisation and low ATP production. This "inefficiency" generates heat. *ADP* – Adenosine Diphosphate, *ATP* – Adenosine Triphosphate, *UCP1* – Uncoupling protein 1

Though it is not possible to definitively trace the lineage of human adipose cells, indirect methods have been utilised. Important data regarding adipocyte turnover has been generated from the study of ^{14}C incorporation from nuclear weapons testing. Adipocytes experience an annual turnover rate of approximately 10% in adult

humans, across all ages and BMI categories (Spalding *et al.,* 2008), and that total adipocyte numbers become "fixed" in childhood or early adulthood. This work has important implications for the treatment of obesity, but also elegantly demonstrates the plasticity of adipose tissue. Perhaps due to the intricacies of the technique and identifying potential study populations, it has not yet been applied to the study of BAT. Tangential anecdotal data may be gleaned from hibernomas, a rare benign tumour of BAT origin typically occurring in adults in the 4th decade of life, which is not reported to metastasise and rarely recurs following resection (Kim and Lee, 2012). Though far from definitive, this suggests that in addition to BAT typically decreasing with age, their precursors may also be scarce in adulthood in contrast to those of WAT.

Adipogenesis

Adipogenesis entails the cellular differentiation of preadipocytes into adipocytes. Expansion of adipose depots is facilitated either by hypertrophy of existing adipocytes or the process of adipogenesis (Jo *et al*., 2009), which gives rise to new adipocytes from a population of precursor cells. In mammalian adipose vascular stroma, these precursors take two forms: pluripotent fibroblasts or unipotent preadipocytes (Cawthorn *et al*., 2012). The differentiation of preadipocyte cells into adipocytes relies on a complex and coordinated network of genetic factors, which may exhibit differing expression patterns temporally, resulting in functional and morphological changes. There exists a complex array of signals influencing preadipocytes, with both inhibitory and stimulatory properties from a variety of sources from within the cell itself, from other adipocytes, and signals of systemic endocrine origin (MacDougald and Mandrup, 2002). Factors influencing preadipocyte cellular fate thus exist in an intricate network, the balance of which ultimately regulates progression of the adipogenic cascade. By measuring gene expression along the time course of differentiation, several markers of adipogenesis have been discovered (Gaillard *et al*., 1989). Glycerol-3-phosphate dehydrogenase (GPDH) expression has been employed as a marker of terminal differentiation for decades,

showing not only an increase in expression over the time course, but robust detection specifically in triglyceride-accumulating cells (Cook and Kozak, 1982). However, further complicating the characterisation of the regulatory network in adipogenesis is the simultaneous function of gene expression regulation and protein-protein interactions.

The central roles of PPARγ and C/EBPα

Central to this adipogenic cascade are Peroxisome Proliferator-Activated Receptor γ (PPARγ) and CCAAT/enhancer-binding protein alpha (C/EBPα). The peroxisome, a membrane-bound organelle, performs a variety of metabolic functions, but perhaps most notably regarding adipose biology breaks down long chain fatty acids via beta oxidation and are closely associated with lipid droplets (Lodhi and Semenkovich, 2014). The ligand-binding cavity of PPARs are uncharacteristically large for nuclear receptors, which confers capacity to utilise a wide range of ligands of varying lengths (Grygiel-Górniak, 2014). These PPARγ ligands include endogenous ligands such as free fatty acids, and fatty acid derived eicosanoids, as well as synthetic ligands such as the thiazolidinedione drug pioglitazone, which is often used for *in vitro* study of adipogenesis. To date, a definitive ligand for PPARγ has not been identified, and synthetic ligands show superior affinity to endogenous ligands which are typically present in tissues in insufficient concentrations for activation *in vivo* (Villacorta *et al*., 2009). Ectopic expression of PPARγ in otherwise non-adipogenic fibroblasts results in adipogenic differentiation (Tontonoz *et al*., 1994), whereas there are no known methods to induce adipogenesis in the absence of PPARγ. This data implicates PPARγ as the single most important determinant of adipogenesis, but in order to bind DNA and be transcriptionally active, it must heterodimerise with the retinoid X receptor (Chawla *et al.,* 2001).

At least four isoforms of PPARγ occur in man via alternative splicing, however these result in only two encoded protein isoforms (Fajas *et al*., 1997; Fajas *et al*., 1998; Sundvold and Lien, 2001). Despite differing expression patterns (isoform 1 is localised to adipose tissue as well as other tissue sites such as liver and skeletal muscle, while isoform 2 is exclusively localised to adipose tissue) both are involved in adipogenesis,

however their relative contributions to the process remain a subject of research (Aprile *et al*., 2014). Some research points toward a more adipogenic effect of the second isoform; in a knockdown study utilising 3T3-L1 cells (a murine embryonic fibroblast cell line used frequently to model adipogenesis), overexpression of isoform 2 rescued adipogenesis, whereas isoform 1 had no effect (Ren *et al.,* 2002). However, studies of this nature may be compromised as ectopic expression of PPARγ2 in fibroblasts appears to result in expression of the endogenous PPARγ gene (Tontonoz *et al*., 1994), and treatment of 3T3-L1 cells sufficient to induce PPARγ1 expression in differentiation-compromised cells leads to expression of PPARγ2 and adipocyte programming (Farmer *et al*., 2002). *In vivo* experiments also reveal a confusing picture, different groups have generated PPARγ2$^{-/-}$ mice, in two of these cases both cohorts exhibited impairments of insulin sensitivity, but one reported decreased adipose mass compared to control (Zhang *et al*., 2004) and another normal adipose morphology and body weight (Medina-Gomez *et al*., 2005). Thus, while the importance of PPARγ to adipogenesis is clear, the differential function of its isoforms is not.

The other central factor in adipogenesis is C/EBPα. C/EBPs are a family of transcription factors characterised by a highly conserved basic-leucine zipper domain, facilitating DNA binding, but also display a variety of protein-protein interactions within and outside of the C/EBP family (Ramji and Foka, 2002). They are involved in differentiation of a variety of different cell types, and several C/EBPs participate in adipogenesis. Typically, this is by inducing expression of C/EBPα, as is the case with C/EBPβ and C/EBPδ (Yeh *et al*., 1995). C/EBPα strongly induces transcription of many adipocyte genes, including PPARγ, which in turn activates promotion of the gene encoding C/EBPα resulting in a positive feedback loop (Wu *et al*., 1999).

C/EBPα and PPARγ induce the expression of a suite of genes involved in the regulation of lipolysis, lipogenesis, and insulin sensitivity, including glucose transporter GLUT4, fatty acid binding protein FABP4, lipoprotein lipase, and the adipokines adiponectin and leptin (Lowe *et al*., 2011). These gene products mediate the metabolic and functional properties of the resultant adipocyte. A representative diagram of some

of the internal and external network of factors regulating adipogenesis and the resultant expression of these functional genes is shown in Figure 1.2.

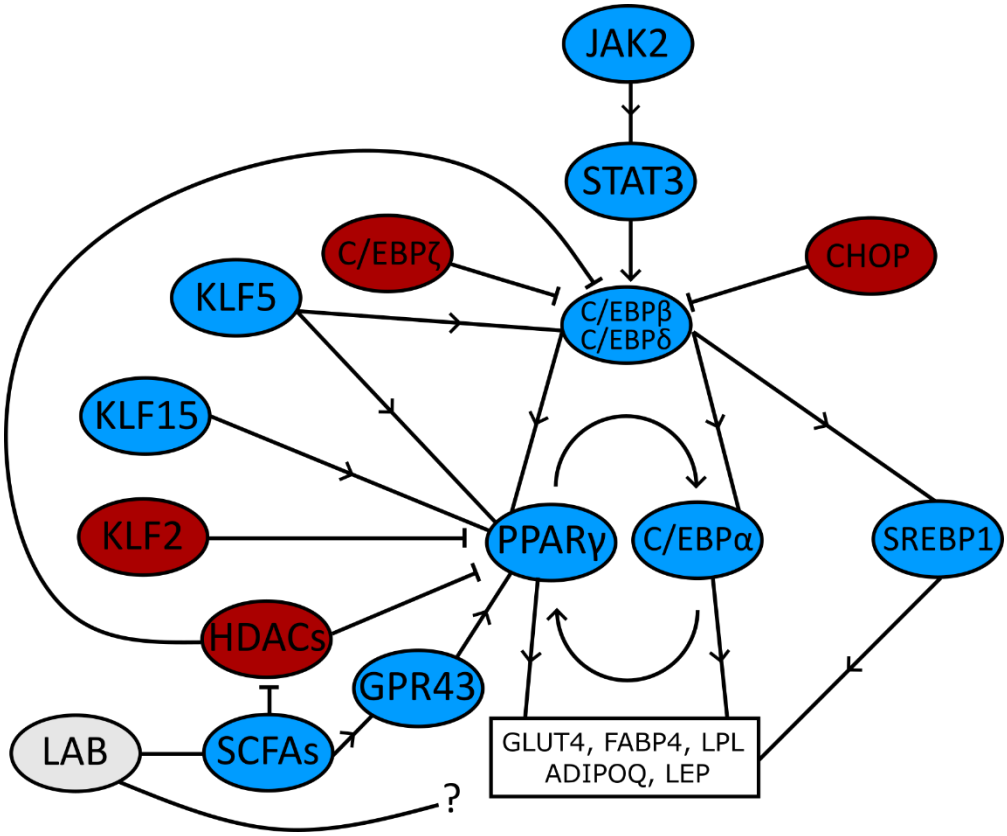

Figure 1.2. – Diagrammatic representation of the regulation of adipogenesis by a network of intra and extracellular factors. Blue ellipses represent pro-adipogenic factors, red ellipses represent anti-adipogenic factors. Arrows represent stimulatory effects, flat-ended arrows represent inhibitory effects. PPARγ is central to the adipogenic cascade, and can be inhibited or stimulated directly or indirectly by a range of factors, inside and outside of the cell. Families of proteins and transcription factors do not exhibit uniform effects; Krüppel Like Factors and C/EBP proteins may both enhance or inhibit adipogenesis. External stimuli such as JAK activation or short chain fatty acid (SCFA) activation of GPR43 can influence adipogenesis. Some cell wall components of lactic acid bacteria have been shown to impact adipose gene regulation; lipoteichoic acid increases adiponectin transcription but decreases resistin transcription, but research in this area remains limited. *C/EBP* - CCAAT/enhancer-binding protein, *CHOP* – C/EBP homologous protein, *GPR43* – G-protein coupled receptor 43, *HDAC* – Histone Deacetylase, *JAK2* – Janus kinase 2, *KLF*

- Krüppel Like Factor, *LAB* – lactic acid bacteria, *PPARγ* – peroxisome proliferator-activated receptor γ, *SCFAs* – short chain fatty acids, *SREBP1* – sterol regulatory element binding protein 1, *STAT3* – signal transducer and activator of transcription 3.

Other factors regulating adipogenesis

While a complete review of signalling factors regulating adipogenesis is beyond the scope of this study, several are conceptually important and potentially directly relevant. Further detail on bacterial components or metabolic products mentioned here is located in chapter 4. As depicted in Figure 1.2, there are a variety of factors capable of influencing adipogenesis both within and outside of the cell, which are mediated by key pathways. The Janus kinase (JAK) family and associated signal transducer and activator of transcription (STAT) are heavily involved in cytokine signalling (Schindler *et al*., 2007). The JAK2/STAT3 pathway has been reported as a regulator of C/EBPβ transcription (Zhang *et al.,* 2011), leading to a clear rationale for immune stimulating components such as bacterial cell walls to impact adipogenesis. Further, short chain fatty acids (SCFAs) are produced in the human colon by resident bacteria, and have been shown to stimulate adipogenesis in brown adipocytes via GPR43 (Hu *et al*., 2016).

As shown in Figure 1.2, several C/EBPs participate in regulating adipogenesis. C/EBPα is one of the central transcriptional players in adipogenesis, but is transcriptionally activated by other C/EBP proteins, notably C/EBPβ and C/EBPδ. However, other members such as C/EBP homologous protein (CHOP) show evidence of an inhibitory role, forming heterodimers with C/EBPβ and preventing its transcriptional activity (Darlington *et al*., 1998).

The Krüppel like factors (KLFs) are a family of zinc finger proteins characterised by three highly conserved C_2H_2 zinc finger motifs at the C-terminus, resulting in similar DNA binding patterns (McConnell and Yang, 2010). As they bind similar regions of DNA, but can associate with different proteins and are subject to various post-translational modifications, as with the C/EBP family they display the potential to either stimulate or inhibit gene transcription, and are important regulatory factors in adipogenesis.

Sterol regulatory element binding protein 1 (SREBP1) is a basic helix-loop-helix transcription factor shown to enhance adipogenesis. Though a simplistic relationship to adipogenesis in which it is induced by C/EBPβ/δ (Payne *et al*., 2009) and activates adipocyte genes (Kim *et al*., 1998a) is shown in Figure 1.2, there is evidence of a more complicated relationship. Further work by Kim *et al*. in the same year (1998b) suggested that SREBP1 activates PPARγ through the production of a PPARγ ligand. However, experiments in mice show that contrary to results in 3T3-L1 cells, overexpression of SREBP1c in adipose tissue results in severe lipodystrophy (Shimomura *et al*., 1998). The reason for the discordance of *in vitro* and *in vivo* data remains obscure but SREBP1 is widely held to be a pro-adipogenic factor.

Histone deacetylases (HDACs) are a family of enzymes involved in epigenetic regulation by facilitating the removal of acetyl groups from lysine residues in the N-terminus of histones, thus compacting chromatin structures (Seto and Yoshida, 2014). As adipogenesis encompasses the transcription of a large amount of genetic material, it logically follows that HDACs inhibit adipogenesis. However, evidence does not uniformly accord with the basic hypothesis; Yoo *et al*. (2006) reported that HDAC1 knockdown in 3T3-L1 cells promoted adipogenesis, while overexpression inhibited differentiation, but chemical HDAC inhibition shows mixed results that appear to be dependent upon class (Lagace and Nachtigal, 2004; Kim *et al*., 2009) and there is evidence in murine embryonic fibroblasts that HDAC gene deletion blocks adipogenesis (Haberland *et al*., 2010). The findings of Kim *et al*. that sodium butyrate can enhance adipogenesis is particularly relevant, as other SCFAs (which are explored in greater detail in chapter 4) also exhibit HDAC inhibitor activity (Latham *et al*., 2012).

Temporal regulation of adipogenesis

The progression of differentiation begins with arrest in the G1 phase of the cell cycle (Scott *et al*., 1982). While *in vitro* cells are cultured to confluency to achieve growth arrest, it is worth noting that confluent 3T3-F442A grown in suspension also retain differentiation capacity, suggestive of a functional cellular change outside of contact inhibition (Pairault and Green, 1979). Thus, while this is an integral step for common

in vitro models, confluence may not be a determining step *in* vivo. Following growth arrest, dependent upon hormonal stimulation, preadipocytes re-enter the cell cycle and undergo mitotic clonal expansion (MCE) (MacDougald and Lane, 1995). Blockade of progression into the S1 phase of the cell cycle during MCE results in complete prevention of adipogenic programming (Tang *et al*., 2003), though the status of MCE as an obligatory process in adipogenesis had previously been challenged (Qiu *et al*., 2001). Several rounds of MCE may occur, which ceases upon expression of PPARγ and C/EBPα (Shao and Lazar, 1997), signalling the onset of early differentiation. In addition to its role in the transcription of adipocyte genes, C/EBPα exerts anti-mitotic effects, facilitating the cessation of MCE (Umek *et al*., 1991). The expression of PPARγ and C/EBPα marks a subsequent and final period of growth arrest, during which fibroblasts acquire a rounded morphology and begin to accumulate lipid droplets and express proteins mediating functions such as lipid transport, synthesis, and insulin sensitivity (Gregoire *et al*., 1998). This period of terminal differentiation takes several days using *in vitro* models such as the 3T3-L1 cell line (Zebisch *et al*., 2012).

Though these stages are often presented as discrete, linear and chronological stages, there is often disagreement about the classification of transcriptional events. For example, lipoprotein lipase is often considered a sign of early differentiation, however reports indicate its expression occurs at growth arrest (Ailhaud *et al*., 1989). Despite complexities in discretely classifying these events, differentiation of adipocytes broadly results in marked temporal changes in gene expression, reflecting an initial multipotent state which is transcriptionally driven towards a specialised function. Resultantly, several genes have been identified and utilised as biomarkers of broad stages of adipocyte development: commitment, early, and terminal differentiation.

As previously mentioned and indicated in Figure 1.2, the Krüppel like factors exhibit inhibitory and stimulatory effects on adipocyte differentiation. KLF2 is robustly expressed in both human and 3T3-L1 preadipocytes, but expression is markedly lower in differentiated cells (Banerjee *et al*., 2003), which see greater expression of KLF5 and KLF15. KLF5 has been associated with early differentiation but is downregulated in mature adipocytes, whereas KLF15 is associated with terminal differentiation. Each

of these KLFs shows evidence of binding to the PPARγ promoter, engendering the hypothesis that KLF2 is sequentially replaced with KLF5, which in turn is replaced with KLF15 (Oishi *et al*., 2005), and that their differing capacity to interact with specific proteins mediates functional changes in the stages of differentiation.

Regulation of thermogenic programming of adipocytes

The regulation of thermogenic programming is less well understood than adipogenesis, however several key components have been identified. PRDM16, a zinc-finger protein, has been shown to strongly induce thermogenic programming when ectopically expressed in WAT (Seale *et al*., 2007). However, PRDM16 does not appear to be essential for the formation of BAT; selective knockout of PRDM16 in BAT progenitors of mice showed no morphological changes in BAT depots on birth, but by 6 months of age BAT associated genes were markedly decreased and adipose depots had physically expanded (Harms *et al*., 2014). Thus, while PRDM16 appears critical to the maintenance of BAT identity, and its expression is sufficient to drive a BAT-like transcriptional programme, it is not a master regulator of BAT development. The full suite of genetic redundancy in BAT development has yet to be elucidated. Early B Cell Factor 2 and Zinc Finger Protein 516 have recently been identified, knockout of the former results in neonatal lethality with dramatically reduced embryonic BAT development (Rajakumari *et al*., 2013), while knockout of the latter results in embryonic lethality with similarly reduced embryonic BAT development (Dempersmier *et al*., 2015). Both of these knockout models display morphologically impaired BAT as well as significant reductions in transcripts of BAT associated genes, but not complete ablation. Ultimately, BAT development still relies on the general adipogenic network (Seale, 2015), but a host of extra factors which are incompletely understood drive development towards a specialised fate.

While ectopic expression of genes such as PRDM16 in WAT can drive a thermogenic transcriptional programme, they do not appear to be involved in the activation of BAT. Cold exposure, the classical activator of BAT, results in secretion of catecholamines that stimulate β-adrenergic receptors in brown adipocytes, which

both acutely activates UCP1 and increases its transcription, enhancing thermogenic capacity of the cell (Seale, 2015). The gene network involved in activation of thermogenesis appears to be distinct from the network regulating BAT development. The best-known gene related to BAT activity is PPARγ coactivator-1α (PGC1-α). PGC1-α is the master regulator of mitochondrial biogenesis, and is thus regulated by a variety of signals related to cellular energy status and demands (Fernandez-Marcos and Auwerx, 2011). Ectopic expression of PGC1-α induces transcription of UCP1 in human WAT (Tiraby *et al*., 2003) and murine 3T3-F442A preadipocytes (Puigserver *et al*., 1998), but knockdown impairs induction of thermogenic genes without altering differentiation in an immortalised cell line generated from murine BAT (Uldry *et al*., 2006).

Activation of the Toll-like receptor (TLR) family of pattern recognition receptors appears to suppress transcription and protein expression of UCP1 in brown adipocytes assessed under basal and isoproterenol-stimulated conditions (Bae *et al*., 2014). Intriguingly TLR activation appears to only suppress PGC1-α transcription under basal conditions, with no significant effect in conjunction with isoproterenol-stimulated uncoupling, and no differences in protein expression of PGC1-α were apparent in either condition. This study utilised both LPS and a synthetic TLR2 ligand. TLR2 can be activated by lipoteichoic acid (Long *et al*., 2009), a component of gram-positive bacterial cell walls and thus these results may have implications for probiotic bacteria. The role of TNF-α is more ambiguous however. Early research efforts involved administration of recombinant human TNF-α in rats, showing upregulation of BAT activity and UCP1 transcription (Coombes *et al*., 1987; Masaki *et al*., 1999), however *in vitro* administration of TNF-α to rat foetal brown adipocytes inhibits transcription (Valladares *et al*., 2001), though the latter study makes no mention of whether rat or human TNF-α was used, and differences may be reflections of experimental platforms used.

In summary, separate gene networks are responsible for BAT development and activity, though ectopic expression of genes from either network in WAT may induce thermogenic programming. Several crucial though not obligatory factors have been identified, and the networks in both development and activity circuits are being

gradually elucidated. PGC1-α, one of the central genes regulating BAT activity, is strongly influenced by a wide variety of signals and is thus seen as a promising target for the treatment of obesity.

Models used for the study of adipogenesis

The 3T3-L1 cell line is a longstanding *in vitro* model of the differentiation of preadipocytes to adipocytes. 3T3-L1 cells are unipotent murine preadipocytes which display fibroblast-like morphology, however under specific culture conditions these cells accumulate lipid and adopt an adipocyte-like phenotype (Farmer, 2006). This process involves mitosis, growth arrest, and the coordinated expression of specific genes, enhancing expression of those related to triglyceride synthesis/storage, and altering expression of structural proteins to facilitate the round phenotype (Rosen and MacDougald, 2006). The process of differentiation requires an adipogenic medium, with maximal differentiation achieved using a combination of glucocorticoids, insulin, a treatment to elevate cAMP intracellularly, and foetal bovine serum (Cristancho and Lazar, 2011). Frequently in the study of adipogenesis using 3T3-L1 cells, treatment groups are cultured in an adipogenic "differentiation medium" (DM) while control groups are cultured in a basal medium containing factors necessary only for the maintenance of growth, termed "complete medium" (CM).

Several investigatory tools are routinely used to quantify adipogenesis to allow statistical comparison between control and treatment groups. The quickest and most practical of these is Oil Red O (ORO) staining. ORO is a lipophilic dye that has been used for the quantification of lipids in *in vitro* models of adipogenesis for several decades (Ramirez-Zacarias *et al*., 1992) and is widely used in histopathology for the investigation of hepatic steatosis (Levene *et al*., 2012). In brief, lipid-soluble ORO is dissolved in a solvent, which is diluted with water prior to use. Owing to the hydrophobic nature of ORO, incubation of tissues with the solution results in the dye associating with lipids, which can then be extracted in alcohol and optical absorbance measured to enable lipid quantification. ORO staining can encounter problems with

nonspecific staining, as fine particulate matter can be difficult to completely wash from cells and will carry over to the final extraction. There have also been reports of non-adipogenic cell staining dependent upon solvents used (Kinkel *et al*., 2004). In summation ORO is a hugely useful tool in the quantification of adipogenesis, but encounters issues with sensitivity. As mentioned previously, several genes have been identified which are involved in the transcriptional regulation of adipogenesis; quantitative polymerase chain reaction (qPCR) is another method frequently used to assess adipogenesis via measurement of transcripts of markers of terminal differentiation. qPCR allows for extremely sensitive measurements in biological samples, but is also more versatile than ORO staining as it allows for the quantification of markers of adipose phenotype and function.

Much of the knowledge of the cellular and genetic processes of adipogenesis has been derived from 3T3-L1 studies. As an *in vitro* model it appears highly physiologically representative; cultured 3T3-L1 adipocytes have been implanted into mice and maintained function (Fischbach *et al.,* 2004) and these implantation methods have also been used to study the differences observed in the function of visceral and subcutaneous adipose tissue with regards to inflammation (Shibasaki *et al*., 2002). While the 3T3-L1 model is held to be an excellent model of white adipose tissue, it is less clear how it applies to the study of thermogenically active adipose phenotypes. 3T3-L1 adipocytes appear to display mixed features of brown and white adipocytes, responding to catecholamines in a manner more representative of beige or BAT, and are capable of significant enrichment of BAT associated genes without increases in UCP1 expression (Morrison and McGee, 2015). Previous studies have tangentially reported the presence of BAT associated genes such as Zinc in Cerebellum 1 (ZIC1) in 3T3-L1 cells (Seale *et al*., 2007), but it remains unclear whether they possess any functional role. In recent years, protocols have been reported allowing the induction of beige-like characteristics, including robust expression of UCP1 (Asano *et al*., 2014), however the expression of beige associated genes was largely unchanged from control adipocytes. Within the past 2 decades, the PAZ6 cell line has been developed for use as a model of human brown preadipocytes (Kazantzis *et al.*, 2012), however its usefulness has been questioned owing to differences

observed in function between PAZ6 and primary cultures (van Beek *et al*., 2008) and work continues in this area of research. Until validated protocols or new models of adipose "browning" appear, 3T3-L1 cells still represent a useful investigatory tool, but caution is required in interpreting results.

Treatment of obesity

Expansion of adipose depots occurs through either hypertrophy of adipocytes or *de novo* adipogenesis. Broadly, there are two phenotypic patterns of obesity, hypertrophic and hyperplasic, though some degree of hypertrophy is characteristic of all obesity (Hirsch and Batchelor, 1976). Hyperplasic obesity is associated with severity of obesity (Hirsch and Batchelor, 1976), however hypertrophic obesity appears to be more metabolically deleterious (Weyer *et al*., 2000; Tchoukalova *et al*., 2008). This difference in metabolic features of adipose tissue may also affect response to treatment; limited data exists on the cellular response of adipose tissue in obesity to treatment, but a suggestion exists that weight loss reduces adipocyte size in large adipocytes, with little effect on smaller adipocytes (Rossmeislová *et al*., 2012).

However, classification and screening of obesity relies on measures applicable at a population level, chiefly BMI, and few patients are examined on a cellular basis. At present, the treatment algorithm for obesity in the United Kingdom is governed by different bodies in different jurisdictions but is broadly similar in England and Wales, employing a tiered approach (NHS England, 2014; Welsh Government, 2016). Tier 1 consists of behavioural change facilitated by public health campaigns such as "Change4Life", tier 2 consists of weight management services delivered in the community, tier 3 consists of clinician led services that may involve pharmacological intervention, and tier 4 consists of bariatric surgery (NHS England, 2014).

Public health campaigns encounter criticism of ineffectiveness and governmental reticence for legislative intervention in environmental factors contributing to obesity (Walls *et al*., 2011; Hafekost *et al*., 2013). Health technology assessment of the clinical effectiveness of weight management services shows that weight reduction tends to

be modest, and regaining weight is common (Loveman *et al*., 2011). Orlistat (tetrahydrolipstatin) therapy is the only pharmacological intervention approved in the UK at present, as sibutramine was withdrawn following concerns about adverse cardiovascular events (European Medicines Agency, 2010). Orlistat is a pancreatic lipase inhibitor, which in a study investigating effectiveness of dosage timing found an increase of 20-27g of faecal fat per day compared to placebo (Hartmann *et al*., 1993). This can result in gastrointestinal discomfort and steatorrhea, and faecal urgency (Jain *et al*., 2011) making it an unattractive treatment for many patients. Bariatric surgery is reserved for the most severely obese patients and appears to be the most effective intervention (Chang *et al*., 2014). However, in addition to attendant risks of surgical procedures such as mortality, there are potential metabolic complications associated with the disruption of normal gastrointestinal physiology. These include micronutrient deficiencies, hypoglycaemia, and metabolic bone disease (Jammah, 2015).

Given the estimated cost of obesity, the significant contribution to ill health, and the ineffectiveness of present treatments, new treatments are desperately needed. Development and licensing of new medications takes significant time and monetary investment, and so existing medications or non-pharmacological interventions are an attractive avenue of research.

1.2 – The gut microbiota and probiotic bacteria

The gut microbiota

The human body is host to a variety of microbial communities inhabiting areas such as skin, eyes, and the intestinal tract. Total bacterial cell numbers inhabiting the human body are estimated to be in the same order as the total somatic cells in an average 70kg man (Sender *et al*., 2016). Of these communities the "gut microbiome" of the large intestine is the largest and most extensively studied. The term microbiome refers to the entire ecological "habitat" and its contents, i.e. the "gut microbiome" would account for the entire bacterial population of the large intestine, as well as components such as viruses and fungi, their genomes, and other abiotic factors. The terms "microbiota" and "microbiome" are often used interchangeably, recent attempts to standardise the language in research propose that "microbiota" be used to refer to "assemblage of microorganisms present in a defined environment", the composition of which is analysed by means such as 16S rRNA sequencing (Marchesi and Ravel, 2015).

Evidence suggests that colonisation of the human gastrointestinal tract may begin *in* utero, as meconium of neonates shares microbiota features of amniotic fluid and placental tissue (Collado *et al*., 2016). It is believed that an increase in foetal swallowing of amniotic fluid increases in the third trimester (Mann *et al*., 1996), which may allow the foetal gut to become colonised, and may explain links between gestational age and faecal microbiota (Hill *et al*., 2017). Mode of delivery appears to exert effects on infant microbiota signatures over at least the first 3 months of life, with Caesarean section notably associated with greater colonisation of *Clostridium* and *Lactobacillus*, whereas *Bifidobacterium* and *Bacteroides* colonisation seems associated with vaginal delivery (Rutayisire *et al*., 2016). Composition of the infant microbiota also varies according to nutritional status. Breast feeding affects development of the infant microbiota not only through the composition of the nutritional milieu, but there is also evidence of a bacterial entero-mammary pathway (Rodríguez, 2014). Immunoglobulins in breast milk are also believed to affect immunoregulation in the infant, promoting tolerance to the endogenous microbiota

(Maynard *et al*., 2012). The establishment of the microbiota and exposure to microorganisms is intrinsically linked to development of the immune system (Renz *et al*., 2011), and development of the microbiota occurs also, with the relatively simple infant microbiota giving way to the more complex adult microbiota by the end of the first year of life (Palmer *et al*., 2007).

The gut microbiome has received considerable research interest in the last decade and has come to be viewed as an extrasomatic organ, representing an abundance of genetic material capable of mediating functions that human genes cannot (Bäckhed *et al*., 2005). Metagenomic analysis of stool samples reveals that a significant amount of total genetic material is related to the fermentation of carbohydrates (Gill *et al*., 2006), producing abundant quantities of SCFAs from undigested material from the host diet, which are estimated to account for between 5-10% of daily energy intake in man (McNeil, 1984). As SCFAs are highly energetic molecules, this is often cited as the most important bacterial contribution to human metabolism, however there is also evidence of processes as diverse as vitamin synthesis, drug metabolism, and bile acid deconjugation (Jandhyala *et al*., 2015). Outside of metabolic processes, the gut microbiota is involved in pathogen exclusion both through competition for resources and production of bacteriocins (Buffie and Pamer, 2013) and is proposed to be a regulatory factor in epithelial homeostasis, affecting transport protein expression through hypoxia (Ward *et al*., 2014).

Modern techniques such as 16S rRNA sequencing allow for far more sensitive analysis of the microbial composition of a sample than traditional culture techniques (Clarridge III, 2004), which were often limited to measuring the growth of aerobic or anaerobic populations (Krook, 1981). These techniques have facilitated the publishing of many studies investigating the association between composition of the gut microbiota and human health, particularly in inflammatory bowel diseases (Prosberg *et al*., 2016). This work builds on an unexpected role of bacteria in human health proposed in the last few decades. The TLR family of pattern recognition receptors which regulate response to pathogenic bacteria, are highly conserved in both vertebrates and invertebrates, and are of distinct evolutionary importance (Roach *et al*., 2005). The “old friends” hypothesis proposed by Rook *et al*. (2004)

builds on the hygiene hypothesis based on the work of Strachan (1989) and accounts for discordant evidence surrounding the contemporary T-helper 1/2 paradigm (Yazdanbakhsh *et al*., 2002). This proposed that a shared evolutionary history with microbial organisms such as certain helminths and species of bacteria primed immunoregulation rather than aggressive inflammatory responses that may be detrimental to the health of the host. This suggestion neatly accounted for the then recent discovery of regulatory T cells (Rook and Brunet, 2005) and links between microbial richness and diversity in the large intestine and human health. The hygiene hypothesis has been proposed to be involved in the growing incidence of autoimmune diseases such as type 1 diabetes mellitus, multiple sclerosis, and inflammatory bowel diseases, which experienced rises of up to 300% between 1950-2000 in some developed nations (Bach, 2002). Various epidemiological studies appear to support the hypothesis, such as the findings of Leibowitz *et al*. (1959) that risk of developing multiple sclerosis in an Israeli population may be related to level of sanitation during childhood, and that early life exposure to siblings is also associated with a reduced risk of multiple sclerosis (Ponsonby *et al*., 2005). While results such as these present interesting hypotheses, they do not establish a causal link. There is however strong evidence of causality in animal models. In both bio-breeding diabetes-prone rats and non-obese diabetic mice the incidence of spontaneous type 1 diabetes mellitus is directly correlated to the infectious burden of the environment (Bach, 2002).

Recently, there has also been considerable interest in the potential role of gut microbiota composition in obesity, T2DM, and metabolic syndrome (Hartstra *et al*., 2015). The high fat diet (HFD) model of obesity in mice results in decreased colonic epithelial integrity (Murakami *et al*., 2016). HFD feeding also disrupts microbial composition of the intestines, increasing lipopolysaccharide content while permitting increased bacterial translocation from the intestinal lumen resulting in “metabolic endotoxemia” (Cani *et al*., 2007). However, colonic bacteria may also affect other adipose depots via systemic effects, synthesising SCFAs and other metabolic products that may be absorbed within the colon and enter systemic circulation via the liver (den Besten *et al*., 2013). The application of techniques for assessing the composition

of the gut microbiota remains a matter of debate; results have proven difficult to reproduce and no standard reference material exists (Sinha *et al*., 2015), in addition to unresolved questions surrounding the effect factors such as intestinal transit time have on results derived from faecal samples (Vandeputte *et al*., 2016).

Intriguingly, a recent meta-analysis into the possible effect of probiotic supplementation on microbiome composition reported no significant effects (Kristensen *et al.,* 2016). While techniques for the robust study of the gut microbiome remain in their infancy, this may be reflective of factors governing ecological niches within the intestines. Some of these are likely to be relatively fixed host factors, such as internal anatomical dimensions and immunological function. However, owing to the microbial richness of the gut microbiota and the abundance of genes facilitating metabolism of remnant dietary material, it is believed that there is a complex network of interdependent microbes and the application of ecological theory to the gut microbiome is an expanding area of research (Pepper and Rosenfeld, 2012). The competitive exclusion principle proposes that species occupying the same ecological niche within the same geographic region cannot coexist, as the slightest imbalance of reproductive rate will cause one species to dominate said niche (Hardin, 1960). Natural selection favours species specialised for niches constructed within the intestine, influenced by host and ecological factors, and it is therefore unsurprising that introduction of exogenous species appears to have little impact.

The ecological view of the gut microbiota is supported by evidence surrounding recurrent *Clostridium difficile* infection. Antibiotics have pronounced effects on the composition and abundance of intestinal bacteria, and alterations can persist after the cessation of treatment, which may prime the environment for *C. difficile* colonisation (Vincent and Manges, 2015). Faecal microbial transplantation appears to be a highly successful strategy for treating recurrent *C. difficile* infection, which at present appears to be superior to probiotic therapy (Crow *et al*., 2015), though there are attendant caveats regarding strains, doses, and methods used. It had been proposed that restoration of an intact microbial community confers resistance to colonisation through niche exclusion, but recent research suggests multiple mechanisms including bile acid metabolism are involved (Mullish *et al*., 2017). The

issue therefore arises of reconciling effects of probiotic supplementation on clinical features such as reduction of serum CRP (Mazidi *et al*., 2017) or prevention of necrotising enterocolitis (Lau and Chamberlain, 2015) with no apparent change in microbiota structure. Evidence suggests that supplementation with probiotic bacteria can induce significant changes in the transcriptional activity of the gut microbiota without apparent effects on richness or diversity. A recent study of 12 elderly Finnish individuals receiving daily doses of a *Lactobacillus rhamnosus* strain for 28 days found no evidence of significant structural changes in subjects' microbiota, however did find significant enrichment of genes of commensal bacteria (Eloe-Fadrosh *et al.,* 2015). These gene sets were primarily related to adhesion and motility of the butyrate producing species *Roseburia* and *Eubacterium*. A separate study in both mice and humans also showed limited evidence of change in microbial community structure with fermented milk supplementation, but significant changes in the faecal metatranscriptome related primarily to carbohydrate metabolism (McNulty *et al*., 2011). It is therefore plausible that probiotic supplementation can induce a change in the *function* of the gut microbiota without changing its population level structure. It is impossible to delineate whether this is due to effects of probiotics on the host, the bacterial community, or both and further research is required. One of the most widely researched aspects of probiotic bacteria is the assessment of anti-inflammatory activity. *In vitro* study of *Lactobacillus* strains suggests that anti-inflammatory effects on human cells are mediated largely by soluble metabolites (Ladda *et al*., 2015), but data relating to effects on adipogenesis (discussed in greater detail later in this chapter) is constrained by methodological oversights.

If the resident bacteria of the colon can account for up to 10% of daily energy intake, and the composition of the gut microbiome is implicated in the "diseases of civilisation", it follows that an increased microbial capacity for energy salvage could contribute towards obesity. Bäckhed *et al*. (2004) showed that a cohort of germ free mice had significantly lower body fat than conventionally raised littermates despite greater food consumption, and that transplantation of caecal material from conventional mice resulted in a 61% increase in body fat despite a reduction in food consumption. Sporadic reports of weight gain in human patients treated for *C.*

difficile infection by faecal transplant occur (Alang and Kelly, 2015), and conversely small randomised controlled trials of faecal transplants from lean donors in patients with metabolic syndrome have shown increases in peripheral insulin sensitivity (Vrieze *et al*., 2012), but definitive evidence of causative microbial shifts in humans remains obscure.

Potential impact of bacteria on adipogenesis

The modern history of utilising lactic acid bacteria (LAB) for effects on human health dates to 1907. Metchnikoff (1907) proposed that as with fermented milk, ingestion of LAB would “arrest intestinal putrefaction”. The ongoing association with ingestible bacterial products and potential health effects led to the creation of the term “probiotic”, defined by the World Health Organization in 2001 as "live micro-organisms which, when administered in adequate amounts, confer a health benefit on the host" (Food and Agriculture Organization and World Health Organization, 2001). Lab4 is a commercial probiotic product comprised of a mixture of *Lactobacillus* and *Bifidobacteria* strains. The composition of both Lab4 and Lab4b products is given in Table 1.1. Lab4 has been studied for potential effects in prevention of upper respiratory infections in children (Garaiova *et al*., 2015), prevention of *C. difficile*-associated diarrhoea (Plummer *et al*., 2004), on symptoms of irritable bowel syndrome (Williams *et al*., 2009), on cholesterol metabolism in mice (Michael *et al*., 2017), and other conditions.

Table 1.1. – Composition of Lab4 and Lab4b products

Product	Bacterial strains
Lab4	*Lactobacillus acidophilus* CUL21 (NCIMB 30156) *Lactobacillus acidophilus* CUL60 (NCIMB 30157) *Bifidobacterium bifidum* CUL20 (NCIMB 30153) *Bifidobacterium animalis subsp. lactis* CUL34 (NCIMB 30172)
Lab4b	*Lactobacillus salivarius* CUL61 (NCIMB 30211) *Lactobacillus paracasei* CUL08 (NCIMB 30154) *Bifidobacterium bifidum CUL20* (NCIMB 30153) *Bifidobacterium animalis subsp. lactis* CUL34 (NCIMB 30172)

NCIMB - National Collection of Industrial, Food and Marine Bacteria

Probiotic bacteria have been assessed for potential ability to ameliorate diet induced obesity in animal models, and for weight loss in humans (Park and Bae, 2015). While results from animal studies indicate the structure of the gut microbiome may modulate obesity, results in human trials remain mixed and multiple recent meta-analyses reach varying conclusions (Park and Bae, 2015; Zhang *et al*., 2016; Borgeraas *et al*., 2017). Borgeraas *et al*. notably found a modest reduction in BMI but insignificant results in fat mass. As probiotic bacteria show species and strain specific effects, attempting to reconcile data for meta-analysis is problematic, and results may be artefacts of inclusion criteria, data availability, or both. Data from animal models is more robust, and notably the Lab4 consortium supplemented with *L. plantarum* CUL66 has already been studied in the context of cholesterol metabolism, with HFD mice gaining significantly less weight after 14 days when supplemented with Lab4 plus *L. plantarum* CUL66 (Michael *et al*., 2017).

Another recent study found that two *Lactobacillus* strains ameliorated weight gain in HFD mice, but also led to statistically significant increases of PGC1-α and decreases of leptin mRNA in mesenteric adipose tissue (Park *et al*., 2017). While these tissues were seemingly not assessed for UCP1 transcription, these findings are suggestive of a potential "browning" effect on adipose tissue following administration of a probiotic, as leptin and BAT genes are reciprocally regulated (Cancello *et al*., 1998), and PGC1-α induces transcription of thermogenic genes such as UCP1 (Harms and Seale, 2013).

The 3T3-L1 model provides an excellent experimental platform to investigate the effects of soluble factors of probiotic bacteria on adipocyte biology and has been frequently used for the study of adipogenesis in relation to obesity (Ruiz-Ojeda *et al*., 2016). Several *in vitro* studies have investigated the effect of probiotic bacteria on adipogenesis, and methods used vary. Lee *et al*. (2015) treated differentiated 3T3-L1 cells for 24 hours with lyophilised kimchi (a fermented cabbage dish) powder dissolved in culture medium, finding reduced mRNA expression of PPARγ, C/EBPα, and fatty acid synthase, as well as what appeared to be reductions in lipid droplet size assessed subjectively by ORO staining. However, this study did not report on cell viability and utilised glyceraldehyde-3-phosphate dehydrogenase (GAPDH) as a reference gene, which is unsuitable in 3T3-L1 cells (Zhang *et al*., 2014). Park *et al*. (2011) found similar results treating 3T3-L1 cells with a probiotic cell extract, reporting reduced mRNA and protein expression of PPARγ2, C/EBPα, fatty acid synthase, and adipocyte-fatty acid binding protein. Ilavenil *et al*. (2015) studied the effect of phenyllactic acid extracted from the supernatant of cultured *Lactobacillus* spp. KCC-10 on 3T3-L1 cells and reported increases in mRNA and protein expression of PPARγ 2, C/EBP-α, adiponectin, fatty acid synthase, and SREBP-1 compared to control. However, this study also used GAPDH as a reference gene and protein, and while it did report data on cell proliferation, this was using a tetrazolium salt based assay which may not be suitable for use with treatments that may increase mitochondrial respiration (discussed further in chapter 3). Park *et al*. (2013) studied the effects of supernatant of a LAB extracted from gajami sik-hae (a fermented fish dish), reporting dose dependent reductions in ORO staining, in addition to dose

dependent reductions in mRNA expression of PPARγ 2, C/EBPα, leptin, adipocyte-fatty acid binding protein, glycerol-3-phosphate dehydrogenase (GPDH), and fatty acid translocase. This study utilised a more suitable reference gene in β-actin, but did not report on cell viability. A 3T3-L1 study utilising both the spent broth and a cell extract of cultures of *L. rhamnosus* isolated from amabere amaruranu, a Kenyan milk product, reported increased protein expression of PPARγ 1, 2, C/EBPα, and adipose tissue triglyceride lipase from spent broth treatment but not cell extract (Kotala, 2015). This study also did not report cell viability. While there are differing methodologies and results, *in vitro* evidence largely suggests potential inhibition of adipogenesis in 3T3-L1 cells with probiotic treatment.

Similar to results seen in other *in vitro* studies mentioned, unpublished data generated in our laboratory by Erika Galgóczi (discussed in further detail in chapter 4.3) suggests that culturing 3T3-L1 cells with Lab4 and Lab4b cell free supernatant (CFS) may influence adipogenesis. ORO staining of 3T3-L1 cells was performed during late adipogenesis, as well as qPCR quantification of markers of terminal differentiation. ORO staining suggested potential enhancement of adipogenesis in cells treated with CFS, with visual features of lipid droplets suggestive of a more advanced stage. However, qPCR data suggested the opposite, with a marker of terminal differentiation appearing lower in cells treated with Lab4 and Lab4b CFS than control in a single experiment.

In sum, there is a scientific rationale behind the potential of bacteria to influence adipogenesis. Further, there is an unmet need in the literature to assess viability of adipocytes treated with bacterial CFS and resultant phenotype, which the present study seeks to address.

1.3 – Hypothesis and aims

Following on from results seen in preliminary data, it is hypothesised that treatment of 3T3-L1 cells with the Lab4 consortium of probiotics will inhibit adipogenesis, with inhibition differing in a strain and time specific manner. It is further hypothesised that culturing 3T3-L1 cells in cell free supernatant of the Lab4 consortia will enrich expression of genes associated with BAT or beige adipose tissue and enhance thermogenic activity.

The aims of this study are to assess the effects of the Lab4 consortium of probiotics on the molecular events of adipogenesis by measuring lipid accumulation and markers of adipose phenotype in the presence or absence of the Lab4 consortia and their constituent strains.

Chapter 2: Standardisation and production of bacterial cell free supernatant

2.1 – Introduction

Probiotic bacteria are studied in a wide variety of contexts, such as research into immunomodulatory capabilities (Chon *et al*., 2009) or mucosal adhesion (Piatek *et al*., 2012). In certain biological contexts such as mucosal adhesion, investigating the effects of viable bacterial cells on *in vitro* cell models can be physiologically relevant. However, in the context of investigating potential effects of bacteria on *in vitro* adipogenesis, different methodology is required. As mentioned in the previous chapter, a large amount of genetic material in the gut microbiota is related to the metabolism of carbon sources, and the gut microbiota can synthesise large amounts of SCFAs from remnant material of the host's diet. This demonstrates a secretory capacity of bacteria resident within the gastrointestinal tract, and though as mentioned bacterial translocation can occur, and probiotic administration in mice has shown effects on mesenteric fat, most adipose depots in an organism will not interact directly with bacteria. Harvesting bacterial metabolites suspended in culture medium for use with *in vitro* cell models of adipogenesis is a simple method to maintain physiological relevance.

In the absence of data on the effects of oral administration of the Lab4 consortium of probiotics on the genetic and molecular events of adipogenesis in previous mouse studies, it is important to standardise any materials used for *in vitro* study to obtain consistent, accurate results, and enable future study. Due to the extremely fast growth rate of many bacteria there are inherent difficulties to standardising either populations or their products. The present study represents the early stages of establishing *in vitro* models of the effects of such probiotic bacteria on adipogenesis and as such there are attendant concerns.

Previous studies investigating the effect of probiotic bacteria on *in vitro* adipogenesis mentioned in chapter 1 have utilised standardisation methods that include lyophilisation and reconstitution of product to a specific weight per given volume of

media. This has advantages such as greater ease of studying dose dependent effects, but as the composition of products remains uncertain, it is unknown what effect the lyophilisation process may have. In order to provide a quantifiable measure for standardisation of CFS without introducing further processing, culture methods developed at Cultech to normalise to number of microorganisms in the starting inoculum were used. As might be expected, bacterial strains within the same species can exhibit significant differences in measures such as cell diameter (Kokkinosa *et al*., 1998), and strains within the same genus can display different rates of production of metabolic products (Liguori *et al*., 2015). As the metabolic products of the bacterial strains used in the present study remain unknown, it was necessary to standardise to a broad measure such as cell number, however this is also advantageous as doses of probiotic products used by humans are routinely given in colony forming units (CFU). Various techniques have been applied for the enumeration of microorganisms in culture. A classical method still widely used today is the "Miles and Misra method" (Miles *et al*., 1938), which though labour intensive, uses bacterial suspensions plated on the surface of agar plates rather than more laborious methods using bacteria incorporated within molten agar.

Time is a necessary variable to control for when culturing bacteria, as bacterial growth is characterised by distinct phases. A "lag" phase in which bacteria acclimate to growth conditions (Rolfe *et al*., 2012), a "log" phase of exponential growth seldom encountered naturally, a stationary phase in which growth plateaus, often restricted by environmental factors such as nutrient availability, followed eventually by a death phase (Navarro Llorens *et al.,* 2010). It is necessary to be able to determine that growth has plateaued at the timepoint which the starting inoculum is used for further experiments in order to standardise bacterial content. There are numerous methods to quantify bacteria, however as with the Miles and Misra method they can be labour intensive and unsuitable for longitudinal determination. A practical method that allows for collection of large amounts of granular, longitudinal data is spectrophotometry. Unlike typical applications of spectrophotometry, the measurement taken is not directly of absorption of light at a specific wavelength as with a dye, but by bacterial suspension scattering light and reducing the amount that

ultimately reaches the photoelectric cell. The measurement obtained therefore is turbidity, and an indirect though semi-quantifiable measure of the number of bacteria in suspension. Measuring optical density of suspensions at 600nm is a common practice in the field of enumeration of microorganisms (Smetnakova *et al*., 2012) but does not itself give direct quantification.

2.2 – Materials and methods

A list of reagents used and their suppliers is given in Appendix 1, Table 1.

Miles and Misra counts

Lyophilised Lab4, Lab4b, *L. paracasei* CUL08, *L. salivarius* CUL61, a Lactobacillus acidophilus mixture comprised of *L. acidophilus* CUL21 and *L. acidophilus* CUL60, and a Bifidobacterium mixture comprised of *B. animalis subsp. lactis* CUL34, *B. bifidum* CUL20 were obtained from Cultech Limited (Port Talbot, UK). The strains comprising the various bacterial cultures are summarised in Table 2.1.

Table 2.1. – Constituent strains of lyophilised bacterial mixtures used

Condition	Constituent strains
1 – Lab4	*Lactobacillus acidophilus* CUL21 (NCIMB 30156) *Lactobacillus acidophilus* CUL60 (NCIMB 30157) *Bifidobacterium bifidum* CUL20 (NCIMB 30153) *Bifidobacterium animalis subsp. lactis* CUL34 (NCIMB 30172)
2 – Lab4b	*Lactobacillus salivarius* CUL61 (NCIMB 30211) *Lactobacillus paracasei* CUL08 (NCIMB 30154) *Bifidobacterium bifidum CUL20* (NCIMB 30153) *Bifidobacterium animalis subsp. lactis* CUL34 (NCIMB 30172)
3 – *Lactobacilli*	*Lactobacillus acidophilus* CUL21 (NCIMB 30156) *Lactobacillus acidophilus* CUL60 (NCIMB 30157)
4 – *Bifidobacteria*	*Bifidobacterium bifidum CUL20* (NCIMB 30153) *Bifidobacterium animalis subsp. lactis* CUL34 (NCIMB 30172)
5 – *L. salivarius*	*Lactobacillus salivarius* CUL61 (NCIMB 30211)
6 – *L. paracasei*	*Lactobacillus paracasei* CUL08 (NCIMB 30154)

NCIMB - National Collection of Industrial, Food and Marine Bacteria

Approximately 10µg of lyophilised bacteria per condition was suspended in 30ml universal containers (Greiner Bio-One, Belgium) containing 10ml MRS broth (reconstituted per manufacturer's instructions), which was then incubated statically for 18 hours inside an Electrotek 400sg anaerobic cabinet (Electrotek, Shipley) at 37˚C. To determine numbers of viable bacteria, serial dilutions were prepared by pipetting 4.5ml of phosphate buffered saline (PBS) into bijou containers (Greiner, Belgium) and transferring 500µl of the prior culture stock sequentially, up to dilutions of 10^{-7}, as summarised in Figure 2.1.

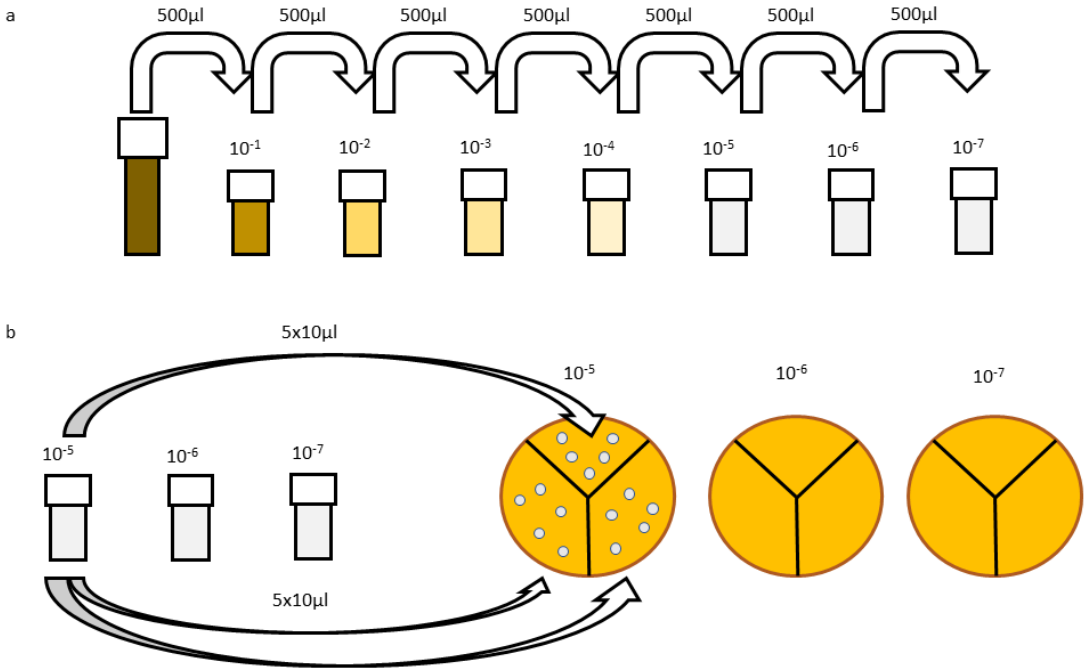

Figure 2.1. – Representative diagram of the Miles and Misra technique. A. Serial dilutions were prepared from a starting inoculum of lyophilised bacteria up to a final concentration of 10^{-7} with the stepwise addition of 500µl of prior suspension to 4.5ml PBS. B. 5 individual 10µl droplets of the final 3 dilutions were added to demarcated segments of agar plates.

Droplets (5 x 10µl) from dilutions 10^{-5}, 10^{-6}, and 10^{-7} were plated on each of 3 demarcated segments of 5 individual MRS agar plates per dilution. Droplets were air dried inside a class 1 biological safety cabinet and then incubated anaerobically for 48 hours. Following this, numbers of visible colonies per segment were counted at 10^{-7}, and the equivalent number of colony forming units at 10^{-1} calculated using the formula:

$$\text{CFU of 50µl at } 10^{-7} \times 20 = \text{CFU of 1ml at } 10^{-7}$$

$$\text{CFU of 1ml at } 10^{-7} \times 1{,}000{,}000 = \text{CFU of 1ml at } 10^{-1}$$

A mean average of the 15 results per condition was then used to calculate a dilution factor to achieve a $1x10^8$ concentration.

Longitudinal evaluation of bacterial growth by spectrophotometry

Lyophilised bacteria were obtained from Cultech Ltd utilising the same strains and culture combinations as in Table 2.1. Cultures were prepared in triplicate by suspending approximately 10µg of lyophilised bacteria in 30ml universal containers containing 10ml MRS broth, then diluted to 1:100 and 1:1000 in MRS within separate universal containers. 100µl of both 1:100 and 1:1000 dilution samples with MRS as negative control were plated in duplicate on 96-well, flat bottomed, untreated plates (Corning, UK). Growth curves were generated by measuring optical density at 600nm every hour for 70 hours using a TECAN infinite 200 pro plate reader (TECAN, Männedorf) housed within an Electrotek SG 400sg anaerobic cabinet. Cultures were shaken with an orbital amplitude of 1mm for 5 seconds before measurement each hour.

Production of bacterial cell free supernatant

Approximately 10µg of lyophilised bacteria per condition (as in Table 2.1) were suspended in 10ml MRS broth within 30ml universal containers for 18 hours inside an Electrotek 400sg anaerobic cabinet at 37˚C.

Following initial incubation, cultures were centrifuged at 3000 rpm for 10 minutes, supernatant discarded, and pellets resuspended in 10ml sterile PBS. PBS suspensions were subsequently centrifuged at 3000 rpm for a further 10 minutes, supernatant discarded, and resuspended in DMEM:F12 tissue culture media (see chapter 3.2 for details), diluted to $1x10^8$ CFU per ml if necessary. Dilutions were performed according to dilution factors derived from Miles and Misra counts (with the exception of *Bifidobacteria*) and are shown in Table 2.2. Dilutions for *Bifidobacteria* were performed according to previous counts generated at Cultech as the $5.8x10^8$ CFU per ml result was deemed to be a statistical outlier. Following adjustment to $1x10^8$ CFU

per ml, DMEM:F12 suspensions were then incubated anaerobically at 37°C for a further 5 hours.

Following final incubation, the DMEM:F12 bacterial suspensions were centrifuged at 3000 rpm for 10 minutes, and supernatant decanted into new universal containers. Supernatants were adjusted to an approximate pH of 7.4 with drop wise addition of NaOH, determined by subjectively matching colour to unadulterated DMEM:F12 (unpublished data generated at Cultech suggests phenol red indicator is accurate for this purpose). 1000µl of penicillin/streptomycin mixture was then pipetted into pH adjusted supernatants, which were then filter sterilised using 0.22 micron filters (Merck-Millipore, UK), collected into labelled 15ml Falcon tubes (Corning, UK) and stored at -20°C.

Table 2.2 – Volumes of DMEM:F12 bacterial suspension and DMEM:F12 used to make 10ml aliquots of cell free supernatant containing $1x10^8$ microorganisms

Condition	Mean CFU per ml at 10^{-1}	Volume of suspension	Volume of DMEM:F12
Lab4	$2.5x10^8$	4ml	6ml
Lab4b	$1x10^8$	10ml	0ml
L. salivarius	$1.6x10^8$	6.25ml	3.75ml
L. paracasei	$1.8x10^8$	5.5ml	4.5ml
Lactobacilli†	$5x10^7$	10ml	0ml
*Bifidobacteria**	$5.8x10^8$	6ml	4ml

*Supplemented with 0.05% cysteine, †*undiluted,* grows to 50% of desired CFU/ml

2.3 – Results

Miles and Misra counts

The Miles and Misra method was applied to quantify the growth of selected probiotic bacteria. All strains showed good viability, with visible colonies formed at 48 hours,

with the exception of *Bifidobacteria.* For assessment of *Bifidobacteria* growth, culture broths are frequently supplemented with 0.05% cysteine (Shah, 2000), and *Bifidobacteria* in the present study displayed visible colonies when MRS was supplemented with 0.05% cysteine. Results of colony counts in each condition assessed are presented in Table 2.3.

Table 2.3. – Colony counts at 48 hours using the Miles and Misra technique

Condition	Mean CFU per ml at 10^{-1}
L. salivarius	$1.6x10^8$
L. paracasei	$1.8x10^8$
Lactobacilli	$5x10^7$
*Bifidobacteria**	$5.8x10^8$

*Supplemented with 0.05% cysteine

Longitudinal evaluation of bacterial growth by spectrophotometry

Longitudinal spectrophotometric measurements of solutions containing bacteria used in this study were performed for 70 hours to assess growth. With the exception of the *Bifidobacteria* condition, all strains displayed approximately plateaued growth within 24 hours. However, Lab4 displayed a long, slow period of growth that continued after the cessation of linear growth. As linear growth had ceased before 24 hours, cell number was deemed to be relatively stable and usable at this time point. A representative growth curve is shown in Figure 2.2, comprehensive growth curve data can be found in appendix Figures A1-A8. MRS control wells showed no evidence of bacterial growth, indicating that environmental contamination was not a major issue.

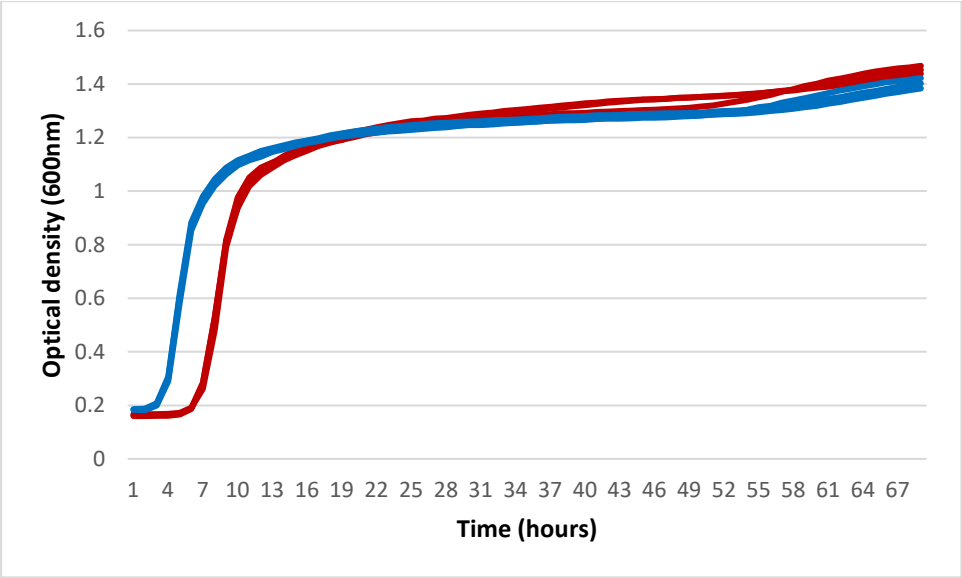

Figure 2.2. – 70-hour growth curve of L. *salivarius* CUL61 diluted to 1:100 and 1:1000 in MRS from starting inoculum. Optical density at 600nm is plotted on the Y axis in arbitrary units. Time is plotted on the X axis in hours. Each coloured line represents readings from 3 wells, 3 biological replicates were plated in technical duplicates. Blue lines represent 1:100 dilutions, red lines represent 1:1000 dilutions. Linear growth of bacteria appears to cease before 24 hours, and appears to reach a stationary phase. Growth reaches the same endpoint despite a 10-fold difference in starting material.

2.4 – Discussion

The Miles and Misra technique has been widely used to enumerate bacteria for decades, and was performed at Cultech's laboratories using established quality control methodology. However, there are potential critiques of the method. Firstly, pipetting error in the large number of required serial dilutions is a potential source of error, however 5 experimental replicates were performed to improve accuracy and should mitigate any potential errors. It is also unclear whether the growth of droplets on MRS agar is necessarily representative of growth in suspension, though the original report of the technique notes that results do not differ significantly from roll-tube agar techniques, and modern validation studies (albeit using different strains to the present study) do not find significant differences between other enumeration

methods (Naghili *et al*., 2013). The technique was used to determine a dilution factor in order to standardise each starting inoculum, but due to time constraints it was not possible to assess any potential impact on organism growth or viability when subsequently cultured in DMEM:F12 for 5 hours. Unpublished data generated previously at Cultech using these methods shows that numbers of viable Lab4 and Lab4b bacteria suspended in RPMI culture medium do not significantly differ after 5 hours of incubation. Future work is needed to ascertain whether the same is true of bacteria cultured in DMEM:F12, and whether individually cultured strains show the same viability. Further, it would be desirable to attempt to perform direct enumeration of bacteria longitudinally rather than turbidimetric measures, as turbidity does not distinguish between live and dead bacteria. However, this would be extremely labour intensive.

The dilution factors derived from enumeration via the Miles and Misra method presented a further issue. *Lactobacilli* grew to only half of the CFU per ml used for standardisation (standardised to growth of Lab4, $1x10^8$ CFU per ml). As it is uncertain what the magnitude of any effects on adipogenesis *in vitro* may be, it was decided not to dilute other conditions down to this level, but to leave the *Lactobacilli* CFS as the only condition below the level of standardisation and be mindful of this when analysing any potential results. As this work represents the early stages of establishing methods to analyse the effects of these probiotic bacteria on *in vitro* adipogenesis, it is reasonable to attempt to standardise materials on the basis of broad measures such as total cell number. It is however possible that bacterial factors which impact adipogenesis are regulated by conditions not accounted for by this simple method, and results should be interpreted cautiously.

There were also unexpected issues that arose from longitudinal growth data. *Bifidobacteria* cultured in the absence of other bacterial strains demonstrated poor growth, and data did not support the assumption that growth had plateaued by 24 hours. As a result, *Bifidobacteria* CFS was not subsequently used to investigate effects on *in vitro* adipogenesis. Despite frequent use, calibration of microplate readers for the purposes of enumerating bacteria is an area of frequent methodological oversight in the literature (Stevenson *et al*., 2016) and variables such as aperture

dimensions and cell diameter can have significant effects. Growth curve data in the present study was used to determine that linear growth ceases before or around 18 hours of incubation, and that variable volumes of starting inoculum have minimal impact on longitudinal growth, suggesting the method is robust enough to mitigate human error.

Bifidobacteria are obligate anaerobes and are routinely supplemented with cysteine, which is not a component of traditional MRS broth, to improve yields, as they are notoriously sensitive to oxygen. It is believed that cysteine acts as a reducing agent aiding recovery of oxygen-stressed bacteria (Nebra *et al*., 2002). As it was not possible to culture *Bifidobacteria* without at some point exposing them to oxygen, this may have had an impact on their viability. Further, should future work seek to incorporate *Bifidobacteria,* it may be necessary to culture each condition both in the presence and absence of cysteine to ensure cysteine supplementation does not have a subsequent effect on variables measured in 3T3-L1 cells. This would have greatly increased the complexity of the present study and contributed to the decision not to investigate the effects of *Bifidobacteria* on adipogenesis.

The data generated from the application of these techniques established dilution factors necessary to standardise the CFU/ml of CFS for all strains utilised in investigating *in vitro* adipogenesis subsequently (with the exception of L. *acidophilus*), allowing direct comparison to be made between treatment groups.

Chapter 3: Effects of bacterial cell free supernatant on viability of 3T3-L1 cells

3.1 – Introduction

As noted in the introductory chapter, numerous studies on the effects of LAB on *in vitro* adipogenesis have been published, though data on cell viability in these studies appears to be a recurrent oversight. To properly assess the impact of a treatment on adipogenesis, especially when using techniques such as ORO staining, it is necessary to show that any potential reduction observed is not simply a result of cell death. Preliminary data reported in the introductory chapter suggests that Lab4 and Lab4b CFS may be able to affect *in vitro* adipogenesis, and that the relative composition of constituent bacteria may alter the magnitude of the effect. In order to determine whether this may be an artefact of reduced viability, viability of 3T3-L1 cells cultured in CFS of Lab4, Lab4b, or their constituent bacterial strains was investigated.

A variety of methods are used for the purposes of assessing viability in cultured cells. Trypan blue staining is a longstanding traditional method that requires manual or semi-automated counting. As a result, it can be a laborious and time-consuming process which can make it unsuitable for use with a large number of experimental conditions. Tetrazolium salt based assays such as 3-(4,5-dimethylthiazol-2-yl)-2,5-diphenyltetrazolium bromide (MTT) and (3-(4,5-dimethylthiazol-2-yl)-5-(3-carboxymethoxyphenyl)-2-(4-sulfophenyl)-2H-tetrazolium) MTS give an indirect measure of cellular viability and are considered far more convenient than traditional methods. While the mechanism is not definitively understood, it is believed that in the case of MTT, reducing molecules chiefly ascribed in the literature to NADH within the mitochondria, reduce the tetrazolium compound to formazan crystals. However, certain cell free experiments have yielded results (Lim *et al*., 2015), and it is no longer believed that MTT is only reduced in the mitochondria. In the case of MTS, an intermediate electron acceptor with the capacity to penetrate viable cells, becomes reduced either within the cytoplasm or at the cell surface, and exits the cell, subsequently converting the tetrazolium compound to soluble formazan (Riss *et al*.,

2013). Evidence suggests that MTS may have a limited capacity to enter cells without the presence of an intermediate electron acceptor, and has some capacity to be reduced at the cell surface (Berridge *et al*., 2005).

3.2 – Materials and methods

A list of reagents used, and their suppliers is given in Appendix 1, Table 1. 3T3-L1 cells were a generous gift from Dr. Lei Zhang and were originally obtained from the American Type Culture Collection (Atlanta, USA).

Media preparation

For preparation of complete medium, DMEM:F12 was supplemented with 10% foetal calf serum (FCS), 2% penicillin/streptomycin, 1% pyruvate, and 1.5% bicarbonate, and stored in sterile universal bottles at 4˚C.

Differentiation medium was prepared with some modifications to the classical method (Student, *et al.* 1980) more similar to Zhang *et al*. (2009). Differentiation medium was routinely prepared in a 2x concentration according to Table 3.1. Initially, 9ml of DMEM:F12 was pipetted into a universal container. 80ml of DMEM:F12 was pipetted into a sterile universal bottle, and penicillin/streptomycin, pyruvate, bicarbonate, and FCS were added via pipette in the volumes given in Table 3.1. Biotin, pantothenate, tri-iodothyronine, hydrocortisone, pioglitazone, and insulin were added via Gilson pipette to the 9ml volume of DMEM:F12 in the volumes given in table 3.1. The contents of the universal container were then passed through a 0.22 micron filter into the universal bottle to produce the 2x concentrated differentiation media.

Complete or differentiation media were diluted 1:1 with either DMEM:F12 or CFS (produced as described in chapter 2.2) and warmed to 37˚C in a heated water bath before use.

Table 3.1 – Composition of standard 2x concentration differentiation media

Component	Volume
DMEM	44.5 mls
Ham`s F12	44.5 mls
Biotin (33µM)	64 µl
Pantothenate (17µM)	200 µl
Tri-iodothyronine (1nM)	1.4 µl
Hydrocortisone (1µM)	20 µl
Pioglitazone (1µM)	20 µl
Insulin (500nM)	570 µl
Penicillin/Streptomycin	4 mls
Pyruvate	2 mls
Bicarbonate	3 mls
FCS	10 mls

Routine cell culture

All cells were routinely incubated in conditions of 37˚C, 5% CO_2 in air.

Trypsinisation of cells

Trypsin IX and complete media were warmed to 37˚C in a heated water bath. Media was aspirated via suction from sub-confluent cells within tissue flasks. Trypsin was added to culture flasks via pipette at the appropriate volume (3ml for T25 flasks, 5ml for T75 flasks) and cells incubated and periodically agitated by gently tapping the sides of the flask and visually assessed by light microscopy to determine when cells had fully detached. Trypsin was then quenched in an equal volume of complete media, cell suspensions pipetted into a universal container, and centrifuged at 1000RPM for 5 minutes. Following centrifugation, media was aspirated without disturbing cell pellets, and gently resuspended by pipette in complete media at the

desired volume (4ml for T25 flasks, 8ml for T75) before being seeded into culture flasks.

Cryopreservation of cells

A "freezing mix" comprised of 90% FCS and 10% dimethyl sulfoxide was prepared and passed through a 0.22 micron filter into a universal container. Cells were trypsinised as above, but cell pellets resuspended in 1ml aliquots of freezing mix via Gilson pipette. Cell suspensions in freezing mix were pipetted into Nalgene cryovials (Fisher Scientific, UK), and stored in a "Mr. Frosty" freezing container (Fisher Scientific, UK) containing 100% isopropyl alcohol at -80˚ for 48 hours before being transferred to liquid nitrogen storage.

Thawing of cryopreserved cells

Cryovials were immersed in a water bath heated to 37˚C such that cell suspensions were just below the water line. Cryovials were checked visually until all ice crystals had nearly thawed. Cryovials were then introduced to a class 2 laminar flow hood and contents poured into a pre-prepared 10ml aliquot of complete media. Cryovials were then washed out with complete media via pipette to ensure maximal cell recovery, and centrifuged at 10000 RPM for 5 minutes. Media was aspirated via suction without disturbing cell pellets, and pellets were gently resuspended by pipette in complete media at the desired volume (4ml for T25 flasks, 8ml for T75) before being seeded into culture flasks.

Cell culture – trypan blue staining

Cryopreserved 3T3-L1 cells at passage 14 were thawed and seeded into a T25 flask as previously described and maintained in undiluted CM until approximately 70% confluent. Cells were trypsinised as previously described and seeded at approximately 100,000 cells per well in 12-well plates and maintained in 1ml undiluted CM per well until 80-90% confluent. Media was replaced in post-confluent cells in triplicate wells in treatment conditions listed in Table 3.2.

CFS was prepared as described in chapter 2.2. Initiation of treatment was designated as day 0, media was changed every 48 hours or sooner if subjective assessment of phenol red indicator was deemed acidic. Trypan blue staining was performed on day 10.

Table 3.2 – Assessment of viability of 3T3-L1 cells in various culture conditions using trypan blue exclusion.

Condition	Composition
CM	Complete media diluted 1:1 with DMEM:F12
DM	Differentiation media diluted 1:1 with DMEM:F12
DM + Lab4	Differentiation media diluted 1:1 with Lab4 CFS
DM+ Lab4b	Differentiation media diluted 1:1 with Lab4b CFS

Cell culture – MTS assay

Cryopreserved 3T3-L1 cells at passage 14 were seeded into a T25 flask and maintained in CM until approximately 70% confluent. Cells were trypsinised and seeded at approximately 50,000 cells per well in 24-well plates and maintained in 0.5ml CM per well until 80-90% confluent. Media was replaced in post-confluent cells in triplicate wells in treatment conditions listed in Table 3.3.

CFS was prepared as previously. Initiation of treatment was designated as day 0, media was changed every 48 hours or sooner if subjective assessment of phenol red indicator was deemed acidic. MTS assay was performed at 72 hours.

Table 3.3 – Assessment of viability of 3T3-L1 cells in various culture conditions using MTS assay.

Condition	Composition
CM	Complete media diluted 1:1 with DMEM:F12
CM + Lab4	Complete media diluted 1:1 with Lab4 CFS
CM + Lab4b	Complete media diluted 1:1 with Lab4b CFS
CM + *L. salivarius*	Complete media diluted 1:1 with *Lactobacillus salivarius* CUL61 CFS
CM + *L. paracasei*	Complete media diluted 1:1 with *Lactobacillus paracasei* CUL08 CFS
CM + *L. acidophilus*	Complete media diluted 1:1 with *Lactobacillus acidophilus* CUL21 and CUL60 CFS

Trypan blue staining and cell counting

Cells were cultured as described previously. Media was aspirated and 0.5ml trypsin pipetted into each well. Plates were incubated at 37˚C and gently agitated periodically to ensure cells fully detached. Trypsinised cells were stained with 1 part trypan blue 0.4% (Sigma-Aldrich) to 1 part trypsin, and 20µl of suspension pipetted into the counting chamber of a Cellometer PD100 slide (Cellometer, UK). Slides were imaged in a Cellometer Auto T4 (Cellometer, UK). Automatic counts were generated and manually adjusted to give correct numbers of stained and unstained cells for all optic fields.

MTS Assay

CellTiter 96® AQ_{ueous} One Solution Cell Proliferation Assay (referred to for convenience as MTS) was obtained from Promega (Promega, UK). At 72 hours, treatment media was aspirated, each well washed once with 1ml PBS, PBS aspirated via suction, and replaced with complete media (diluted 1:1 with DMEM:F12) at a volume of 200µl per well. Equal volume of media was also pipetted into 3 cell-free

"blank" wells. 40µl of MTS solution was pipetted into each well and incubated for one hour at 37˚C, 5% CO_2. Following incubation, 100µl of solution was transferred by pipette into a 96 well microplate, and optical density measured at 490nm in a Dynex Opsys microplate reader. Values for cell-free blank wells were subtracted from readings to obtain final optical density readings.

Statistics

Statistical analysis throughout this thesis was performed with IBM SPSS statistics version 23 (IBM Corporation, New York). Statistical outliers were identified using built-in SPSS functions and manually removed from data before analysis. Data in text are presented as mean ± SD, data in graphs is presented as mean ± SEM for legibility.

3.3 – Results

Trypan blue staining and cell counting

Post-confluent 3T3-L1 cells were maintained in CM or DM diluted 1:1 with DMEM:F12, or DM diluted 1:1 with CFS of Lab4/Lab4b for 10 days. Trypan blue staining was performed, and viability expressed as unstained cells as a percentage of total number of cells (shown in Figure 3.1). Treatment with DM + DMEM:F12 appeared to result in mild cytotoxic effects (78.3% ± 9.4% viability), but DM in conjunction with Lab4 or Lab4b had a more pronounced cytotoxic effect (57.8% ± 6.3% And 55.2% ± 10.7% viability respectively). Data are also presented expressed as untransformed total viable cell counts in Figure 3.2.

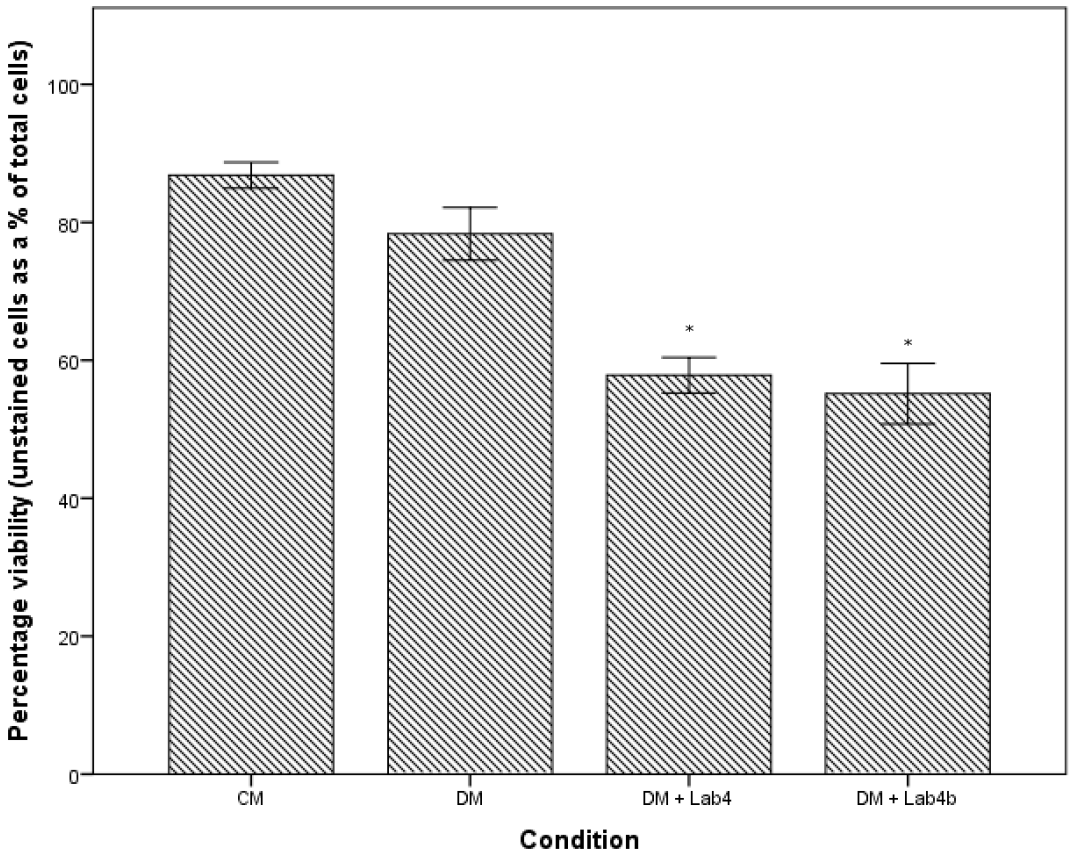

Figure. 3.1. – Cell viability assessed by trypan blue staining in 3T3-L1 cells after 10 days, expressed as a percentage of total cells. 3T3-L1 cells were maintained in either CM diluted 1:1 with DMEM:F12 (CM), DM diluted 1:1 with DMEM:F12 (DM), or DM diluted 1:1 with Lab4 or Lab4b CFS (DM + Lab4 and DM + Lab4b). Treatment with Lab4 or Lab4b resulted in significantly reduced percentage of viable cells (p=0.002 and p=<0.001 respectively) compared to DM control. Experiments were performed in triplicate wells, bars represent the mean of 2 individual experiments, error bars represent SEM. Asterisk denotes significant difference at p=<0.05 from DM.

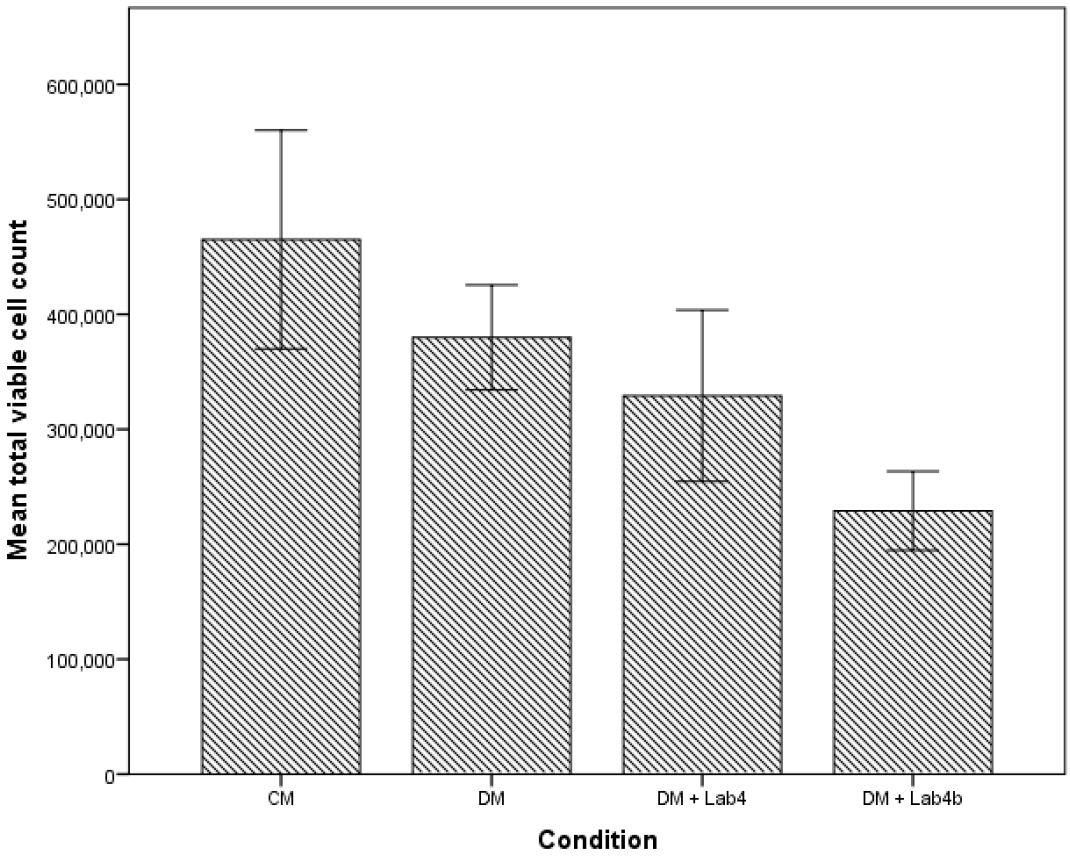

Figure. 3.2 – Cell viability assessed by trypan blue staining in 3T3-L1 cells after 10 days, expressed as total viable cells. 3T3-L1 cells were maintained in either CM diluted 1:1 with DMEM:F12 (CM), DM diluted 1:1 with DMEM:F12 (DM), or DM diluted 1:1 with Lab4 or Lab4b CFS (DM + Lab4 and DM + Lab4b respectively). No treatment condition resulted in significantly different numbers of total viable cells. Bars represent the mean of 2 individual experiments, error bars represent SEM.

One-way between subjects ANOVA tests were conducted on untransformed data of total viable cell counts, and no significant differences were observed between conditions at p=<0.05 (F (3,20) = 2.179, p=0.122).

One-way between subjects ANOVA tests were also conducted on transformed data (viable cells as a percentage of total cell counts). There was a significant effect of the media used on the percentage of viable cells at p=<0.05 (F (3,20) = 21.822, p=<0.001). Post-hoc comparisons using the Tukey HSD test indicated no significant difference between percentage of viable cells between CM + DMEM:F12 (86.833% ± 4.579%)

and DM + DMEM:F12 (78.333% ± 9.374%, p=0.297), but that percentage of viable cells was significantly lower after treatment with DM diluted 1:1 with Lab4 (57.833% ± 6.306%, p=0.002) or Lab4b CFS (55.167% ± 10.741%, p=<0.001) than DM + DMEM:F12.

MTS assay

Post-confluent 3T3-L1 cells were treated for 72 hours with CM diluted with CFS of several bacterial strains. At 72 hours, a spectrophotometric MTS assay was performed, results of which are shown in Figure 3.3. When assessed by MTS assay, treatment of 3T3-L1 cells with CFS did not appear to negatively impact cell viability, though Lab4 treatment appeared to have a more variable effect than other treatments. All conditions except for CM + Lab4b (96.8% ± 3.56%) reported greater values than control.

One-way between subjects ANOVA tests were conducted on spectrophotometric data (corrected by subtracting the average value of 3 cell free blank wells), and no significant differences were observed between conditions at p=<0.05 ($F(5,27) = 2.029$, p=0.106).

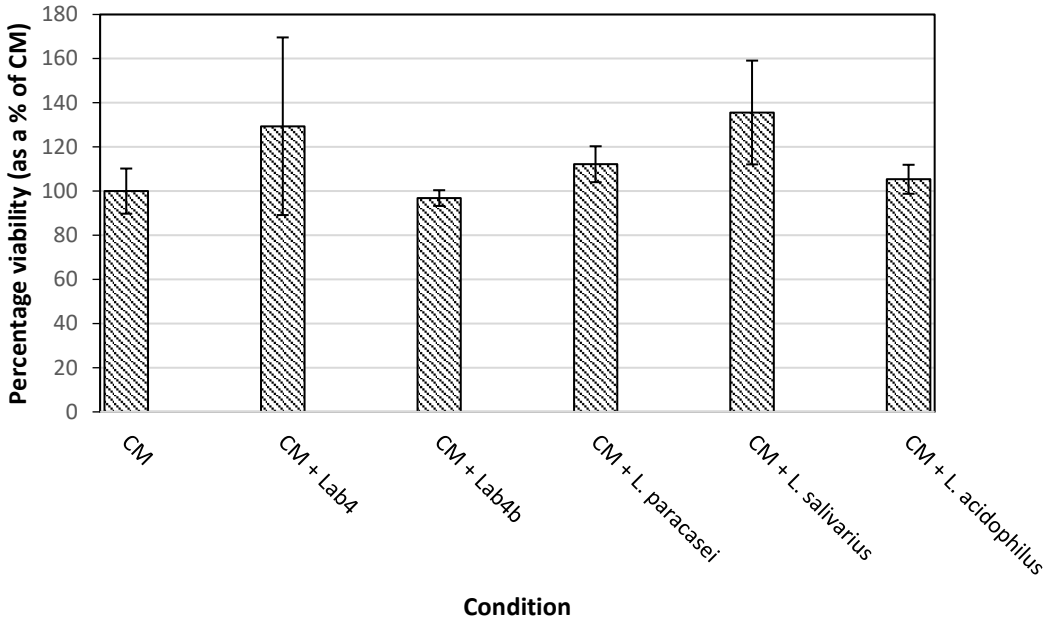

Figure. 3.3 – Cell viability assessed by MTS assay in 3T3-L1 cells after 72 hours, expressed as a percentage of control. 3T3-L1 cells were maintained in either CM diluted 1:1 with DMEM:F12 (CM), or CM diluted 1:1 with CFS of Lab4, Lab4b, *L. paracasei*, *L. salivarius*, or *L. acidophilus*. No treatment condition assessed by MTS was significantly different than control, though most showed non-significant mean increases. Bars represent the mean of 2 individual experiments, error bars represent SEM.

3.4 – Discussion

Cell viability measured via trypan blue exclusion assay is non-significantly decreased in DM, and further significantly reduced in the presence of Lab4 or Lab4b CFS. This significance is only achieved when data is expressed as viable cells as a percentage of total cells, which may be a result of error distortion. However, when measured indirectly via MTS assay results in most conditions seem to indicate an increase in cell number and/or activity. It should also be noted that the MTS assay utilised only complete media due to concerns that differentiation media may affect proliferation, as tetrazolium salt based assays are also used for indirect measures of proliferation. Acute exposure in CM may not be reflective of chronic exposure in DM. Differences

in data may be accounted for by a functional change in differentiating 3T3-L1 cells, and more study is needed to reconcile these data sets.

A prior study using the progenitor 3T3 fibroblast cell line categorised cytotoxicity data (generated via MTT assay) as: non-cytotoxic (>90% of control), slightly cytotoxic (60-90% of control), moderately cytotoxic (30-59% of control), and severely cytotoxic (<30% of control) (Basak *et al*., 2016). Though data in the present study is limited, it is reasonable to suggest that there is some cytotoxic effect of the use of bacterial CFS generated from the Lab4 consortium in 3T3-L1 cells, but that the true magnitude of this effect requires more investigation. Unfortunately, due to time constraints, it was not possible to perform trypan blue exclusion assays on all treatment conditions.

The clearly discordant data between both viability assays used suggests either a striking difference between CM and DM conditions and/or exposure times, or potentially some alteration of the redox state of whichever cellular components interact with MTS and/or its intermediate electron acceptor. The “browning” of adipocytes has recently been proposed as a mechanism to alleviate redox pressure (Jeanson *et al*., 2015), and treatment of murine primary white adipocytes with lactate induces an increase in the NADH:NAD ratio (Carrière *et al*., 2014), which may confer an increased ability to reduce MTS and/or its intermediate electron acceptor. MTS assays were shown to be useful in the study of NADH and NADPH reducing activity in cell free studies shortly after its introduction for use in measuring cell viability (Dunigan *et al*., 1995). Recent data generated at Cultech (unpublished) indicates that CFS of certain bacterial strains may have antioxidant capacity, which is a possible explanation. However, cells were washed in PBS and media replaced with CM diluted with DMEM:F12, so carryover of significant quantities of CFS is unlikely. As the composition of the CFS used in the present study is as yet uncharacterised, only speculative hypotheses can be derived from this data, however the presence of lactate may explain these results and is highly likely to be present. Other strains of *L. acidophilus* have previously been shown to efficiently produce lactic acid when cultured in MRS broth (Juárez Tomás *et al*., 2003). Phenol red indicator showed CFS to be at a pH of approximately 7.4. Under these conditions, a majority of lactic acid is believed to be present in its dissociated form, lactate (Lampe *et al*., 2009).

Statistical significance is not necessarily practical significance in cell biology. Since the widespread adoption of formazan based assays, cytotoxicity data is typically reported as a percentage of control, and analysed on this basis. In the present study, cytotoxicity assays utilised only two individual experiments plated in triplicate, and data collected is therefore not particularly large or robust. Statistical significance was only achieved with transformation of data to a percentage, which is open to methodological criticism. However, the practical significance of a reduction of viable cells measured by trypan blue staining to between 50-60% is potentially large, and may impact data generated using these cells.

Murine adipocytes and 3T3-L1 cells possess TLR9 receptors. TLR9 can be activated by unmethylated CpG dinucleotides (Ashkar and Rosenthal, 2002), which are abundant in bacterial genomes, though stimulation of TLR9 by bacterial DNA shows species dependent effects on activation (Dalpke *et al*., 2006). Batra *et al*. (2007) showed significantly increased interleukin-6 release in adipocytes from wild type mice stimulated with a TLR9 ligand, while no such increase was seen in 3T3-L1 adipocytes. Batra *et al*. also reported that the TLR2 ligand zymosan did not appear to significantly stimulate interleukin-6 production in either wild type murine or 3T3-L1 preadipocytes and adipocytes. It may be that the doses used in Batra *et al*. were not sufficient, but it appears to suggest that in 3T3-L1 cells, these TLRs are relatively insensitive. The presence of bacterial DNA and lipoteichoic acid, which could stimulate TLR9 and 2 respectively, have not been confirmed in CFS produced using methods in the present study, as their composition remains unknown. However, they are potential candidate components that could impact cell viability. In future study it would be beneficial to ascertain any dose-response effect of CFS on 3T3-L1 cell viability, and determine its cause.

MTS assay and potentially other assays based on the reduction of a tetrazolium salt to formazan may be unsuitable for assessing cytotoxicity of bacterial CFS in 3T3-L1 cells. The effects of acute exposure in cells maintained in CM may not reflect the effects of chronic exposure in differentiating cells. Classical cell viability assays are recommended for future study as treatment may influence redox state.

Chapter 4: Effects of bacterial cell free supernatant on adipogenesis in 3T3-L1 cells

4.1 – Introduction

Preliminary data discussed in the introductory chapter indicates a potential effect of Lab4 and Lab4b CFS to reduce adipogenesis in 3T3-L1 cells. However, data generated in the present study suggests that this effect may be at least partially accounted for by changes in cell viability induced by treatment with CFS. Subjective visual analysis of images of ORO stained 3T3-L1 cells treated with Lab4 or Lab4b CFS generated by Erika Galgóczi suggested that adipogenesis in cells surviving cytotoxic effects of treatment exhibited features of enhanced adipogenesis, in particular differentiation was accelerated compared with DM controls. As Lab4 and Lab4b are multi-strain products, further investigation was warranted to determine whether a particular bacterial strain mediates potential effects on adipogenesis. Investigations into effects of Lab4 and Lab4b CFS on adipogenesis measured via ORO staining were repeated, alongside additional experiments utilising CFS of the *L. acidophilus* strains present in Lab4 in an attempt to identify whether any constituent strains were responsible for different effects seen in Lab4 and Lab4b treatment in preliminary data.

Various methods are routinely employed to assess adipogenesis in 3T3-L1 cells, both qualitative and quantitative. Qualitative methods include visual assessment by light microscopy to identify features such as morphologic changes characteristic of differentiating cells, such as “rounding off” and the accumulation of lipid droplets. Quantitative methods include ORO staining and dye extraction, as previously described, and qPCR quantification of gene transcripts whose expression is associated with particular temporal stages or functions of adipogenesis. Temporal regulation of adipogenesis is covered in chapter 1.1, but the process broadly occurs in 4 contiguous stages: growth arrest, MCE, early differentiation, and finally terminal differentiation. Induction of PPARγ and C/EBPα is considered to be a marker of early differentiation (Ntambi and Kim, 2000), whereas genes such as GPDH have long been used as markers of terminal differentiation (Darimont *et al*., 1993). qPCR is frequently

used to assess not just the presence of these markers, but their quantities. qPCR is frequently applied to cell biology in two different forms. Relative quantification of gene transcripts entails comparing the expression of a gene in an experimental condition relative to the expression in control. This technique allows for the fast generation of data and semi-quantitative analysis of the degree of change induced by experimental conditions, reported as "fold change". However, application of relative qPCR has disadvantages, notably that by measuring only relative change, small changes in genes expressed at a low level appear the same as large changes in highly expressed genes. Absolute quantification via qPCR avoids this, but is a comparatively more laborious technique, requiring external standards for the construction of a standard curve to compare against. Quantification by qPCR also requires a reference gene that is stably expressed through the time course of differentiation. As mentioned in the introductory chapter, numerous studies of the effects of bacteria on *in vitro* adipogenesis have utilised unsuitable reference genes, and application of the technique requires careful consideration of many factors. Data previously generated in our laboratory suggests that ARP is stably expressed during differentiation and has been frequently used as a reference gene in 3T3-L1 cells in data generated by this research group (Zhang *et* al., 2009; Draman *et al*., 2013).

4.2 – Materials and methods

A list of reagents used, and their suppliers is given in Appendix 1, Table 1. Media was prepared as in chapter 3.2.

Cell culture – 3T3-L1 adipogenesis experiments

Cryopreserved 3T3-L1 cells at passage 14 were seeded into a T25 flask as described in chapter 3.2 and maintained in undiluted CM until approximately 70% confluent. Cells were trypsinised as described in chapter 3.2 and seeded at approximately 100,000 cells per well in 12-well plates and maintained in 1ml undiluted CM per well until 80-90% confluent. Media was replaced in post-confluent cells in triplicate wells

using either CM or DM diluted 1:1 with CFS (as in treatment conditions listed in Table 3.3) or diluted with DMEM:F12 for control.

Initiation of treatment was designated as day 0, media was changed every 48 hours or sooner if subjective assessment of phenol red indicator was deemed acidic. RNA extraction was performed on day 10, ORO staining was performed on days 3, 6, and 9.

ORO staining

ORO was prepared on the day of each experiment at the designated timepoint. 0.125g of ORO powder was weighed and placed in a universal container containing 25ml 100% isopropanol, then thoroughly vortexed to produce a 0.5% stock solution. 12ml of ORO stock solution was pipetted into a separate universal container containing 8ml distilled water to produce a working solution, and left to stand for 15 minutes at room temperature. ORO working solution was then filtered through Whatman No. 1 filter paper and protected from light.

Media was aspirated from cells, which were subsequently washed with 1ml PBS per well. PBS was aspirated, cells were fixed by pipetting 500µl 60% isopropanol into each well and left for 10 minutes before aspirating and washing with PBS again. 100µl of ORO working solution was pipetted into each well and incubated for 15 minutes at room temperature. Following incubation, cells were rinsed in 1ml 60% isopropanol, followed by 1ml of water, and imaged (Nikon Diaphot Microscope, Nikon) at 10x magnification by light microscopy using ViewFinder software (version 3.0.1, Better Light Inc., California, USA). Following imaging, cells were rinsed in 1ml 60% isopropanol once, then 1ml distilled water 4 times. Following the final distilled water rinse, water was aspirated and 200µl 100% isopropanol was pipetted into each well and incubated at 37˚C for 10 minutes. After incubation, contents of each individual well were mixed gently by pipetting then transferred into 96 well microplates. Optical density at 490nm was read in a Dynex Opsys MR microplate reader (Aspect Scientific, Cheshire, UK) using Dynex Revelation 4.24 software. Blank values were subtracted from data before analysis.

RNA extraction

Media was aspirated from all wells, cells washed in 1ml PBS, then aspirated. 1ml of tri-reagent was pipetted directly into each well and gently mixed by pipetting ensuring no bubbles formed until all cells were visibly detached from plates. Samples were transferred to labelled Eppendorf tubes and stored at -80˚C for 24 hours. After 24 hours, cell lysates were incubated at room temperature until thawed, 200µl of chloroform pipetted into each Eppendorf tube, and vigorously hand shaken for one minute. Eppendorf tubes were incubated at room temperature for 3 minutes, then centrifuged at 13000 RPM for 15 minutes at 4˚C.

Following centrifugation, the upper aqueous phase was transferred by pipette to a new Eppendorf tube, and 500µl isopropanol added by pipette. Eppendorf tubes were then incubated at room temperature for 10 minutes before further centrifugation at 13000 RPM for 15 minutes at 4˚C. Liquid was decanted and Eppendorf tubes blotted upside down on absorbent paper. 1ml of 75% ethanol was pipetted into each Eppendorf and briefly agitated by vortex mixing to wash RNA pellets. Eppendorf tubes were then centrifuged at 8600 RPM for 5 minutes at 4˚C.

Following final centrifugation, liquid was decanted and Eppendorf tubes air dried upside down on absorbent paper for 10 minutes, following which fluid droplets were removed by pipette ensuring not to disturb the pellet area. 6µl of molecular biology grade water was added to each Eppendorf tube before being briefly vortex mixed and pulled down by centrifuge 3 times. RNA was then stored at -80˚C until use.

Reverse transcription

RNA was thawed on ice, and then briefly vortex mixed and pulled down by centrifuge. 1µl of RNA was then measured using a Nanodrop Lite spectrophotometer (Thermo Fisher, UK) and ratio of absorbance at 260nm:280nm and concentration recorded. A 260nm:280nm absorbance ratio of ~2 was used as a measure of pure RNA. RNA samples were diluted with molecular biology grade water to a total of 1000ng RNA in

6µl water in Micro Eppendorf tubes, or undiluted if RNA yields were too low to achieve 1000ng.

Micro Eppendorf tubes were placed in a heating block at 60˚C for 10 minutes then immediately transferred to ice for 5 minutes to prevent secondary structure reformation. A master mix for reverse transcription was prepared according to Table 4.1 (multiplied as required) and was added to each Micro Eppendorf tube. Micro Eppendorf tubes were vortex mixed and pulled down by centrifugation twice, then transferred to a thermocycler programmed for incubation at 37˚C for one hour, 95˚C for 5 minutes, and then cooled to 4˚C before resulting cDNA was stored at -20˚C until use.

Table 4.1. – Volumes of reagents used for reverse transcription master mix per single experiment

Volume	Reagent
4µl	dNTPs (2mM)
4µl	Oligo dT Primer
4µl	5x Buffer
1µl	RNAse Inhibitor
1µl	Reverse Transcriptase

Production of standards for qPCR

3T3-L1 cells were cultured as described previously for trypan blue exclusion assay in chapter 3.2, but using undiluted CM and DM in cells seeded on 6-well plates. Post-confluent cells were cultured in DM for 7 days. At day 7, RNA was extracted, and reverse transcribed as described previously. A master mix for polymerase chain reaction (PCR) was prepared using cDNA generated with volumes according to Table 4.2 (multiplied as necessary). Forward primer used for ARP used the sequence GAGGAATCAGATGAGGATATGGGA, reverse primer used the sequence AAGCAGGCTGACTTGGTTGC. Forward primer for GPDH used the sequence ATGCTCGCCACAGAATCCACA, reverse primer used the sequence AACCGGCAGCCCTTGACTTG.

24µl of master mix was pipetted into Micro Eppendorf tubes stored on ice, 1µl cDNA added by pipette, and transferred to a thermocycler programmed according to Table 4.3.

Table 4.2. – Volumes of reagents used for polymerase chain reaction master mix per single experiment

Volume	Reagent
0.5µl	dNTPs (2mM)
2.5l	10x Buffer
1.5µl	$MgCl_2$
0.5µl	Forward + reverse primer mix
0.125µl	Amplitaq Gold Polymerase
18.875µl	Molecular biology grade water

Table 4.3. – Thermocycler settings for polymerase chain reaction.

Step		Temperature	Time
Initial denaturation		95	10 min
PCR cycles (40)	Denature	95	15 sec
	Anneal	60	30 sec
	Extend	72	30 sec
Final extension		72	5 min
Hold		4	indefinitely

Agarose gel was prepared by heating 2g agarose and 5µl ethidium bromide in 100ml 1x TAE buffer in a microwave until a clear solution was formed, then poured into moulds and allowed to set. PCR products were added to load dye (Promega, UK) in a 5:1 proportion and subjected to gel electrophoresis submerged in 1x TAE buffer supplemented with 5µl ethidium bromide per 100ml at 100v for 30 minutes. Gels were assessed under UV light for expected amplicon size (72bp and 124bp for ARP and GPDH respectively) against 100bp molecular ladders. PCR products were excised from gel bands and resultant DNA purified using the Wizard SV Gel and PCR Clean-Up System (Promega) according to manufacturers' instructions to remove unincorporated dNTPs and primers.

DNA was measured using a Nanodrop Lite spectrophotometer and absorbance ratio at 260nm:280nm and concentration recorded. Using amplicon sequence length and the assumption of an average base pair weight of 650 Daltons, number of copies per µl was estimated using the calculation:

$$\text{No. of copies} = (\text{ng of DNA X } (6.022 \text{ X } 10^{23})) / (\text{amplicon length x } 1x10^{9} \text{ x } 650)$$

These samples were then used to construct a standard curve for absolute qPCR quantification, using serial dilutions to obtain standards for $x10^{2}$ – $x10^{6}$.

qPCR quantification of gene transcripts in 3T3-L1 cells

3T3-L1 cells were cultured, RNA extracted, and reverse transcribed as described above. A qPCR master mix was prepared according to Table 4.4 (multiplied as necessary). ARP was used as a reference gene and transcripts of GPDH expressed per 1000 ARP transcripts. Primer sequences for ARP and GPDH are as given previously.

Table 4.4. – Volumes of reagents used for qPCR master mix per single experiment

Volume	Reagent
12.5µl	Platinum SYBR Green qPCR SuperMix-UDG
0.5µl	Forward + reverse primer mix
11µl	Molecular biology grade water

24µl of master mix was pipetted into 96 well lidded qPCR plates and 1µl cDNA added, plated in technical duplicates per each biological replicate. Technical duplicates of standards produced as described previously were also plated between 10^2 and 10^6 on each plate to construct standard curves. Plates were centrifuged for 3 minutes at 1000 RPM and then ran on a Stratagene MX3000 light cycler (Stratagene, California) for 40 cycles, temperatures and timings programmed per Table 4.5. Results were analysed using MxPro version 4.10 (Stratagene, California) and dissociation curves examined to ensure no primer-dimer formation. Comparison against standard curves allowed estimation of absolute transcript numbers, ARP was utilised as a reference gene and results are expressed as gene transcript copy numbers per 1000 ARP transcripts.

Table 4.5. – Temperatures and duration of an individual cycle used in qPCR protocol

Segment	Temperature	Duration
Initial denaturation	95˚C	2 minutes
Denature	95˚C	15 seconds
Anneal	60˚C	30 seconds
Final extension	72˚C	5 minutes
Final hold	10˚C	Indefinitely

4.3 – Preliminary data

Oil Red O data

ORO staining of 3T3-L1 cells was performed by Erika Galgóczi during late adipogenesis in three independent experiments (day 7 in the first instance, day 8 in the latter two) in 12 well plates following the methods described prior. Dye was extracted in isopropanol, and optical density measured via spectrophotometry at 490nm. One-way between subjects ANOVA tests were conducted in both complete and differentiation medium (CM and DM respectively) diluted 1:1 with Lab4 or Lab4b CFS, with results compared to CM/DM diluted 1:1 with DMEM:F12 as appropriate for control.

In DM, there was not a significant effect of the use of CFS observed at p=<0.05 (F (2,15) = .267, p=0.769), though both Lab4 and Lab4b treatment conditions did show a nonsignificant mean decrease compared to DM control. However, in complete medium, there was a significant effect of the use of CFS observed at p=<0.05 (F (2, 15) = 6.194, p=0.011) compared to CM control (results shown in Figure 4.1). Post hoc comparisons using the Tukey HSD test indicated a significant difference (p=0.021) in mean optical density at 490nm in cells cultured with CM diluted 1:1 with Lab4b CFS (0.427 ± 0.109) compared to control (0.275 ±0.772). A significant (p=0.024) difference was also observed in optical density at 490nm between CM + Lab4b and CM + Lab4 (0.276, ±0.670) groups. However, CM and CM + Lab4 groups did not differ significantly (p=1). Despite this increase in adipogenesis in CM + Lab4b, levels of

adipogenesis were markedly lower than in DM conditions, indicating that adipogenesis was strongly induced by DM treatment. In summary, this preliminary data suggests that Lab4 and Lab4b CFS may affect differentiation of adipocytes, with increased adipogenesis shown in complete (basal) medium, and a non-significant decrease in adipogenesis seen in DM.

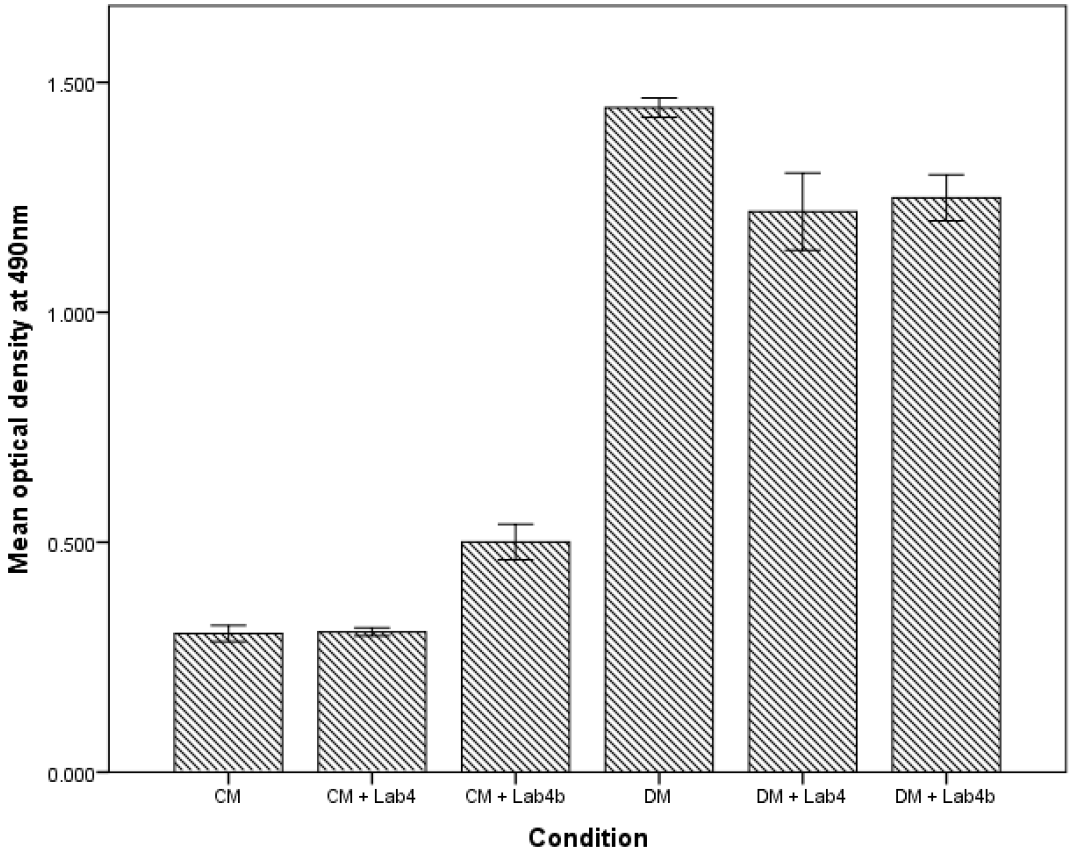

Figure 4.1. – Quantification of ORO staining of 3T3-L1 cells treated with DM diluted 1:1 with Lab4/b cell free supernatant after 7/8 days. Y axis represents absorbance at 490nm (arbitrary units), with conditions grouped along the X axis. Experiments were performed in duplicate wells, bars represent the mean of 3 individual experiments. Error bars represent SEM. CM = Complete media, CM + Lab4 = Complete media diluted 1:1 with Lab4 CFS, CM + Lab4b = Complete media diluted 1:1 with Lab4b CFS. DM = Differentiation Media diluted 1:1 with DMEM:F12, DM + Lab4 = Differentiation media diluted 1:1 with Lab4 CFS, DM + Lab4b = Differentiation media diluted 1:1 with Lab4b CFS.

Visual assessment of 3T3-L1 cells during these experiments indicated that those treated with Lab4 or Lab4b appeared to be in a more advanced stage of adipogenesis at the same timepoints. Experiments were repeated using a timepoint of 48 hours of treatment to represent early adipogenesis. In DM, there was not a significant effect of the use of CFS observed at p=<0.05 (F (2,9) = 1.871, p=0.209), though both Lab4 and Lab4b treatment conditions did show a nonsignificant mean increase compared to DM control. Similar results were yielded in CM, with no significant differences observed at p=<0.05 (F (2,5.547) = .794, p=0.298), these data violated the assumption of homogeneity of variances necessitating a Welch F test. Results are summarised in Figure 4.2.

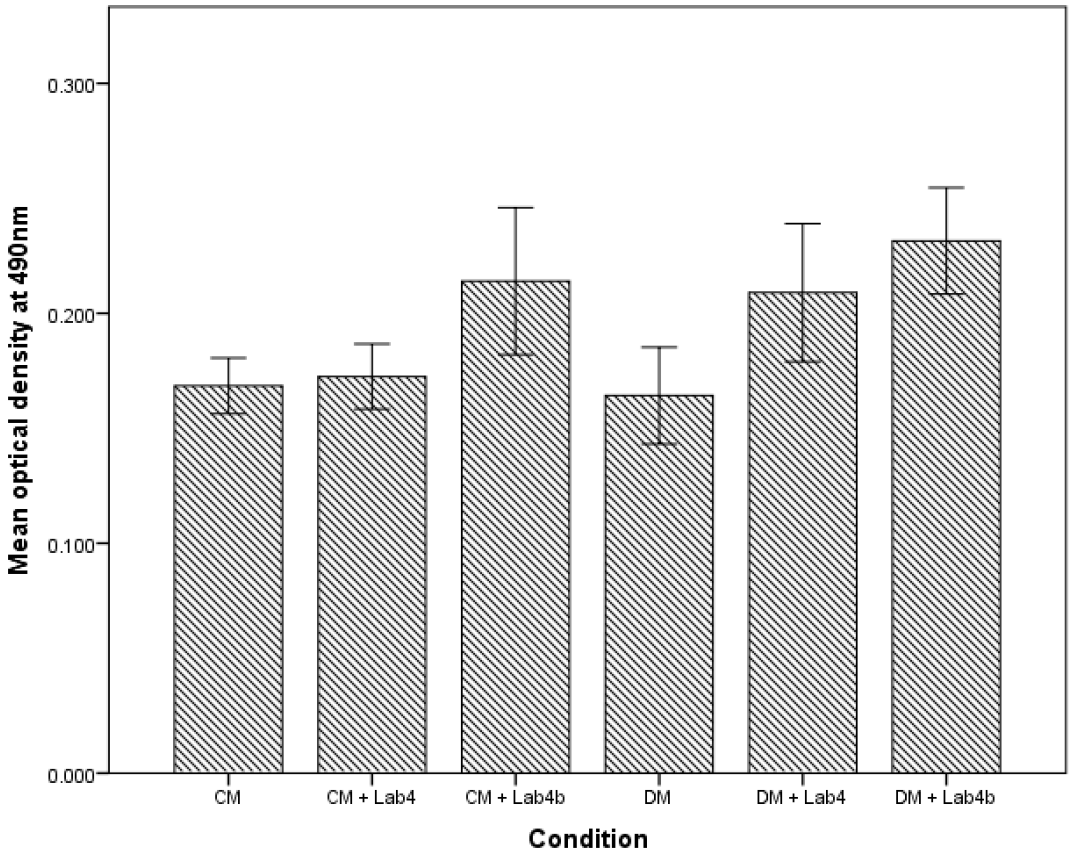

Figure 4.2. – Quantification of ORO staining of 3T3-L1 cells treated with DM diluted 1:1 with Lab4/b cell free supernatant after 48 hours. Y axis represents absorbance at 490nm (arbitrary units), with conditions grouped along the X axis. Experiments were performed in duplicate wells, bars represent the mean of 3 individual

experiments. Error bars represent SEM. CM = Complete Media, CM + Lab4 = Complete media diluted 1:1 with Lab4 CFS, CM + Lab4b = Complete media diluted 1:1 with Lab4b CFS. DM = Differentiation media, DM + Lab4 = Differentiation media diluted 1:1 with Lab4 CFS, DM + Lab4b = Differentiation media diluted 1:1 with Lab4b CFS.

qPCR data

Following the results gathered from ORO staining, the extent of adipogenesis in 3T3-L1 cells treated with the Lab4 consortium was investigated on a transcriptional level using GPDH as a marker of terminal differentiation normalised to expression of acidic ribophosphoprotein (ARP) as previously used in our laboratory (Draman *et al*., 2013). In brief, a single experiment was performed in which 3T3-L1 cells were plated in duplicate on 12 well plates and maintained in CM until confluent. Post-confluent cells were then maintained for 7 days in CM or DM diluted 1:1 with Lab4 or Lab4b CFS, with CM/DM diluted 1:1 with DMEM:F12 for control as appropriate (full methods are given in chapter 2). RNA was extracted and reverse transcribed, and transcript copy numbers of target genes were measured using SYBR green and a Stratagene MX3000 light cycler (La Jolla, California). Quantification of GPDH transcripts as a marker of terminal differentiation yielded a different pattern of results to ORO staining.

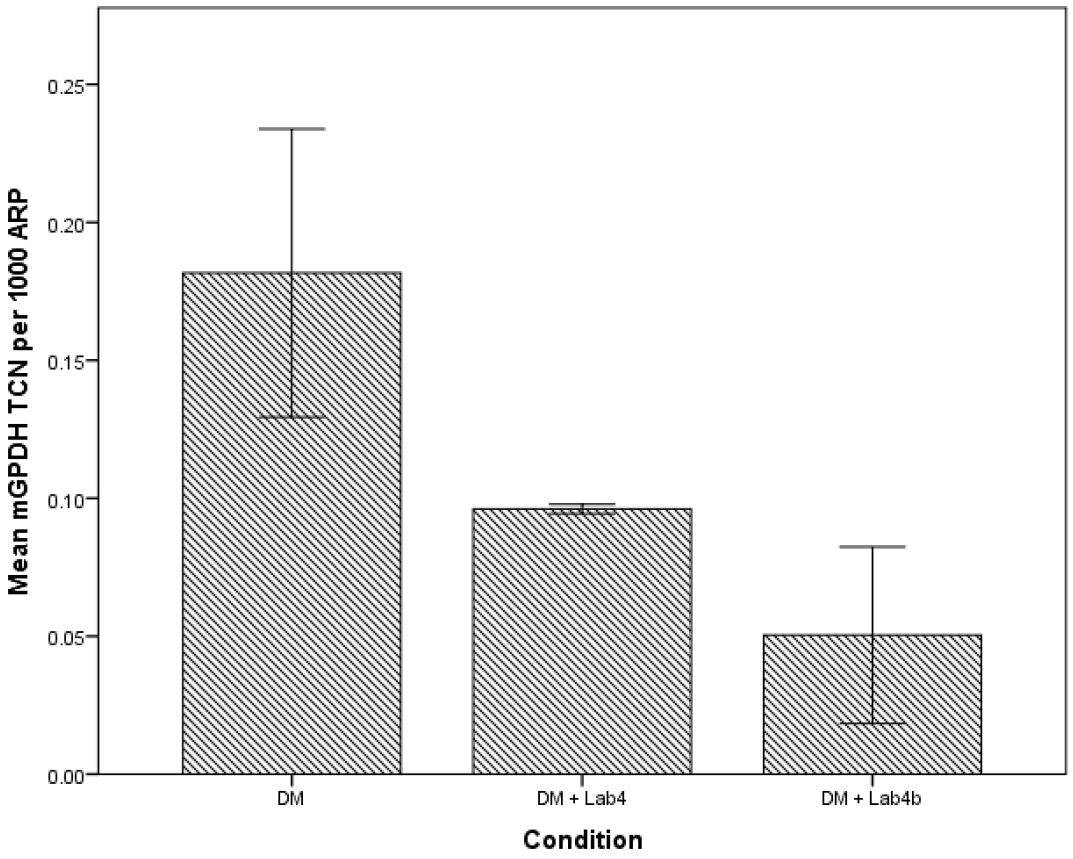

Figure 4.3. – qPCR quantification of GPDH in 3T3-L1 cells treated with DM diluted 1:1 with Lab4/b cell free supernatant after 7 days. Y axis represents total GPDH transcript copy number expressed per 1000 ARP transcript copy number, with conditions grouped along the X axis. Experiments were performed in duplicate wells, bars represent a single experiment. Error bars represent SEM. DM = differentiation media, DM + Lab4 = DM diluted 1:1 with Lab4 CFS, DM + Lab4b = DM diluted 1:1 with Lab4b CFS.

One-way between subjects ANOVA tests were conducted in both complete and differentiation medium (CM and DM respectively) diluted 1:1 with Lab4 or Lab4b CFS, with results compared to CM/DM (diluted 1:1 with DMEM:F12) as appropriate for control. In DM, there was not a significant effect of the use of CFS observed at p=<0.05 ($F(2,3) = 3.548$, p=0.162), though both Lab4 and Lab4b treatment conditions did show a nonsignificant mean decrease compared to control (results shown in Figure 4.3) as in ORO staining data at 7/8 days (results shown in Figure 4.1). In CM

conditions, qPCR data diverged from ORO staining data, with a non-significant decrease of GPDH compared to control in both treatment groups at p=<0.05 ($F(2,3) = 7.354$, p=0.70) (results shown in Figure 4.4) compared to a significant increase in optical density at 490nm in CM + Lab4b (results shown in Figure 4.1). Despite a similar pattern of results in qPCR data in CM and DM conditions, spontaneous adipogenesis assessed by GPDH transcription in CM occurred at minimal levels, with ~1000 times greater expression in DM conditions.

Though this preliminary data is the result of a single experiment, it serves as an interesting investigatory starting point. Visual assessment of cells in late adipogenesis suggested features of enhanced adipogenesis, and ORO staining data showed significantly increased lipid accumulation in CM + Lab4b CFS, but not Lab4. Further, qPCR data appeared to suggest that treatment with CFS reduced adipogenesis in both CM and CM conditions, with potentially greater reductions in Lab4b treated cells. The difference between Lab4 and Lab4b (summarised in Table 2.1) is the substitution of *L. acidophilus* strains with *L. salivarius* and *L. paracasei*, and suggests potential strain specific effects of probiotic bacteria on adipogenesis *in vitro*.

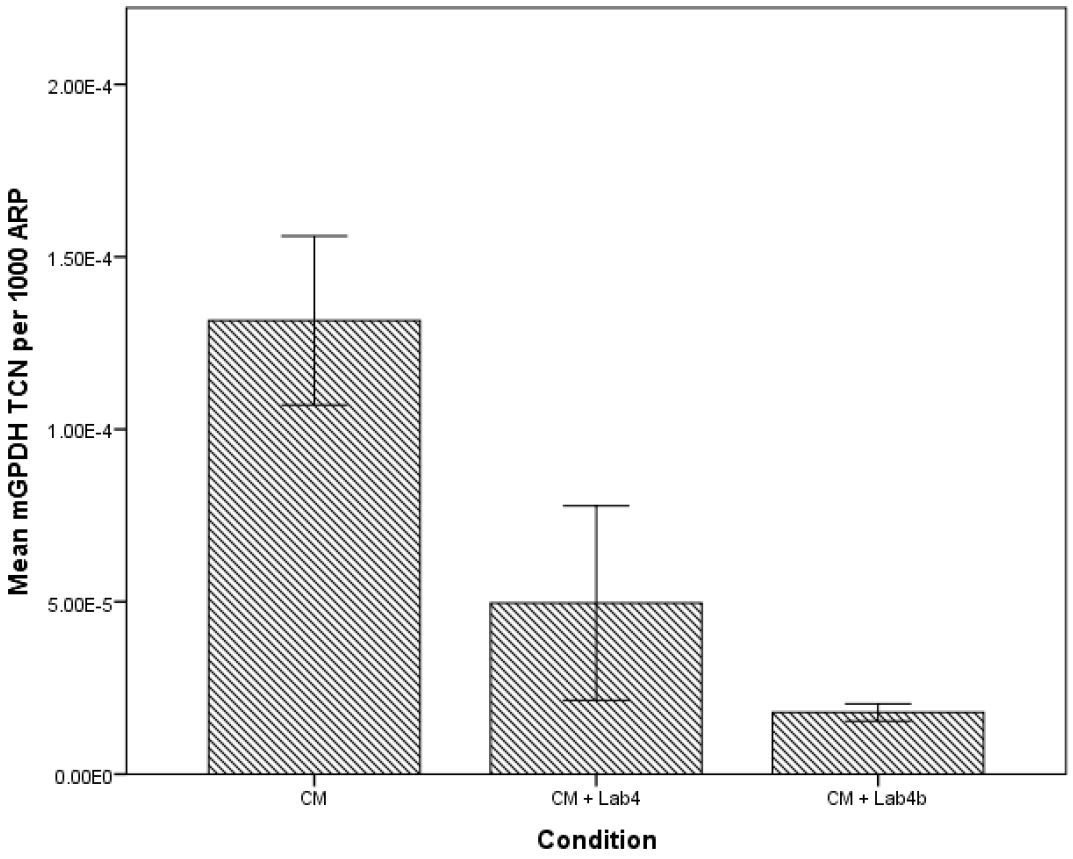

Figure 4.4. – qPCR quantification of GPDH in 3T3-L1 cells treated with CM diluted 1:1 with Lab4/b cell free supernatant after 7 days. Y axis represents total GPDH transcript copy number expressed per 1000 ARP transcript copy number, with conditions grouped along the X axis. Experiments were performed in duplicate wells, bars represent a single experiment. Error bars represent SEM. CM = complete media, CM + Lab4 = CM diluted 1:1 with Lab4 CFS, CM + Lab4b = CM diluted 1:1 with Lab4b CFS.

4.3 – Results

ORO staining

Post-confluent 3T3-L1 cells were treated for up to 9 days in DM diluted with CFS of several bacterial strains, and ORO staining and dye extraction performed at regular intervals. Due to time constraints, it was not possible to perform experiments using the full suite of bacterial strains. CFS of Lab4, Lab4b, and the *L. acidophilus* strains

contained in Lab4 but not Lab4b were used to attempt to generate data explaining differences seen in preliminary ORO staining data reported in the introductory chapter. Appearance of ORO stained droplets increased throughout the time course of experiments, indicating that adipogenesis was induced by DM (images shown in Figure 4.5). At day 3, cells appeared similar between conditions, displaying morphological rounding and limited lipid accumulation. However, by day 6, visible differences began to appear in lipid droplet appearance.

In DM, at day 6, most cells have accumulated lipids. Most of these lipid droplets remain small, with a moderate number of slightly enlarged lipid droplets. At day 9, again a majority of cells display lipid accumulation, but the size of individual lipid droplets is larger and less multilocular than at day 6.

In cells treated with DM + Lab4 CFS, at day 6 less cells show evidence of lipid accumulation than DM, but a population of cells appear to have accumulated larger numbers of lipid, displaying enlarged lipid droplets. There is also greater evidence of loss of cells compared to DM. By day 9, a greater number of cells have accumulated lipids than at day 6, but there is evidence of further cell loss. Additionally, several of the large lipid droplets appear to be coalescing, possibly in the process of formation of a single unilocular lipid droplet characteristic of terminal differentiation.

In cells treated with DM + Lab4b CFS, at day 6 there is pronounced evidence of cell loss, however remaining cells appear to have accumulated large amounts of lipid compared to DM, resembling cells treated with Lab4 CFS at day 9. At day 9, cells treated with Lab4b CFS display evidence of further cell loss, which may be a result of either death of cells or non-adherence upon terminal differentiation. At this stage, the number of cells displaying large lipid droplets is decreased, but a population of cells also appear to be in an earlier stage of adipogenesis, displaying several small lipid droplets.

In cells treated with DM + *L. acidophilus* CFS, at day 6 cells appear to possibly be forming larger numbers of lipid droplets of a smaller diameter than in DM. There is also evidence of cell loss. By day 9, appearance of lipid droplets in cells appears similar

to DM at day 9, but with lipid droplets of a slightly larger diameter. However, there remain unstained patches consistent with loss of cells.

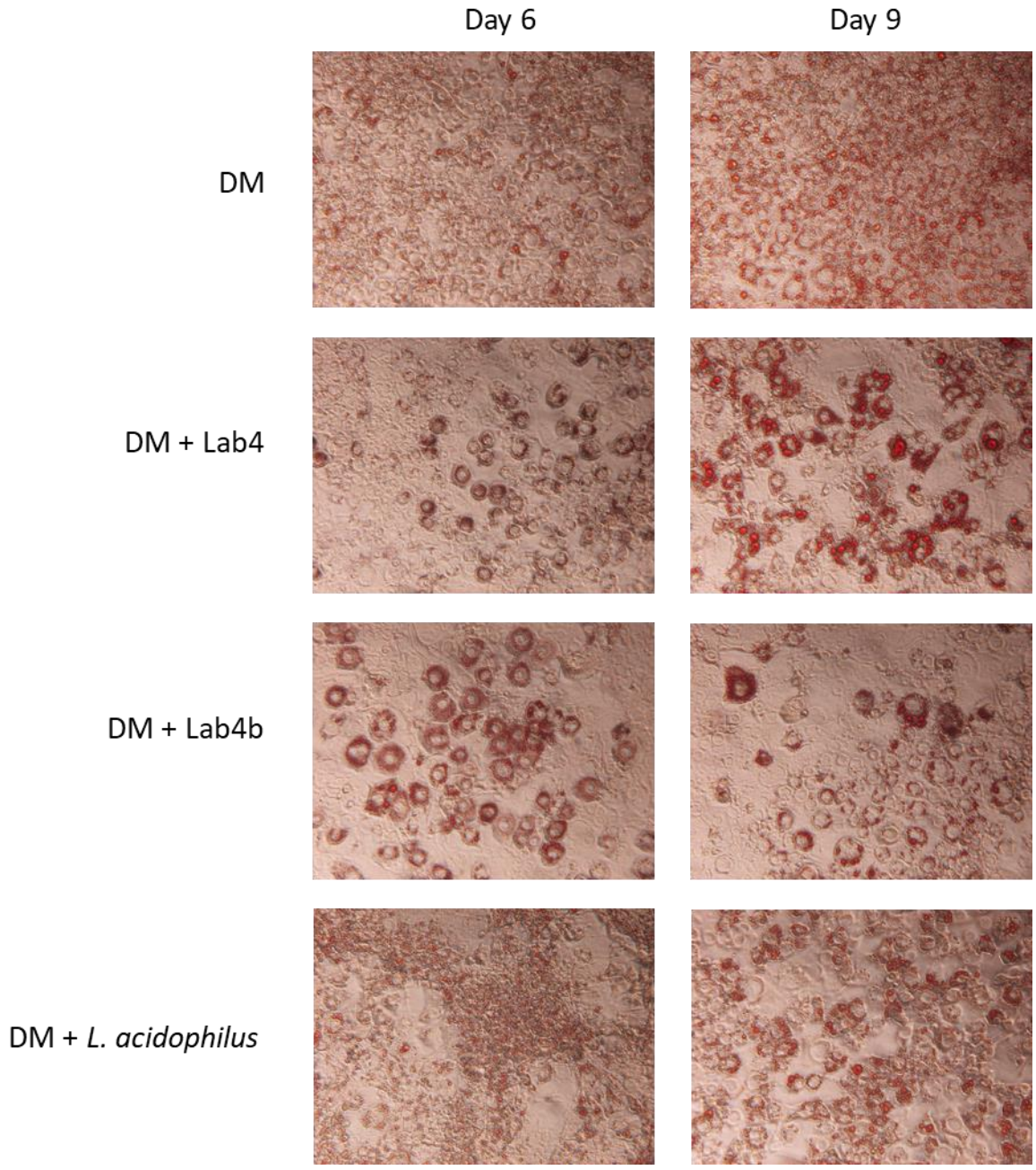

Figure. 4.5 – Representative images of Oil Red O stained 3T3-L1 cells at days 6 and 9. Post-confluent 3T3-L1 cells were maintained in either DM diluted 1:1 with DMEM:F12 (DM), or DM diluted 1:1 with CFS of Lab4, Lab4b, or *L. acidophilus* (DM + Lab4/Lab4b/*L. acidophilus*). Cells were imaged prior to dye extraction.

Throughout the time course, all conditions showed a steady increase in lipid accumulation measured by ORO staining, demonstrating that adipogenesis was induced in all conditions. One-way between subjects ANOVA tests were conducted on spectrophotometric data (corrected by subtracting the value of blank wells):

ORO staining data generated at day 3 of treatment indicated that there was not a significant effect of the use of CFS observed at p=<0.05, data violated the assumption of homogeneity of variances, necessitating a Welch F test. (F (3,7.562) = 0.727, p=0.565)

ORO staining data generated at day 6 of treatment indicated that there was a significant effect of the use of CFS observed at p=<0.05, however data also violated the assumption of homogeneity of variances, necessitating a Welch F test (F (3,6.412) = 8.062, p=0.014). A post-hoc Dunnett's T3 test was performed and no significant differences were observed in optical density at 490nm between conditions, however differences between Lab4 (0.585 ± 0.011 AU) and Lab4b (0.460 ± 0.051 AU) treated conditions were perhaps trending toward significance (p=0.052). Neither Lab4, Lab4b, nor *L. acidophilus* treated conditions were significantly different from control (p=1, 0.889, and 0.471 respectively).

However, in ORO staining data generated at day 9 a significant effect of the use of CFS was observed at p=<0.05 (F (3,16) = 14.450, p=<0.001). Post-hoc comparisons using the Tukey HSD test indicated no significant difference in optical density at 490nm between DM + DMEM:F12 (0.862 ± .043 AU) and DM + Acidophilus CFS (0.774 ± 0.485 AU, p=0.205), but that optical density at 490nm was significantly lower after treatment with DM + Lab4 (0.694 ± 0.081, p=0.006) or Lab4b CFS (0.595 ± 0.114, p=<0.001) than DM + DMEM:F12. Results are shown in Figure 4.6.

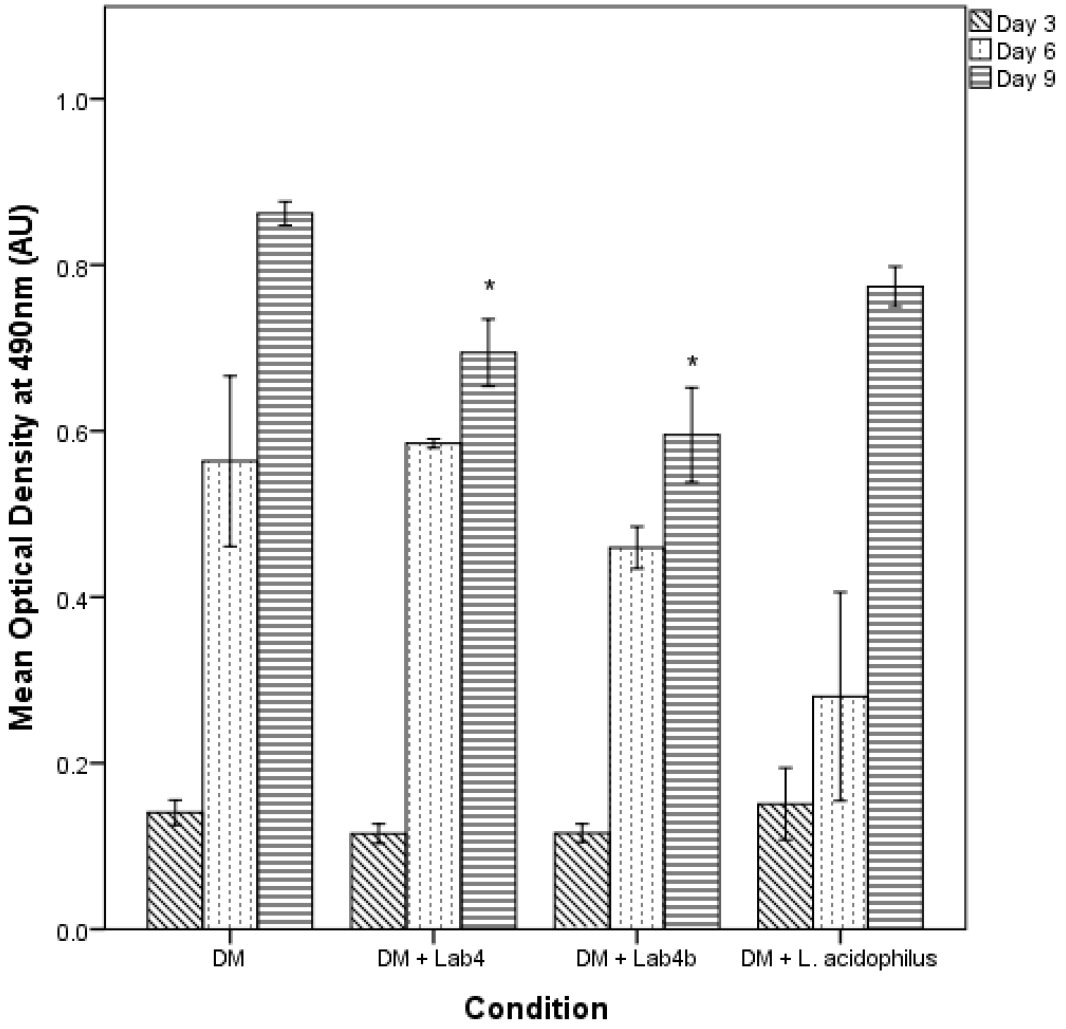

Figure. 4.6 – Oil Red O staining of 3T3-L1 cells at day 3, 6, and 9 after treatment with cell free supernatant. Post-confluent 3T3-L1 cells were maintained in either DM diluted 1:1 with DMEM:F12 (DM), or DM diluted 1:1 with CFS of Lab4, Lab4b, or *L. acidophilus* (DM + Lab4/Lab4b/*L. acidophilus*). ORO staining was performed, and dye extracted at day 3 (diagonally striped bars), day 6 (stippled bars), and day 9 (horizontally striped bars). No significant differences from control were observed at any timepoint except for day 9, where optical density at 490nm in DM + Lab4 and DM + Lab4b were significantly lower than control (p=0.006 and p=<0.001 respectively). Asterisks represent significant differences from control. Experiments were performed in triplicate wells, bars represent the mean of 2 individual experiments, error bars represent SEM.

qPCR quantification of a marker of terminal differentiation in 3T3-L1 cells

Post-confluent 3T3-L1 cells were treated for 10 days with CM or DM diluted with CFS of several bacterial strains, RNA extracted, reverse transcribed, and transcript levels of numerous genes measured via qPCR against standard curves for absolute quantification. GPDH transcripts (a terminal marker of differentiation) were detectable in CM conditions only at very low levels (below 0.1 transcripts per 1000 ARP). Transcription was comparatively far greater in DM conditions, demonstrating induction of adipogenesis, with the lowest value observed in DM + L. *acidophilus* treated cells (10.4 ± 8.94 transcripts per 1000 ARP), and the highest in DM control (46.1 ± 46.6 transcripts per 1000 ARP). One-way between subjects ANOVA tests were conducted on transcripts of GPDH expressed per 1000 transcripts of ARP as a reference gene. In DM conditions, a significant effect of the use of CFS observed at p=<0.05, however data violated the assumption of homogeneity of variances, necessitating a Welch F test ($F(5,12.121) = 5.814$, p=0.006). A post-hoc Dunnett's T3 test was performed for pairwise comparison, the only significant difference observed was between *L. salivarius* (38.3 ± 4.61 transcripts per 1000 ARP) and *L. acidophilus* (10.4 ± 8.94) treated conditions (p=0.009).

No significant differences were observed between conditions in cells maintained in CM conditions, data also violated the assumption of homogeneity of variances, necessitating a Welch F test ($F(5,7.637) = 1.020$, p=0.468). Results are summarised in Figures 4.7 and 4.8 respectively.

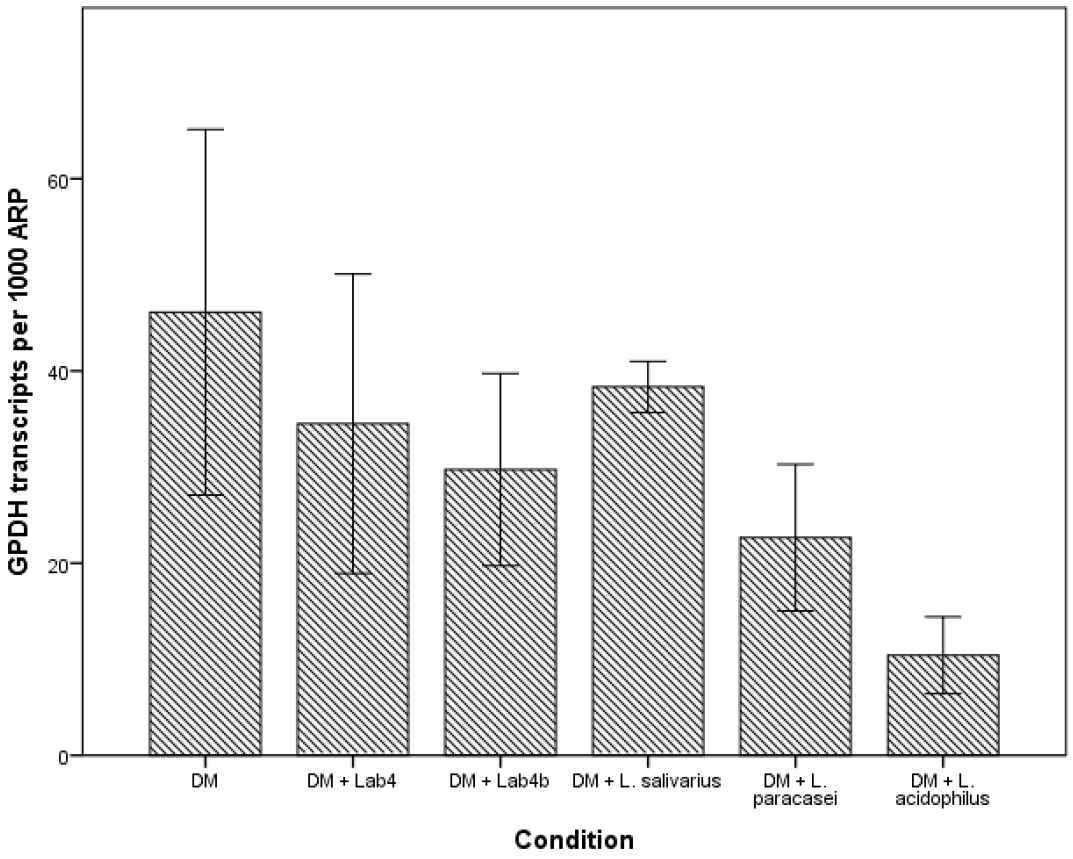

Figure. 4.7 – qPCR quantification of GPDH in 3T3-L1 cells treated with DM diluted with DMEM:F12 or cell free supernatant of several bacterial strains after 10 days. Post-confluent 3T3-L1 cells were maintained for 10 days in either DM diluted 1:1 with DMEM:F12 (DM), or DM diluted 1:1 with CFS of various bacterial strains (DM + Lab4/Lab4b/*L. salivarius*/*L. paracasei*/*L. acidophilus*), RNA extracted, reverse transcribed, and subjected to qPCR. GPDH transcripts at day 10 did not show significant differences to control in any condition (p=0.481). Experiments were performed in triplicate wells, bars represent the mean of 2 individual experiments, error bars represent SEM.

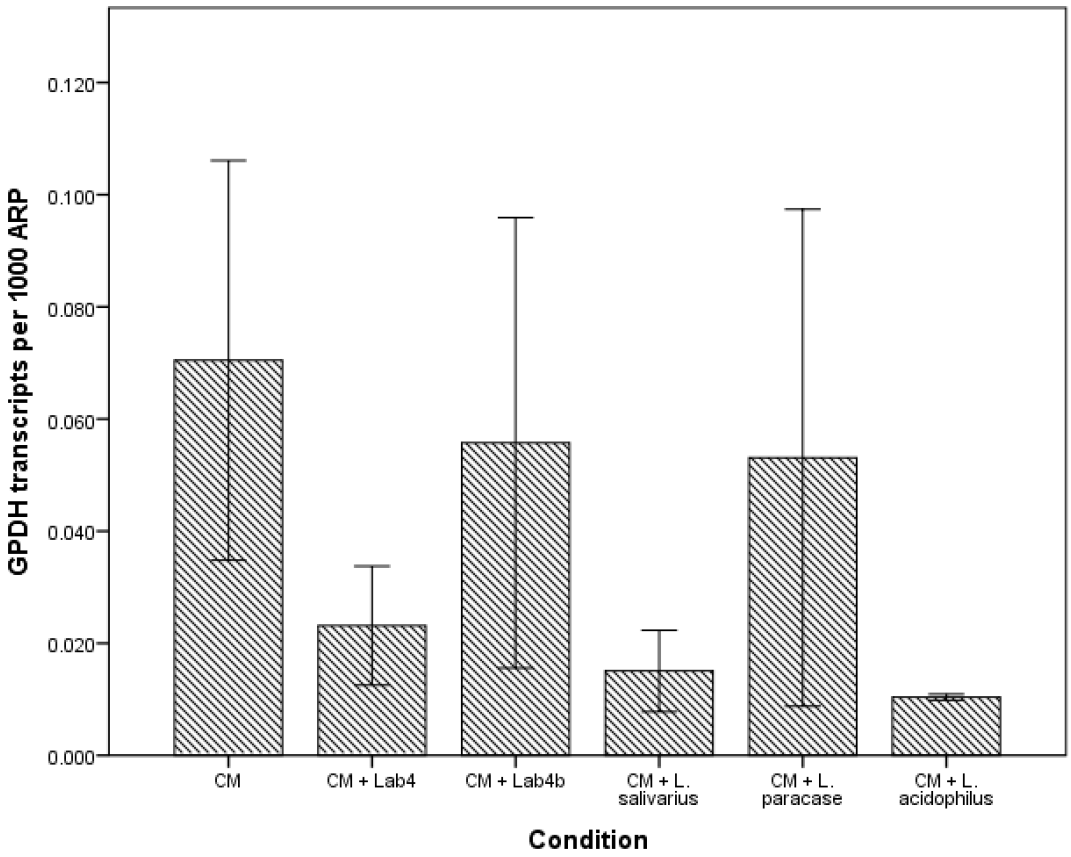

Figure. 4.8 – qPCR quantification of GPDH in 3T3-L1 cells treated with CM diluted with DMEM:F12 or cell free supernatant of several bacterial strains after 10 days. . Post-confluent 3T3-L1 cells were maintained for 10 days in either DM diluted 1:1 with DMEM:F12 (CM), or CM diluted 1:1 with CFS of various bacterial strains (CM + Lab4/Lab4b/*L. salivarius*/*L. paracasei*/*L. acidophilus*), RNA extracted, reverse transcribed, and subjected to qPCR. GPDH transcripts at day 10 did not show significant differences to control in any condition (p=0.635). Experiments were performed in triplicate wells, bars represent the mean of 2 individual experiments, error bars represent SEM.

4.4 – Discussion

Quantification of adipogenesis

ORO staining of differentiating 3T3-L1 cells treated with Lab4 and Lab4b CFS showed a significant reduction in optical density at 490nm only during late adipogenesis at day 9, but showed similar levels of adipogenesis to control at 3 and 6 days (Figure 4.6) despite an apparent reduction in cell viability. It had been hypothesised on examining images generated in preliminary data presented in the introductory chapter that cells treated with CFS had morphological features of *enhanced* adipogenesis despite non-significant reductions in ORO and GPDH transcripts. Images of cells from the present study shown in Figure 4.5 display visibly larger lipid droplets at day 9 in Lab4 and Lab4b treated cells, alongside evidence of fewer cells compared to control. A complication of studies with 3T3-L1 cells is that while preadipocytes are adherent, fully mature adipocytes are not (Draman *et al*., 2013), and will be removed in culture medium when aspirated. Time can therefore be a critical variable, which contributed to the decision to perform ORO staining at different time points. It is possible that the similar optical density between conditions in ORO staining data at days 3 and 6 is a function of coinciding reductions in cell viability and enhancement of adipogenesis, however more granular data for both viability and adipogenesis is required to draw any conclusions.

Data in the present study suggests an effect of treatment with Lab4 and Lab4b CFS on late adipogenesis when measured via ORO staining, however in conjunction with potential effects on viability and morphology that may oppose one another, more data is needed to determine effects at earlier stages. Data generated from trypan blue exclusion assays gives strong evidence of reduced viability of 3T3-L1 cells when treated with CFS of Lab4 and Lab4b, however evidence for the supposition of increased adipogenesis is thus far only qualitative, derived from subjective analysis of visual features of cells. It would therefore be useful to employ a full factorial experimental design accounting for both duration and concentration of exposure, but was not possible in the present study due to time constraints. A potential step for further study of the interaction between time of treatment, adipogenesis, and cell

viability is to culture cells used for viability assays and ORO staining on the same plate, and express data as a function of the number of viable cells at a given timepoint.

Transcripts of GPDH, a marker of terminal differentiation, were also used to assess the effects of CFS on adipogenesis in 3T3-L1 cells. No significant differences were observed between any treatment condition and control. This suggests that the effects seen in ORO data may be a reflection of a reduction in cell viability. However, due to time constraints means observed result from only two experiments . Preliminary data reported in the introductory chapter used a different timepoint for extraction of RNA (7 days) compared to experiments performed in this chapter (10 days), making comparison particularly of a marker of terminal differentiation difficult. GPDH transcripts reported in DM control in preliminary data displayed a mean of 0.181 (± 0.074) transcripts per 1000 ARP, and previous data generated in our laboratory in 3T3-L1 cells at day 7 showing a mean of ~1.6 GPDH transcripts per 1000 ARP (Draman *et al*., 2013), though this was using undiluted DM. Other data generated in our laboratory at day 9 in differentiating 3T3-L1 cells (again using undiluted DM) reported ~11 GPDH transcripts per 1000 ARP (Zhang *et al*., 2009). Though these results are taken from different timepoints from three different researchers, they suggest that GPDH transcription may be highly variable in 3T3-L1 cells during late adipogenesis. As such, the large variation in data in the present study may be a result of this variability, but is likely a result of inexperience when conducting the initial experiment, and further data is needed to draw firmer conclusions and improve accuracy.

Despite aforementioned issues and a lack of statistically significant results in overall data, the *L. acidophilus* treatment group showed the lowest mean GPDH transcript copy number in overall data from CM and DM experiments. The *L. acidophilus* condition contained half the CFU/ml as other treatment conditions in its starting inoculum, and a decision was made not to dilute other conditions down to this level due to concern about being able to observe results. If future study were to generate data maintaining this pattern of results and achieve significance, it would be necessary to determine whether this is due to a reduction in adipogenesis or perhaps

a result of not being as pro-adipogenic as other conditions due to lower cell numbers in starting inoculum.

Chapter 5: Effects of bacterial cell free supernatant on markers of adipose phenotype in 3T3-L1 cells

5.1 – Introduction

Though trypan blue staining reported in chapter 3.3 seemed to indicate a significant impact of Lab4 and Lab4b CFS on viability in differentiating 3T3-L1 cells, data generated via MTS assay did not. It was hypothesised that this may be the result of uncoupled respiration induced by some factor in CFS. Resultantly, it was decided to investigate expression of gene markers of adipose phenotype and function in 3T3-L1 cells to determine whether treatment with CFS may induce a "browning" effect.

Since the discovery of functional BAT in adult humans there has been wide interest in identifying gene markers of adipose phenotype. It has previously been shown that it is possible to induce a beige-like phenotype in 3T3-L1 adipocyte cells in the presence of the β adrenergic receptor agonist isoproterenol, and that subsequent UCP1 expression is modulated by the hormonal environment of the culture medium (Asano, *et al*. 2014). Notably, despite the evidence of increased UCP1 transcription, the relative levels of putative beige adipocyte selective markers were not significantly different. As the capacity of the 3T3-L1 cell line to display a thermogenic phenotype is a relatively recent discovery, there are no markers specifically validated for phenotypic characteristics in 3T3-L1 cells. There are however numerous markers of adipose phenotype that have been proposed in mice, primers for several of these have already been developed in our laboratory.

ZIC1 is used as a marker of "classical" BAT in mice (Harms and Seale, 2013), and has been previously identified in 3T3-L1 cells by Seale *et al*. (2007). Seale *et al*. reported a >5-fold greater mRNA expression in immortalised brown adipose cells compared to immortalised white adipose cell lines such as 3T3-L1, though data relating to 3T3-L1 expression was not shown.

UCP1 can be used as a marker of thermogenic capacity in adipocytes, and has previously been shown to be inducible in 3T3-L1 cells via treatment with the β-adrenergic agonist isoproterenol (Miller *et al*., 2015). Contrary to the results of Asano

et al. (2014) Miller *et al*. found dose and time-dependent increases in certain putative beige-selective markers, though timepoints used were 6 and 48 hours of treatment compared to 4 hours in Asano *et al*.

PGC1-α has also been proposed as a marker of a non-specific beige/brown adipose phenotype (Harms and Seale, 2013). PGC1-α is inducible in HIB1b cells (an *in vitro* model of murine BAT) upon cAMP stimulation, but expression in 3T3-L1 cells appears cAMP insensitive under normal conditions (Karamanlidis *et al*., 2007).

Cbp/p300-interacting transactivator 1 (CITED1) has been proposed as a marker of a beige adipose phenotype in murine adipose tissue (Sharp *et al*., 2012) and its expression in 3T3-L1 cells has previously been shown to be responsive to the PPARγ agonist rosiglitazone in specific treatment conditions (Asano *et al*., 2014).

Leptin is considered a classical marker of white adipose tissue (Ussar *et al.,* 2014), and in murine BAT appears reciprocally regulated with UCP1 (Cancello *et al*., 1998). Gene expression of leptin in 3T3-L1 cells can notably be both inhibited and stimulated by the presence of triiodothyronine dependent upon dose and length of treatment (de Oliveira *et al*., 2015), though concentrations were 10-1000 times greater than in the present study.

5.2 – Materials and methods

A list of reagents used, and their suppliers is given in Appendix 1, Table 1. Media was prepared as in chapter 3.2. Cells for qPCR experiments were cultured as in chapter 4.2. qPCR was performed as in chapter 4.3.

Isolation of brown adipose tissue markers from 3T3-L1 cells

3T3-L1 cells were cultured, RNA extracted and reverse transcribed, and PCRs performed as described in chapter 4.2, but using primers for genes listed in Table 5.1. PCR products were subjected to gel electrophoresis, gel bands excised, and DNA obtained as described previously for production of standards for qPCR in chapter 4.2

UCP1 and CITED1 were identified by the presence of appropriately sized bands on gel electrophoresis alone but PCR amplicons for ZIC1 and PGC1-α underwent sequence analysis to confirm their identity Their column purified DNA was subjected to BigDye Terminator V1.1 cycle sequencing according to manufacturers' instructions and BigDye PCR product precipitated by sodium acetate precipitation as follows.

A master mix was prepared containing 1.5µl sodium acetate, 31.5µl 100% ethanol, and 7µl molecular biology grade water per volume, mixed thoroughly by vortexing then 40µl pipetted into each Micro Eppendorf tube containing BigDye PCR product. Micro Eppendorf tubes were then incubated at room temperature for 15 minutes before being centrifuged at 13000 RPM for 20 minutes at 4˚C. Following centrifugation, supernatant was discarded and 250µl 70% ethanol was pipetted into each Micro Eppendorf tube. Micro Eppendorf tubes were then centrifuged at 13000 RPM for 10 minutes at 4˚C and supernatant discarded. Following this, Micro Eppendorf tubes were placed in a heating block at 95˚C for one minute with lids open to evaporate fluid, then stored at -20˚C.

Precipitates were sent to Cardiff University's Central Biotechnology Services for Sanger sequencing. Sequence data was analysed with DNA Baser v4.36.0 software and high-quality sequence data trimmed. Sequence data was subsequently searched for in a murine database using the online Basic Local Alignment Search Tool (National Center for Biotechnology Information, 2017).

Production of standards for qPCR

Following positive identification by sequencing or gel electrophoresis, procedures for production of standards given in chapter 4.2 were repeated using primer sequences for genes shown in Table 5.1. PCR products were subjected to gel electrophoresis, and DNA retrieved using the Wizard SV Gel and PCR Clean-Up System as described previously.

Table 5.1. – Primers and exon locations used for polymerase chain reaction

Gene (product size)	Forward Primer (exon location)	Reverse Primer (exon location)
ARP (72bp)	GAGGAATCAGATGAGGATATGGGA (exon 7)	AAGCAGGCTGACTTGGTTGC (exon 7)
GPDH (124bp)	ATGCTCGCCACAGAATCCACAC (exon 8)	AACCGGCAGCCCTTGACTTG (exon 8)
UCP1 (84bp)	GGCCTCTACGACTCAGTCCA (exon 2)	TAAGCCGGCTGAGATCTTGT (exon 3)
PGC1-α (161bp)	CCCTGCCATTGTTAAGACC (exon 4/5)	TGCTGCTGTTCCTGTTTTC (exon 5)
ZIC-1 (194bp)	AGAGCAGAGCAACCACATCT (exon 1)	CCCCTGTGTGTGTCCTTTTG (exon 1/2)
CITED1 (288bp)	CCTCAGCTCCTGTGAGCTTTC (exon 1)	CGTTGGCTTTGGCTCCATTT (exon 3)
Leptin (226bp)	CCAGGATCAATGACATTTCACACA (exon 1)	TTGGAGAAGGCCAGCAGATG (exon 2)

ARP - acidic ribophosphoprotein*, GPDH* - glycerol-3-phosphate dehydrogenase*, UCP1* – Uncoupling Protein 1, *PGC1-α* - peroxisome proliferator-activated receptor gamma coactivator 1-alpha*, ZIC-1* – Zinc in Cerebellum 1*, CITED1* - Cbp/p300-interacting transactivator 1*.*

DNA was measured using a Nanodrop Lite spectrophotometer and absorbance ratio at 260nm:280nm and concentration recorded. Using amplicon sequence length and the assumption of an average base pair weight of 650 Daltons, number of copies per µl was estimated using the calculation:

No. of copies = (ng of DNA X (6.022×10^{23})) / (amplicon length x 1×10^{9} x 650)

These samples were then used to construct a standard curve for absolute qPCR quantification, using serial dilutions to obtain standards for $\times 10^{2}$ – $\times 10^{6}$.

5.3 – Results

Presence of brown adipose tissue markers in 3T3-L1 cells

Sanger sequencing data (shown in Appendix 2) for presumed ZIC1 and PGC1-α samples received from Cardiff University's Central Biotechnology Services was trimmed to high-quality sequence and searched for in a murine database as previously described. Search results indicated query cover of 100% for both sequence queries. Identity scores were 98% and 95% for ZIC1 and PGC1-α samples respectively. E values of $2x10^{-63}$ and $7x10^{-42}$ were returned for ZIC1 and PGC1-α respectively. No untargeted gene matches occurred. This data appears to confirm the presence of these gene transcripts in 3T3-L1 cells.

qPCR data for all genes investigated is presented in tables 5.2 and 5.3 for cells maintained in CM and DM conditions respectively. ARP was used as a reference gene. Though some conditions (such as CM + Lab4b) display a larger standard deviation than others, suggesting it may not have been stably transcribed, this was believed to be related to reduced RNA yields in certain conditions falling below the limit needed to use 1000ng input RNA. ARP transcription did not appear to be impacted by either adipogenesis or treatment.

As would be expected, in differentiating cells GPDH was the most abundantly detected gene, whereas in CM conditions it appeared minimally transcribed. Statistical analysis of GPDH transcripts is given in chapter 4.3.

Leptin transcription was detectable in all cells, though at low levels. In line with expectations, leptin was detected at higher levels in cells maintained in DM compared to CM, though was not robustly transcribed in either. The greatest mean leptin transcription was seen in cells treated with DM + L. *salivarius* CFS, though there was also a large standard deviation.

Of the phenotypic genes investigated, UCP1 displayed the highest level of transcription, which again were comparatively several times greater in DM conditions compared to CM. Results in DM conditions were suggestive of all conditions with the

exception of L. *acidophilus* potentially decreasing UCP1 transcription, whereas L. *acidophilus* displayed a potential increase in transcription.

PGC1-α transcription also appeared increased in DM conditions compared to CM, and though not as robustly induced as UCP1, transcripts were detected in greater quantities than leptin or CITED1. Again, the greatest level of PGC1-α transcripts were observed in DM + L. *acidophilus*, though the increase appeared less pronounced than that seen in UCP1 transcription.

As with other genes, CITED1 transcription appeared greater in DM conditions compared to CM. However, transcription was generally low. No condition appeared to increase CITED1 transcription, though in DM conditions all treatment groups except DM + Lab4 CFS showed a lower mean than control.

Representative images of a standard curve for PGC1-α, as well as an amplification plot and dissociation curve obtained from a DM well assessed for PGC1-α transcription are shown in Figures 5.1, 5.2, and 5.3 respectively.

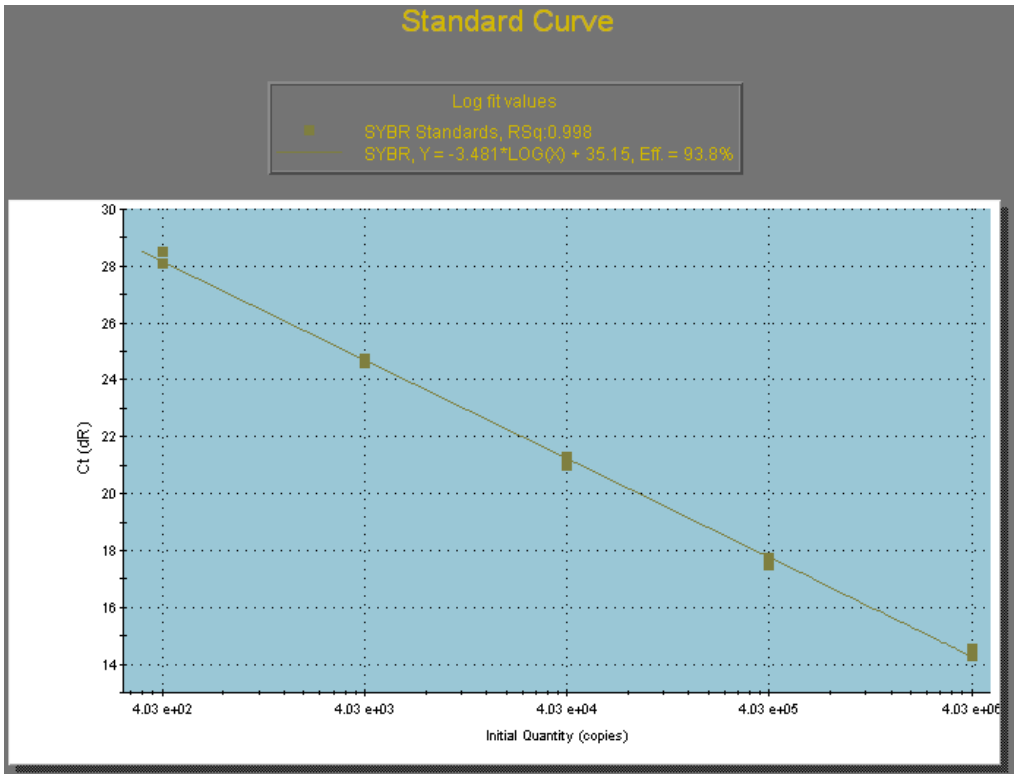

Figure 5.1. – Representative image of a qPCR standard curve plot using MXPro software. Standards for PGC1-α were produced from PCR products and serial dilutions of known concentrations plated in duplicate alongside cDNA produced from experimental samples. Ct is plotted on the Y axis and number of transcripts on the X axis.

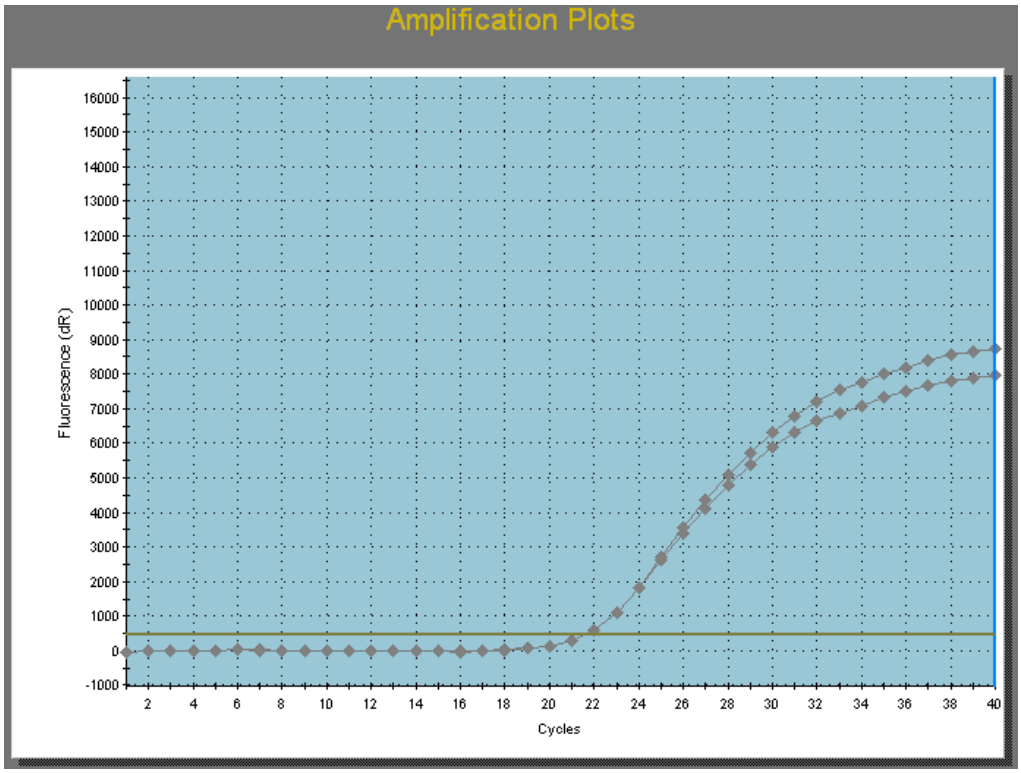

Figure 5.2. – Representative image of a qPCR amplification curve plot using MXPro software. cDNA produced from an experimental sample maintained in DM was plated in duplicate and assessed via qPCR for PGC1-α transcripts. Fluorescence is plotted on the Y axis and PCR cycle number on the X axis.

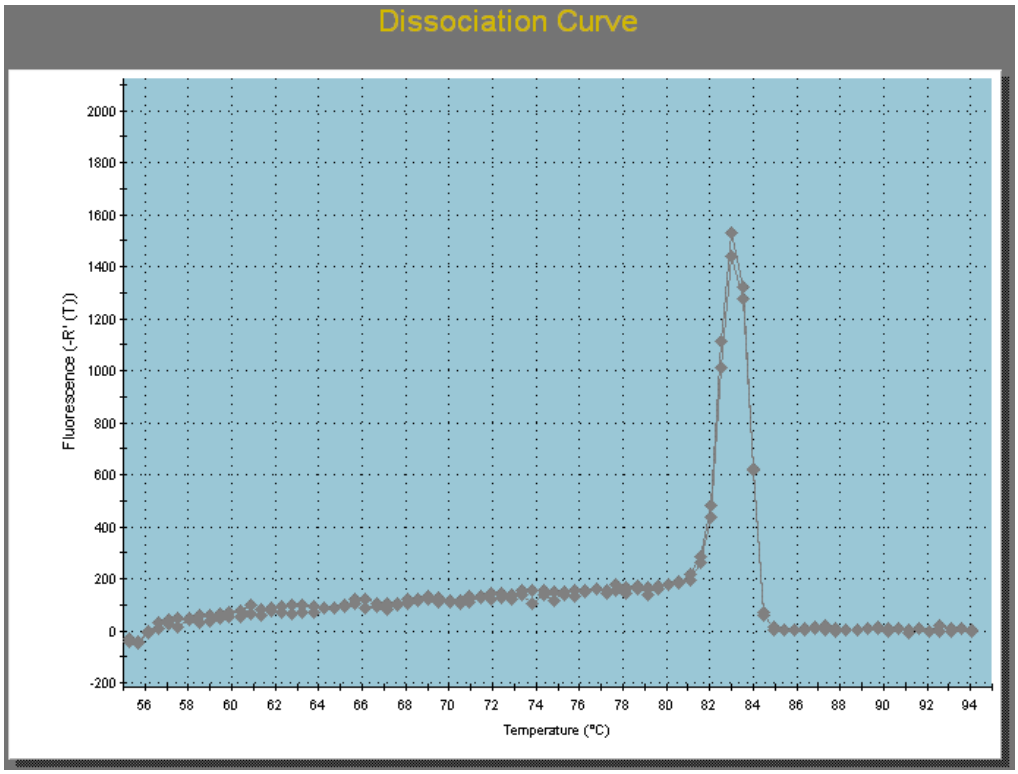

Figure 5.3. – Representative image of a qPCR dissociation curve plot using MXPro software. cDNA produced from an experimental sample maintained in DM was plated in duplicate and assessed via qPCR for PGC1-α transcripts. Fluorescence is plotted on the Y axis and temperature on the X axis. A single product peak was observed around 83˚C.

Table 5.2. – qPCR data for all genes investigated in 3T3-L1 cells maintained in CM conditions for 10 days

Condition	ARP TCN	ARP Ct	Leptin TCN	Leptin Ct	UCP1 TCN	UCP1 Ct	PGC1-α TCN	PGC1-α Ct	CITED1 TCN	CITED 1 Ct	GPDH TCN	GPDH Ct
CM	$2.71x10^{6}$ ± $2.68x10^{6}$	17.4 ± 1.82	$7.89x10^{-3}$ ± $9.02x10^{-3}$	37.8 ± 1.31	$759x10^{-2}$ ± $1.14x10^{1}$	32.5 ± 2.31	$7.17x10^{-1}$ ± $7.85x10^{-1}$	31.3 ± 8.1	$8.86x10^{-3}$ ± $1.76x10^{-3}$	33.2 ± 0.79	$7.05x10^{-2}$ ± $8.73x10^{-2}$	34.7 ± 2.35
CM + Lab4	$2.20x10^{6}$ ± $2.30x10^{6}$	18.1 ± 2.33	$2.20x10^{-2}$ ± $3.19x10^{-2}$	38.4 ± 0.80	$227x10^{-2}$ ± $112x10^{-2}$	33.2 ± 0.30	$7.97x10^{-1}$ ± $7.21x10^{-1}$	30.4 ± 6.8	$1.11x10^{-2}$ ± $5.03x10^{-3}$	33.2 ± 1.24	$2.31x10^{-2}$ ± $2.12x10^{-2}$	34.3 ± 1.95
CM + Lab4b	$2.79x10^{6}$ ± $3.01x10^{6}$	18.7 ± 3.49	$2.81x10^{-2}$ ± $5.93x10^{-2}$	38.0 ± 0.76	$636x10^{-2}$ ± $567x10^{-2}$	31.4 ± 1.28	$6.21x10^{-1}$ ± $5.07x10^{-1}$	30.8 ± 7.24	$1.46x10^{-2}$ ± $7.10x10^{-3}$	32.3 ± 0.76	$5.57x10^{-2}$ ± $8.02x10^{-2}$	33.8 ± 2.40
CM + L. *salivarius*	$3.91x10^{6}$ ± $2.58x10^{6}$	16.9 ± 2.03	$1.28x10^{-2}$ ± $2.05x10^{-1}$	37.3 ± 0.60	$198x10^{-2}$ ± $3.90x10^{-1}$	32.0 ± 0.07	$6.01x10^{-1}$ ± $3.5x10^{-1}$	27.9 ± 6.24	$4.08x10^{-3}$ ± $1.32x10^{-3}$	34.3 ± 0.45	$1.51x10^{-2}$ ± $1.45x10^{-2}$	34.9 ± 3.10
CM + L. *paracasei*	$3.62x10^{6}$ ± $3.94x10^{6}$	17.9 ± 2.89	$4.36x10^{-2}$ ± $5.94x10^{-2}$	37.3 ± 0.96	$190x10^{-2}$ ± $2.71x10^{-1}$	32.6 ± 0.15	$9.07x10^{-1}$ ± $1.23\ x10^{-1}$	27.6 ± 5.1	$9.41x10^{-3}$ ± $2.43x10^{-3}$	33.8 ± 2.91	$5.31x10^{-2}$ ± $8.86x10^{-2}$	33.9 ± 2.49
CM + L. *acidophilus*	$4.24x10^{6}$ ± $2.21x10^{6}$	15.9 ± 0.49	$1.02x10^{-3}$ ± $9.40x10^{-4}$	37.6 ± 1.61	$474x10^{-2}$ ± $4.39x10^{-1}$	31.4 ± 0.27	$105x10^{-2}$ ± $1.77x10^{-1}$	26.4 ± 3.4	$9.57x10^{-3}$ ± $6.72x10^{-3}$	33.2 ± 1.54	$1.04x10^{-2}$ ± $1.09x10^{-3}$	34.3 ± 2.18

ARP - acidic ribophosphoprotein*, CITED1* - Cbp/p300-interacting transactivator 1, *GPDH* - glycerol-3-phosphate dehydrogenase*, PGC1-α* - peroxisome proliferator-activated receptor gamma coactivator 1-alpha, *TCN* – Transcript Copy Number *UCP1* – Uncoupling Protein 1*.* Transcripts are given per 1000 ARP transcripts, with the exception of ARP which are reported as raw values.

Table 5.3. – qPCR data for all genes investigated in 3T3-L1 cells maintained in DM conditions for 10 days

Condition	ARP TCN	ARP Ct	Leptin TCN	Leptin Ct	UCP1 TCN	UCP1 Ct	PGC1-α TCN	PGC1-α Ct	CITED1 TCN	CITED 1 Ct	GPDH TCN	GPDH Ct
DM	$1.51x10^{6}$ ± $1.44x10^{6}$	18.1 ± 1.45	$1.60x10^{-2}$ ± $7.07x10^{-3}$	35.9 ± 1.82	$2.55x10^{1}$ ± $413x10^{-2}$	29.9 ± 2.80	$842x10^{-2}$ ± $903x10^{-2}$	27.6 ± 7.2	$1.79x10^{-1}$ ± $5.03x10^{-1}$	31.6 ± 5.32	$4.61x10^{1}$ ± $4.66x10^{1}$	24.2 ± 6.25
DM + Lab4	$1.44x10^{6}$ ± $1.17x10^{6}$	17.8 ± 0.84	$2.08x10^{-1}$ ± $2.04x10^{-2}$	36.1 ± 1.17	$1.17x10^{1}$ ± $565x10^{-2}$	31.5 ± 0.71	$741x10^{-2}$ ± $923x10^{-2}$	26.9 ± 5.6	$1.89x10^{-1}$ ± $1.05x10^{-1}$	29.7 ± 0.93	$3.45x10^{1}$ ± $3.82x10^{1}$	24.2 ± 4.6
DM + Lab4b	$6.65x10^{5}$ ± $5.59x10^{5}$	19.0 ± 0.85	$1.52x10^{-1}$ ± $7.60x10^{-3}$	36.8 ± 1.30	$1.38x10^{1}$ ± $170x10^{-2}$	32.3 ± 0.16	$594x10^{-2}$ ± $571x10^{-2}$	28.3 ± 5.9	$5.56x10^{-1}$ ± $3.50x10^{-1}$	33.5 ± 1.99	$2.97x10^{1}$ ± $2.45x10^{1}$	25.5 ± 5.20
DM + L. *salivarius*	$2.69x10^{6}$ ± $2.33x10^{6}$	18.0 ± 3.08	$9.54x10^{-2}$ ± $8.56x10^{-2}$	34.2 ± 3.02	$1.17x10^{1}$ ± $227x10^{-2}$	30.5 ± 0.76	$466x10^{-2}$ ± $296x10^{-2}$	24.0 ± 4.21	$5.21x10^{-1}$ ± $3.35x10^{-2}$	32.6 ± 4.00	$3.83x10^{1}$ ± $461x10^{-2}$	26.5 ± 10.2
DM + L. *paracasei*	$2.01x10^{6}$ ± $1.36x10^{6}$	17.4 ± 1.60	$2.08x10^{-2}$ ± $2.95x10^{-3}$	35.0 ± 2.41	$1.40x10^{1}$ ± $134x10^{-2}$	30.8 ± 0.07	$875x10^{-2}$ ± $792x10^{-2}$	25.9 ± 6.0	$7.73x10^{-1}$ ± $7.87x10^{-2}$	32.5 ± 3.60	$2.27x10^{1}$ ± $1.87x10^{1}$	24.2 ± 5.42
DM + L. *acidophilus*	$4.39x10^{6}$ ± $5.50x10^{6}$	16.3 ± 1.17	$1.02x10^{-2}$ ± $4.20x10^{-3}$	35.0 ± 0.96	$4.79x10^{1}$ ± $1.96x10^{1}$	28.27 ± 0.90	$1.78x10^{1}$ ± $1.67x10^{1}$	22.8 ± 4.2	$1.22x10^{-1}$ ± $1.19x10^{-1}$	30.28 ± 2.34	$1.04x10^{1}$ ± $894x10^{-2}$	23.7 ± 1.27

ARP - acidic ribophosphoprotein*, CITED1* - Cbp/p300-interacting transactivator 1, *GPDH* - glycerol-3-phosphate dehydrogenase*, PGC1-α* - peroxisome proliferator-activated receptor gamma coactivator 1-alpha, *TCN* – Transcript Copy Number *UCP1* – Uncoupling Protein 1. Transcripts are given per 1000 ARP transcripts, with the exception of ARP which are reported as raw values.

qPCR quantification of leptin transcripts in 3T3-L1 cells

Post-confluent 3T3-L1 cells were treated for 10 days with CM or DM diluted with CFS of several bacterial strains, RNA extracted, reverse transcribed, and transcript levels of numerous genes measured via qPCR against standard curves for absolute quantification. Leptin transcripts were detectable in CM conditions at very low levels, below 0.05 transcripts per 1000 ARP, with the lowest value observed in cells treated with CM + L. *acidophilus* (0.001 ± 0.0009) and the highest observed in cells treated with CM + L. *paracasei* (0.04 ± 0.06). Transcription in DM conditions was around ~0.01 per 1000 ARP in all conditions except for DM + L. *salivarius* (0.10 ± 0.09) which was roughly 10-fold higher, indicating a potential effect of this treatment on leptin transcription.

Leptin was used as a potential marker of a WAT-like phenotype in 3T3-L1 cells. One-way between subjects ANOVA tests were conducted on transcripts of leptin expressed per 1000 transcripts of ARP as a reference gene. Data violated the assumption of homogeneity of variances, necessitating a Welch F test. No significant effect of the use of CFS was observed on leptin transcripts at p=<0.05 ($F(5,11.107) = 1.609$, p=0.236) in DM conditions, though there appeared to be a large but non-significant mean increase in DM + *L. salivarius* CFS, results shown in Figure 5.4.

One-way between subjects ANOVA tests were similarly conducted In CM conditions, data again violated the assumption of homogeneity of variances, necessitating a Welch F test. No significant differences were observed between conditions at p=<0.05 ($F(5,13.016) = 0.958$, p=0.226), results shown in Figure 5.5.

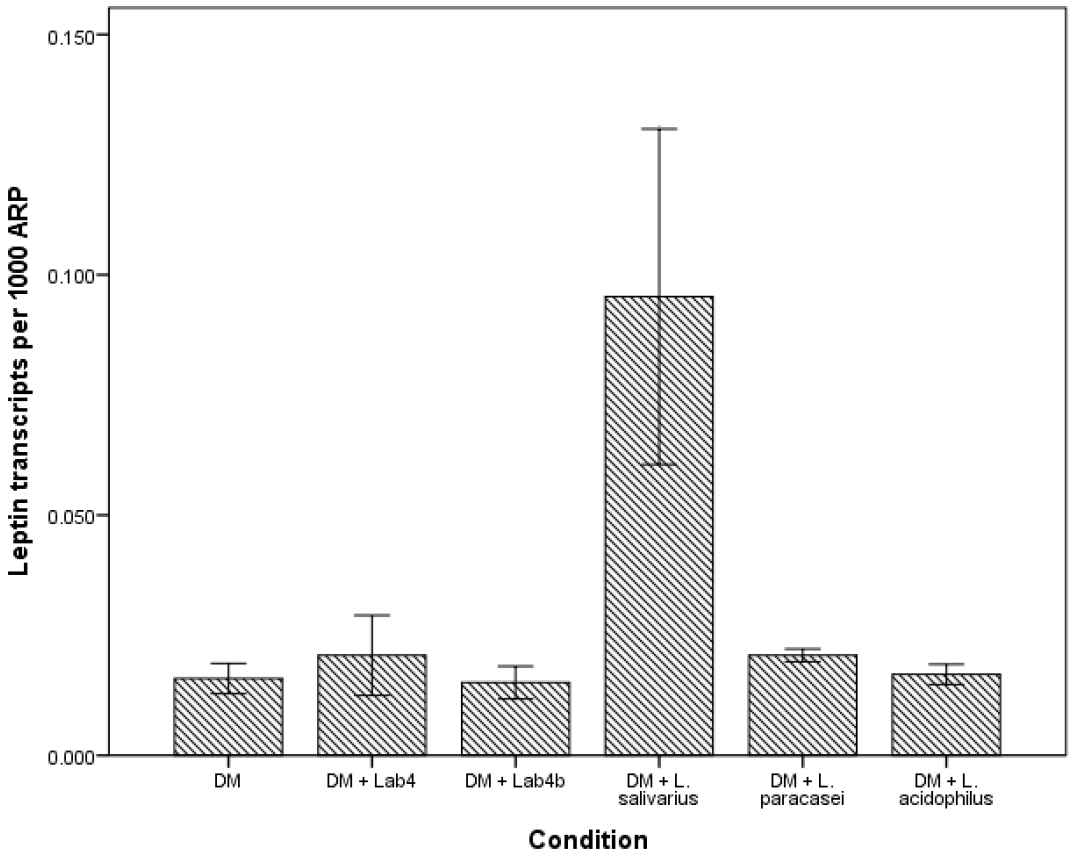

Figure. 5.4 – qPCR quantification of leptin in 3T3-L1 cells treated with DM diluted with DMEM:F12 or cell free supernatant of several bacterial strains after 10 days. Post-confluent 3T3-L1 cells were maintained for 10 days in either DM diluted 1:1 with DMEM:F12 (DM), or DM diluted 1:1 with CFS of various bacterial strains (DM + Lab4/Lab4b/*L. salivarius*/*L. paracasei*/*L. acidophilus*), RNA extracted, reverse transcribed, and subjected to qPCR. Leptin transcripts at day 10 were not significantly different between any treatment condition, though *L. salivarius* treatment showed a non-significant increase compared to control (p=0.236). Experiments were performed in triplicate wells, bars represent the mean of 2 individual experiments, error bars represent SEM.

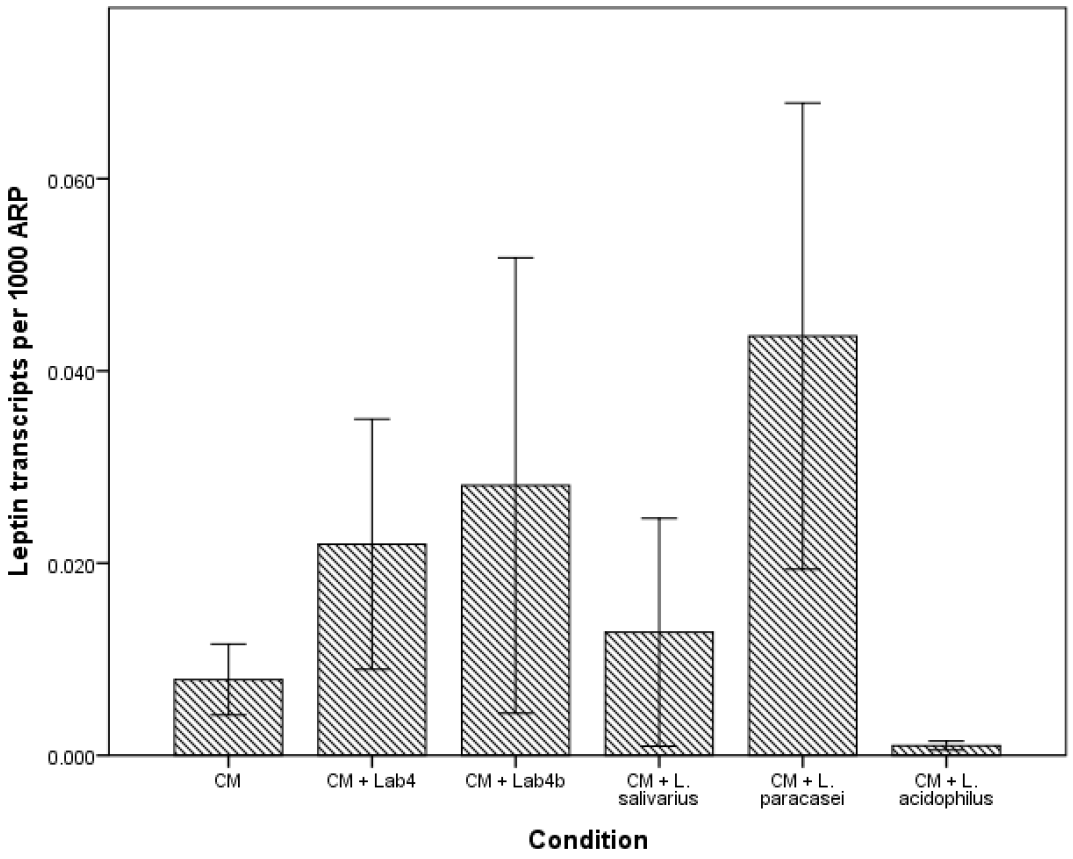

Figure. 5.5 – qPCR quantification of leptin in 3T3-L1 cells treated with CM diluted with DMEM:F12 or cell free supernatant of several bacterial strains after 10 days. Post-confluent 3T3-L1 cells were maintained for 10 days in either DM diluted 1:1 with DMEM:F12 (CM), or CM diluted 1:1 with CFS of various bacterial strains (CM + Lab4/Lab4b/*L. salivarius*/*L. paracasei*/*L. acidophilus*), RNA extracted, reverse transcribed, and subjected to qPCR. Leptin transcripts at day 10 did not show significant differences to control in any condition (p=0.226). Experiments were performed in triplicate wells, bars represent the mean of 2 individual experiments, error bars represent SEM.

qPCR quantification of ZIC1 transcripts in 3T3-L1 cells

ZIC1 was positively identified in 3T3-L1 cells in the present study through Sanger sequencing of PCR products obtained from cells differentiated for 7 days in undiluted DM for the purposes of producing standards for absolute quantification of transcripts

by qPCR. Despite this positive identification, ZIC1 mRNA was not found subsequently in either control or experimental conditions assessed via qPCR.

qPCR quantification of UCP1 transcripts in 3T3-L1 cells

UCP1 transcripts were detectable in CM conditions at lower levels than DM conditions, ranging from 1.04 ± 0.19 to 4.74 ± 0.44 UCP1 transcripts per 1000 ARP in CM control and CM + L. *acidophilus* respectively. Transcription in DM conditions was markedly higher, ranging from ~25 to ~50 UCP1 transcripts per 1000 ARP. Interestingly, most treatment conditions displayed a lower mean level of UCP1 transcription than DM control (25.5 ± 4.13), whereas the DM + L. *acidophilus* treated group displayed an increased mean of 47.9 ± 19.6 UCP1 transcripts per 1000 ARP.

One-way between subjects ANOVA tests were conducted on transcripts of UCP1 expressed per 1000 transcripts of ARP as a reference gene. A significant effect of the use of CFS was observed on UCP1 transcripts in DM conditions at p=<0.05, data violated the assumption of homogeneity of variances, necessitating a Welch F test (F (5,5.385) = 4.815, p=0.049). Post-hoc comparisons were performed using the Dunnett's T3 test. Post-hoc pairwise comparisons revealed that no condition was significantly different from any other, though treatment with DM + *L. salivarius* (11.7 ± 2.27) non-significantly reduced transcripts of UCP1 compared to control (25.5 ± 4.13) (p=0.082). The only treatment condition showing a mean increase in transcripts of UCP1 compared to control was DM + *L. acidophilus* (47.9 ± 19.6), though this was also non-significant (p=0.645). Results are summarised in Figure 5.6.

In CM conditions, a significant effect of the use of CFS was observed on UCP1 transcripts at p=<0.05, data violated the assumption of homogeneity of variances, necessitating a Welch F test (F (5,5.337) = 13.397, p=0.005). Post-hoc comparisons were performed using the Dunnett's T3 test. All conditions except CM + *L. acidophilus* displayed no significant difference to control, whereas CM + *L. acidophilus* treatment significantly increased UCP1 transcription (4.74 ± 0.44) compared to CM control (1.04 ± 0.19) (p=0.008), results shown in Figure 5.7. Caution should be applied interpreting results for UCP1 transcription as data are from a single experiment.

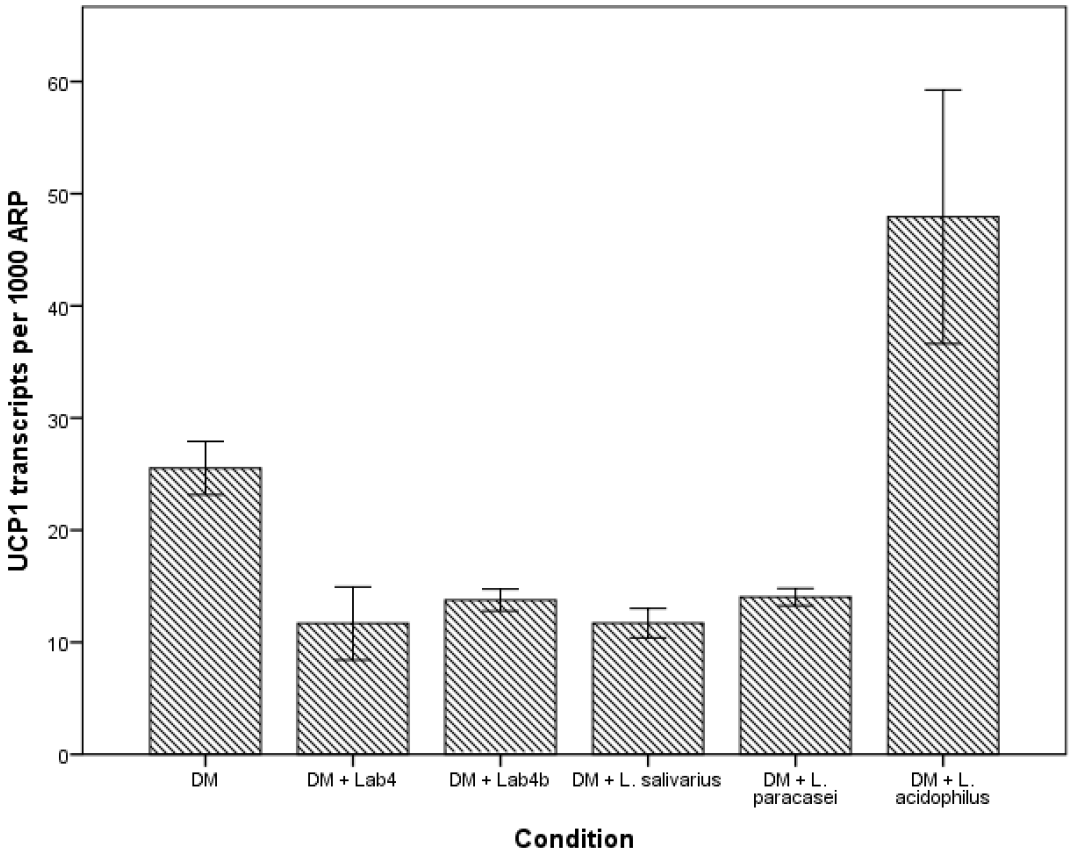

Figure. 5.6 – qPCR quantification of UCP1 in 3T3-L1 cells treated with DM diluted with DMEM:F12 or cell free supernatant of several bacterial strains after 10 days. Post-confluent 3T3-L1 cells were maintained for 10 days in either DM diluted 1:1 with DMEM:F12 (DM), or DM diluted 1:1 with CFS of various bacterial strains (DM + Lab4/Lab4b/*L. salivarius*/*L. paracasei*/*L. acidophilus*), RNA extracted, reverse transcribed, and subjected to qPCR. UCP1 transcripts at day 10 did not show significant differences to control in any condition, nor were significant differences observed between treatment conditions. DM + L. *salivarius* showed non-significantly decreased UCP1 transcription compared to control (p=0.082). Experiments were performed in triplicate wells, bars represent the mean of a single experiment, error bars represent SEM.

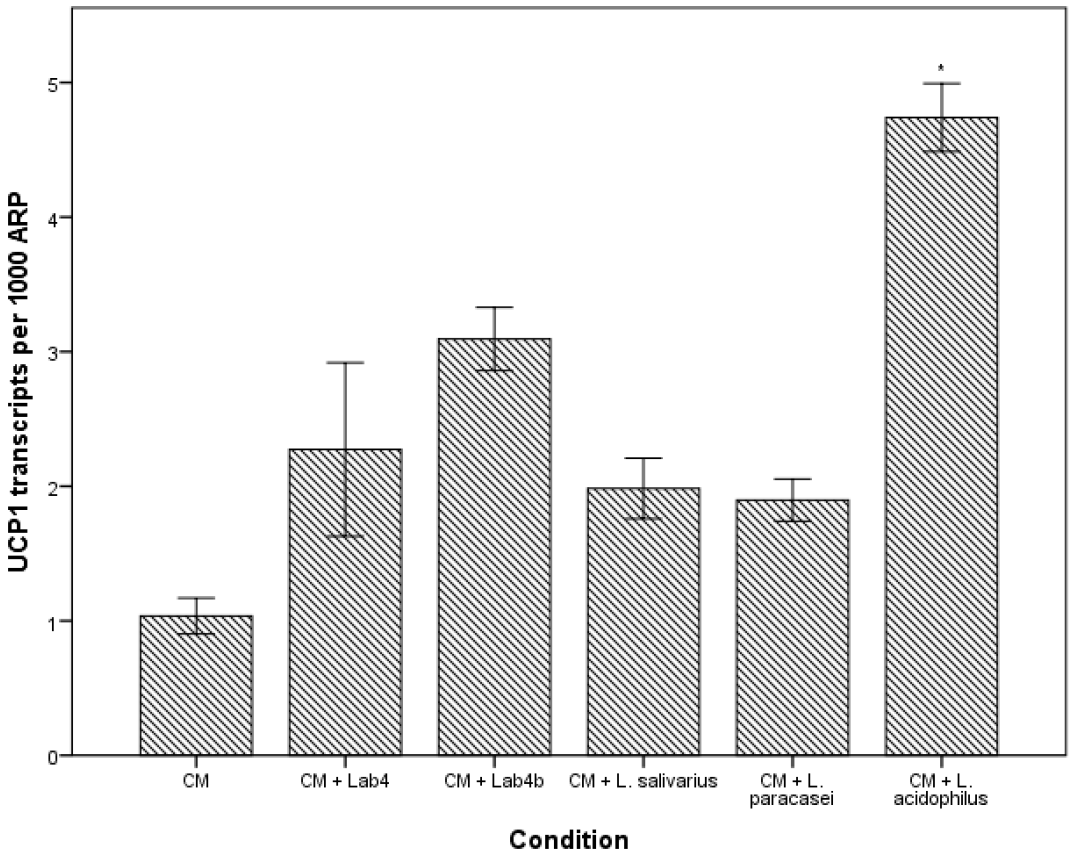

Figure. 5.7 – qPCR quantification of UCP1 in 3T3-L1 cells treated with CM diluted with DMEM:F12 or cell free supernatant of several bacterial strains after 10 days. Post-confluent 3T3-L1 cells were maintained for 10 days in either CM diluted 1:1 with DMEM:F12 (CM), or CM diluted 1:1 with CFS of various bacterial strains (CM + Lab4/Lab4b/*L. salivarius*/*L. paracasei*/*L. acidophilus*), RNA extracted, reverse transcribed, and subjected to qPCR. UCP1 transcripts at day 10 were significantly higher in CM + *L. acidophilus* compared to control (p=0.008). Experiments were performed in triplicate wells, bars represent the mean of a single experiment, error bars represent SEM.

qPCR quantification of PGC1-α transcripts in 3T3-L1 cells

Similar to UCP1, PGC1-α transcripts were more abundant in DM conditions than CM conditions. In CM conditions, transcripts ranged from 0.60 ± 0.35 per 1000 ARP in CM + L. *salivarius* treated cells to 1.05 ± 0.18 per 1000 ARP in CM + L. *acidophilus* treated cells, though no condition seemed markedly different from another despite results in

UCP1. In DM conditions, transcripts ranged from 4.66 ± 2.96 per 1000 ARP in DM + L. *salivarius* treated cells to 17.8 ± 16.7 per 1000 ARP in DM + L. *acidophilus* treated cells.

One-way between subjects ANOVA tests were conducted on transcripts of PGC1-α expressed per 1000 transcripts of ARP as a reference gene. In DM conditions, no significant effect of the use of CFS was observed on PGC1-α transcripts at p=<0.05, data violated the assumption of homogeneity of variances, necessitating a Welch F test ($F(5,12.343) = 0.757$, p=0.597). Results are summarised in Figure 5.8.

Similarly, in CM conditions, no significant effect of the use of CFS was observed on PGC1-α transcripts at p=<0.05, data violated the assumption of homogeneity of variances, necessitating a Welch F test ($F(5,10.257) = 1.218$, p=0.367). Results summarised in Figure 5.9.

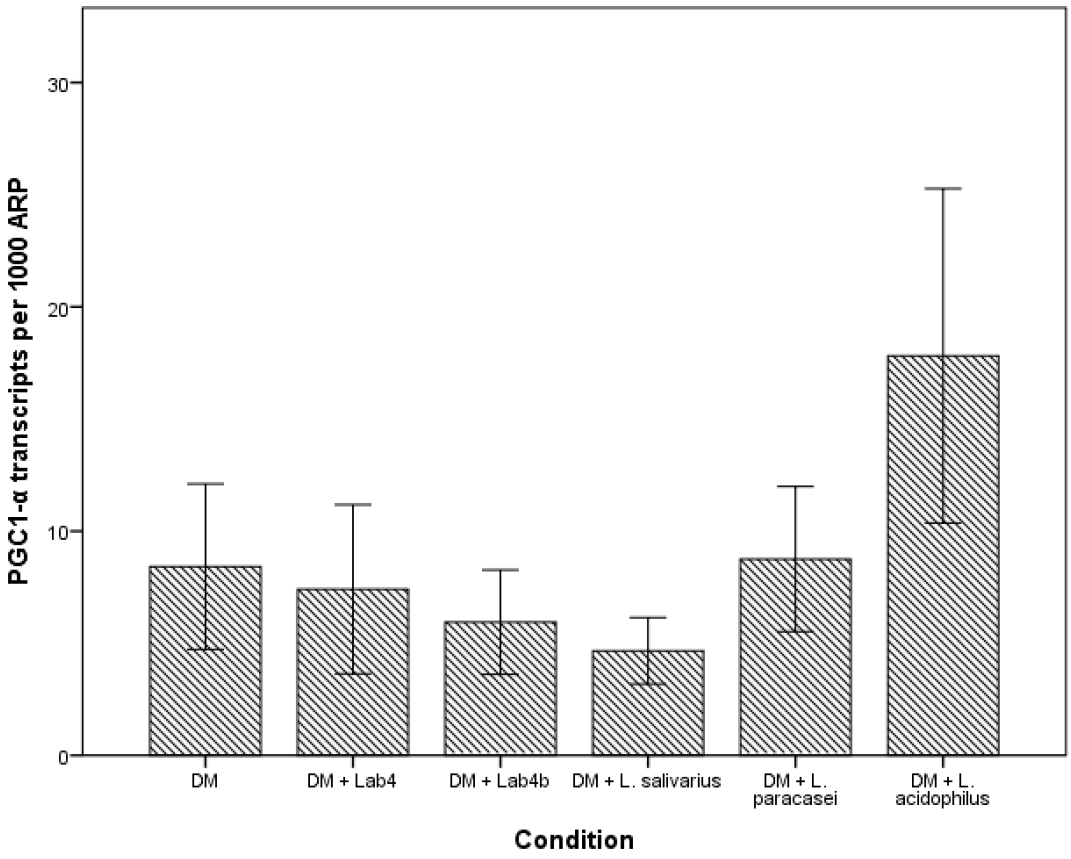

Figure. 5.8 – qPCR quantification of PGC1-α in 3T3-L1 cells treated with DM diluted with DMEM:F12 or cell free supernatant of several bacterial strains after 10 days. Post-confluent 3T3-L1 cells were maintained for 10 days in either DM diluted 1:1 with DMEM:F12 (DM), or DM diluted 1:1 with CFS of various bacterial strains (DM + Lab4/Lab4b/*L. salivarius*/*L. paracasei*/*L. acidophilus*), RNA extracted, reverse transcribed, and subjected to qPCR. PGC1-α transcripts at day 10 did not show significant differences to control in any condition (p=0.597). Experiments were performed in triplicate wells, bars represent the mean of 2 individual experiments, error bars represent SEM.

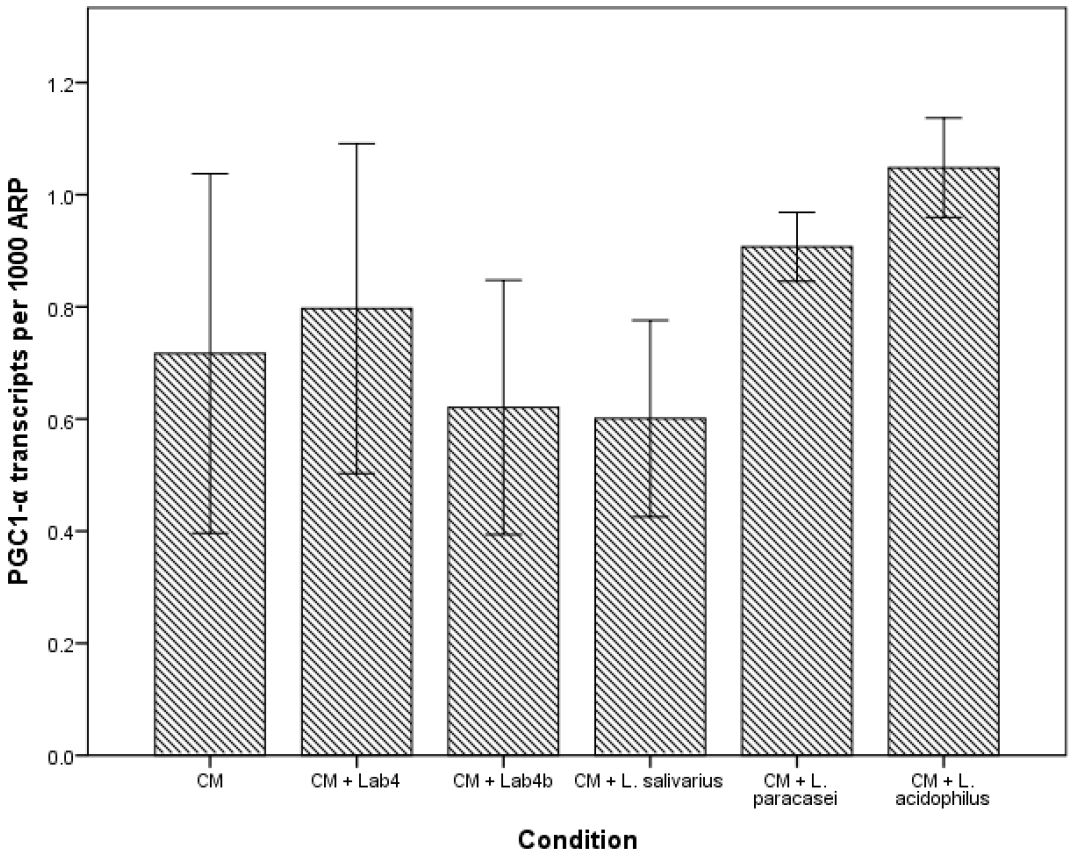

Figure. 5.9 – qPCR quantification of PGC1-α in 3T3-L1 cells treated with CM diluted with DMEM:F12 or cell free supernatant of several bacterial strains after 10 days. Post-confluent 3T3-L1 cells were maintained for 10 days in either CM diluted 1:1 with DMEM:F12 (CM), or CM diluted 1:1 with CFS of various bacterial strains (CM + Lab4/Lab4b/*L. salivarius*/*L. paracasei*/*L. acidophilus*), RNA extracted, reverse transcribed, and subjected to qPCR. PGC1-α transcripts at day 10 did not show significant differences to control in any condition (p=0.367). Experiments were performed in triplicate wells, bars represent the mean of 2 individual experiments, error bars represent SEM.

qPCR quantification of CITED1 transcripts in 3T3-L1 cells

As seen in UCP1 and PGC1-α data, transcripts of CITED1 were roughly 10 times more abundant in DM conditions compared to CM conditions. However, transcription was more in line with leptin data, and was not as robustly transcribed as UCP1 and PGC1-α. In CM conditions, transcripts ranged from 0.004 ± 0.001 per 1000 ARP in CM + L.

salivarius treated cells to 0.015 ± 0.007 per 1000 ARP in CM + Lab4 treated cells, though most conditions appeared similar to control. In DM conditions, transcripts ranged from 0.05 ± 0.03 per 1000 ARP in DM + L. *salivarius* treated cells to 0.19 ± 0.10 per 1000 ARP in DM + Lab4 treated cells.

One-way between subjects ANOVA tests were conducted on transcripts of CITED1 expressed per 1000 transcripts of ARP as a reference gene. In DM conditions, no significant effect of the use of CFS was observed on CITED1 transcripts at p=<0.05, data violated the assumption of homogeneity of variances, necessitating a Welch F test ($F(5,8.744) = 1.606$, p=0.255). Results are summarised in Figure 5.10.

Similarly, in CM conditions no significant effect of the use of CFS was observed on CITED1 transcripts at p=<0.05, data violated the assumption of homogeneity of variances, necessitating a Welch F test ($F(5,6.415) = 1.606$, p=0.056). Due to the Welch F test suggesting a possible trend towards significance, post-hoc comparisons were performed using the Dunnett's T3 test. Post-hoc pairwise comparisons revealed that no condition was significantly different from any other, though treatment with CM + *L. salivarius* (0.004 ± 0.001) non-significantly reduced transcripts of CITED1 compared to control (0.009 ± 0.002) (p=0.150).Results are summarised in Figure 5.11.

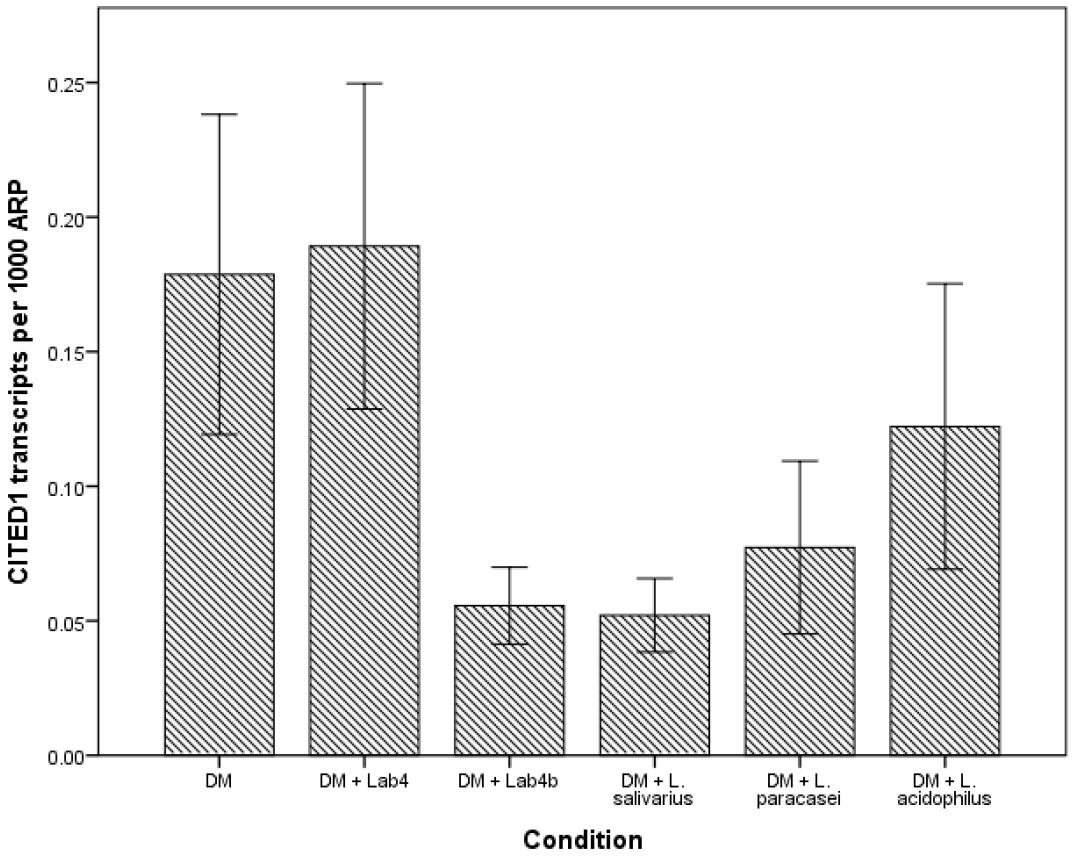

Figure. 5.10 – qPCR quantification of CITED1 in 3T3-L1 cells treated with DM diluted with DMEM:F12 or cell free supernatant of several bacterial strains after 10 days. Post-confluent 3T3-L1 cells were maintained for 10 days in either DM diluted 1:1 with DMEM:F12 (DM), or DM diluted 1:1 with CFS of various bacterial strains (DM + Lab4/Lab4b/*L. salivarius*/*L. paracasei*/*L. acidophilus*), RNA extracted, reverse transcribed, and subjected to qPCR. CITED1 transcripts at day 10 did not show significant differences to control in any condition (p=0.255). Experiments were performed in triplicate wells, bars represent the mean of 2 individual experiments, error bars represent SEM.

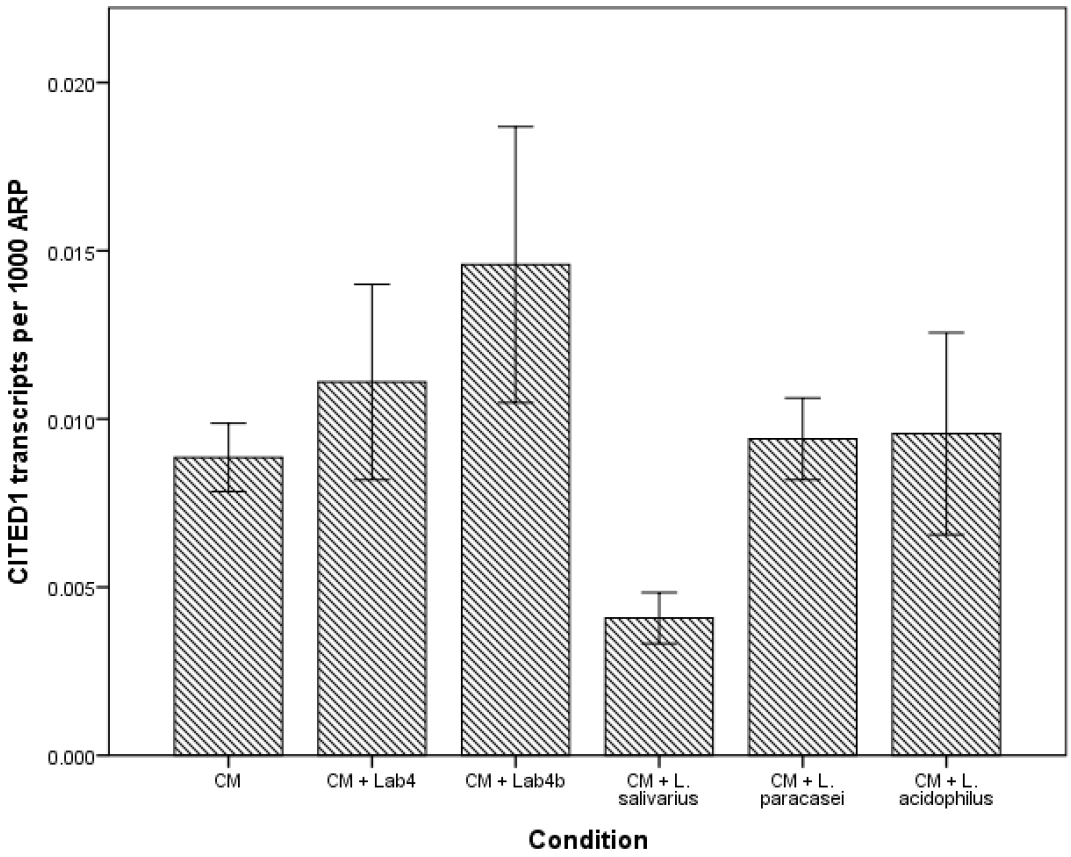

Figure. 5.11 – qPCR quantification of CITED1 in 3T3-L1 cells treated with CM diluted with DMEM:F12 or cell free supernatant of several bacterial strains after 10 days. Post-confluent 3T3-L1 cells were maintained for 10 days in either CM diluted 1:1 with DMEM:F12 (CM), or CM diluted 1:1 with CFS of various bacterial strains (CM + Lab4/Lab4b/*L. salivarius*/*L. paracasei*/*L. acidophilus*), RNA extracted, reverse transcribed, and subjected to qPCR. CITED1 transcripts at day 10 did not show significant differences to control in any condition (p=0.056). Experiments were performed in triplicate wells, bars represent the mean of 2 individual experiments, error bars represent SEM.

5.4 – Discussion

Leptin

Leptin has been widely used as a marker of WAT in primary cultures, and is considered a classical marker of WAT (Ussar *et al*., 2014). However, expression of leptin in 3T3-L1 cells is markedly lower than in primary adipocytes; leptin mRNA is mostly absent in 3T3-L1 preadipocytes, but transcription increases during the course of differentiation (MacDougald *et al*., 1995). This low level of expression in 3T3-L1 cells appears to be an accepted phenomenon (Kuroda *et al*., 2016), but no work in the literature appears to address its validity as a marker in 3T3-L1 cells. No significant differences were observed in the gene expression of leptin in any conditions used in the present study. However, there was an intriguing non-significant increase in leptin transcripts in the DM + *L. salivarius* CFS treatment condition. Leptin transcripts were roughly 10-fold higher in DM conditions compared to CM conditions, indicating as in MacDougald *et al.* (1995) that transcription increases during the course of adipogenesis.

Due to wide variations in gene expression data mentioned in the course of the present study, data has proven challenging and due to a lack of robust data it remains difficult to draw conclusions. The finding that treatment of differentiating 3T3-L1 cells with *L. salivarius* non-significantly *increased* leptin transcription (results shown in Figure 5.4) was particularly puzzling; it is difficult to reconcile this finding with visual assessment of the cells during the differentiation period. *L. salivarius* CFS appeared to dramatically impact viability of cells, with a substantial number visibly detaching throughout treatment. Despite 3T3-L1 cells being a unipotent and presumably homogeneous population, some cells appeared resistant to this effect and maintained attachment to tissue culture plates. In DM, by the 10^{th} day of differentiation, a majority of cells display visible lipid droplets (Figure 5.12A), however when treated with *L. salivarius* CFS there are a large number of cells that do not display lipid accumulation, alongside a number of what were presumed to be lipid containing cells with enlarged cytoplasmic compartments (Figure 5.12B). However,

some of the spherical structures within these enlarged cells may be autophagosomes, and it remains to be seen whether this enlargement is a transient or stable event.

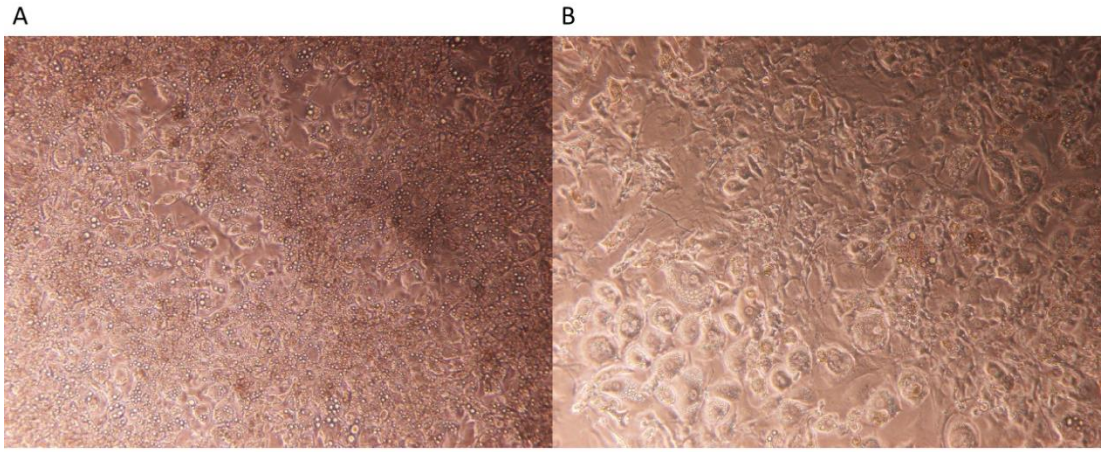

Figure 5.12 – Images of 3T3-L1 adipocytes at day 10. (A) 3T3-L1 cells maintained for 10 days post confluence in DM diluted 1:1 with DMEM:F12. A majority of cells display lipid droplet accumulation and rounded morphology. (B) 3T3-L cells maintained for 10 days post confluence in DM diluted 1:1 with CFS of *L. salivarius*. Some cells do not display lipid accumulation, while many of those that do have aberrant morphology and enlarged cytoplasm.

Given the typically low levels of expression in 3T3-L1 cells, any practical significance of an increase from 0.016 (± 0.007) transcripts per 1000 ARP transcripts to 0.095 (± 0.086) is unclear. The large standard deviation displayed in the DM + *L. salivarius* treatment reflects the fact that one well in the experimental condition displayed leptin gene expression near identical to DM, while the other 5 were between ~10-50 fold higher, but was not statistically deemed an outlier and thus not removed from data to prevent distortion by subjective determination of outliers. This single low reading may be reflective of death of cells in this well, but further data is needed.

This finding was initially believed to be an artefact of loss of cells reducing RNA yields in the first experiment, however this reduction of RNA yield did not occur in the second experiment. In terms of absolute numbers of transcripts, in the first experiment leptin transcripts were broadly similar to control, while ARP was proportionally lower, in accord with reduced RNA yield. In the second experiment, total ARP transcripts were broadly similar (though surprisingly slightly higher in the *L.*

salivarius treated condition) while total transcripts of leptin were an order of magnitude higher than control. This data seems to indicate that the increase in leptin gene expression is not merely a distortion caused by the loss of cells, however the similar level of ARP transcripts in the second experiment remains surprising given the widespread cell detachment. It is possible that the unusually large morphology of some of the cells counteracts this loss, but treatment may also impact transcription of ARP. Further research is needed to determine these results are upheld with further experimental repeats.

Serum leptin concentrations have been shown to correlate with BMI and adiposity in numerous human populations (Ruhl *et al*. 2007; Hu *et al*., 2001; Al Maskary and Alnaqdy, 2006). Adipocyte volume has also been shown to be associated with leptin secretion in human adipocytes (Skurk *et al*., 2007), and murine studies suggest a complex relationship in which adipose hypertrophy results in higher total leptin secretion, but lower levels of leptin secretion per volume of lipid (Guo *et al*., 2004). This raises the possibility that the possible increase in leptin mRNA in *L. salivarius* treated 3T3-L1 adipocytes is a reflection of the volume of the cell, but the reason and mechanisms for this expansion remains unclear.

ZIC1

Gene markers that may help distinguish between brown and beige adipocytes are an active area of research. One of the proposed BAT exclusive gene markers is Zinc in Cerebellum 1 (ZIC1), which displays robust expression in human brown adipocytes and is often undetectable in cultured white and beige adipocytes (Petrovic *et al.,* 2010; Waldén *et al*., 2012), and has been validated as a marker of murine BAT (de Jong *et al*., 2015). Its presence in 3T3-L1 cells has previously been obliquely referenced in the literature as detectable, though data was not shown (Seale *et al*., 2007). In the present study, while ZIC1 was apparently detected in 3T3-L1 cells used initially for sequencing and the production of standards, it was not detectable by qPCR in any condition in subsequent experiments. Standards were prepared using standard PCR, so relative quantities of transcripts in 3T3-L1 cells used for production

of standards compared to experimental cells are unknown. The low levels of ZIC1 expression in 3T3-L1 cells reported in the literature suggest it may be difficult to amplify consistently, it may still be present under experimental conditions, but below the limit of detection.

Under normal differentiation conditions, 3T3-L1 cells show gene expression similar to WAT, but are capable of displaying phenotypic characteristics of beige/BAT tissue (Morrison and McGee, 2015). The results shown in Morrison and McGee are particularly intriguing as under normal conditions 3T3-L1 cells displayed significantly greater expression of PGC1-α than BAT, but also that norepinephrine treated cells demonstrated increased transcription of pyruvate dehydrogenase kinase 4, which like ZIC1 is proposed to be a BAT selective marker (Wang and Seale, 2016). It should be noted that many proposed beige/BAT selective markers have been subsequently found not to be as useful for tissue classification as believed (de Jong *et al*., 2015), but the ability of 3T3-L1 cells to adopt beige/BAT characteristics and their relevance remains an open question. A study investigating knockdown of fat specific protein 27 in 3T3-L1 cells showed some morphological features consistent with beige/BAT (multilocular lipid droplets and increased mitochondrial number) without affecting expression of BAT associated genes (Keller *et al*., 2008). Keller *et al*. reported that ZIC1 is present in 3T3-L1 cells used in their study, but not in appreciable quantities. The role of ZIC1 in 3T3-L1 cells is thus uncertain and likely limited. To date no studies have shown conditions that enrich its expression in 3T3-L1 cells, which appears consistent with its use as a model of white adipocytes and ZIC1 as a marker of classical BAT. Difficulty detecting ZIC1 in the present study is therefore not an unexpected result.

UCP1

Results in the present study for UCP1 gene expression warrant extreme caution in interpretation. Data only represent results from a single experiment, and so results may simply display variation around a mean. The finding of a statistically significant increase of UCP1 transcripts in the CM + *L. acidophilus* condition is surprising and

intriguing. UCP1 is activated via lipolysis (Cannon and Nedergaard, 2004), but it has been suggested that undifferentiated 3T3-L1 cells show similar levels of lipolysis to differentiating cells, but that a greater proportion of fatty acids liberated through lipolysis become re-esterified within differentiating cells (Carnicero, 1984). UCP1 may therefore be present and functional in preadipocytes, however the practical significance of the observed increase in transcription is questionable, as transcripts increased from 1.04 ± 0.19 per 1000 ARP to 4.74 ± 0.44. As would be expected, transcription was more pronounced in DM treated conditions. Though the mean increase of UCP1 transcription in DM + *L. acidophilus* was non-significant, the broad effect of treatment seen in CM conditions was recapitulated, and it is possible with further experimental replicates that significance could be achieved. UCP1 and leptin transcription are reciprocally regulated in murine BAT (Cancello *et al*., 1998) and though decreases in leptin transcripts in CM + L. *acidophilus* treated cells were not statistically significant, this does suggest that there is a potential effect on adipose phenotype. However, there was also a non-significant increase of UCP1 transcripts in cells maintained in DM + L. *acidophilus,* but in these cells leptin transcription remained indistinguishable from DM control. UCP1 transcription appeared non-significantly lower in DM + L. *salivarius* treated cells, which did see a striking though non-significant increase in leptin transcription. However, cells maintained in DM + Lab4, Lab4b, and L. *paracasei* CFS also show similar levels of UCP1 transcripts to L. *salivarius* treated cells, but do not appear to have any increase in leptin transcription.

A possible explanation for the effect seen in L. *acidophilus* treated cells lies in the presumed content of the CFS. LAB such as L. *acidophilus* have been shown to efficiently produce lactic acid when cultured in MRS broth (Juárez Tomás *et al*., 2003). Phenol red indicator showed CFS to be at a pH of approximately 7.4. Under these conditions, a majority of lactic acid is believed to be present in its dissociated form, lactate (Lampe *et al*., 2009). Cold exposure, the classical activator of BAT, transiently raises circulating plasma lactate in mice, and lactate administration to both murine and human adipocytes *in vivo* induces thermogenic gene expression (Carrière *et al*., 2014). However, oral administration of butyrate increases UCP1 and PGC1-α expression in mice (Gao *et al*., 2009), and it appears that in BAT most fatty acids

activate UCP1, with effect dependent upon chain length (Shabalina *et al*., 2008). Thus, there is a scientific rationale for specific metabolic products of LAB to activate UCP1. However, further work is required to determine whether these results are reproducible in more than a single experiment, and what the precise composition of the CFSs used is. As leptin is expressed at a markedly lower level in 3T3-L1 cells compared to murine tissue, it is unclear whether the reciprocal transcriptional relationship is maintained in 3T3-L1 cells, and these results provide conflicting evidence.

PGC1-α

Though used as a non-specific marker of beige/BAT, PGC1-α has previously been shown to be highly expressed in differentiating 3T3-L1 adipocytes (Morrison and McGee, 2015). This data is likely to confound the use of PGC1-α as a marker of phenotype in 3T3-L1 cells, and much work is still needed to validate markers used for the classification of murine tissues for use in 3T3-L1 studies. In the present study, no treatment conditions significantly affected gene expression of PGC1-α. As mentioned in the introductory chapter, knockdown of PGC1-α in an immortalised cell line generated from murine BAT impairs induction of thermogenic genes without altering differentiation (Uldry *et al*., 2006). PGC1-α appears to be dispensable for BAT differentiation, but has a greater link to response to cold exposure. As cells in the present study were maintained at 37˚C, cold exposure was an infrequent occurrence experienced only transiently by cultured cells during visual assessment and infrequent media changes. A previous study has shown that 3T3-L1 cells robustly express UCP1 when cultured at 31˚C, and in 3T3-F442A adipocytes both UCP1 and PGC1-α are inducible by temperature manipulation (Ye *et al*., 2013). Notably, Ye *et al*. showed that UCP1 transcription increased roughly 2-fold compared to control following only 1 hour of exposure to 31˚C. *In vivo* evidence suggests that paradoxically, following induction of transcription, UCP1 mRNA has a longer half-life in animals reintroduced to room temperature than in those maintained at 4˚C (Jacobsson *et al*., 1987). This raises the possibility that thermogenic gene

transcription can be induced with acute exposure to cold even in *in vitro* models, and that maintenance at physiological temperatures may prolong the period in which transcripts can be detected. It remains to be seen if this PGC1-α function is seen in 3T3-L1 cells, but if PGC1-α is more linked to the functional response to cold exposure than BAT identity then temperature would be an interesting variable to consider in any future study.

Unfortunately, the primers used in the present study target exons 4 and 5. PGC1-α in mice exists in multiple isoforms, often truncated due to alternative splicing introducing an in-frame stop codon. At least 2 isoforms (PGC1-α2 and PGC1-α3) do not contain exons 4 and 5, and novel isoforms are discovered with some regularity (Martínez-Redondo *et al*., 2015). While evidence suggests that the various PGC1-α isoforms exist at broadly similar levels in a range of murine tissues including BAT (Ruas *et al*., 2012) the same is not known in 3T3-L1 cells. Therefore, the results in the present study may underestimate total PGC1-α present in 3T3-L1 cells, and any future work seeking to quantify PGC-1α transcription should use primers specific to exon 2, which to the best of present knowledge is valid for all PGC1-α isoforms. It would also be useful to determine protein levels, which were not investigated in the present study due to time constraints. However, despite potential underestimation, data indicates that for a majority of known PGC1-α isoforms, the treatment of 3T3-L1 cells with CFS has no significant effect on gene expression.

CITED1

CITED1 was proposed to be a beige selective tissue marker, but has subsequently been shown to be less informative regarding tissue classification, though it may be reflective of norepinephrine response (de Jong *et al*., 2015). No statistically significant differences were observed in the present study, and levels of expression were uniformly low. Interestingly, though non-significant, CITED1 transcription was lowest in L. *salivarius* treated cells, which may be a reflection of the non-significant increase in leptin transcripts seen in CM + L. *salivarius* treated cells if CITED1 is valid as a marker of adipose phenotype in 3T3-L1 cells. As in all other genes, expression of

CITED1 appeared greater overall in DM conditions than CM conditions, suggesting its expression increases during the course of differentiation. The lack of any significant differences between conditions accords with its proposed functional role in norepinephrine response, which would not be expected in cells cultured in conditions as used in the present study, however the non-significant decreases seen in certain treatment conditions is an avenue of further research that may be worth exploring alongside further data on leptin transcription.

Chapter 6: Effects of bacterial cell free supernatant on adipogenesis in human primary preadipocytes

6.1 – Introduction

Research into the microbiota is complicated due to the complexity of the field, and the nascent state of many techniques. Present data indicates that *Lactobacilli* are vastly more abundant in the murine microbiota than in humans (Nguyen *et al*., 2015), and as there is a suggestion that microorganisms have evolved alongside humans and are involved in innate immunity, it is possible that murine and human cells possess different responses to certain bacteria. Further, though the 3T3-L1 cell line has been the source of much knowledge regarding the processes of adipogenesis, murine and human adipogenesis have notable differences. It has been suggested that MCE is not an obligatory process for the induction of adipogenesis in primary human preadipocytes, with reports of human preadipocytes not displaying evidence of MCE (Newell *et al*., 2006) and experiments using mitotic inhibitors not preventing differentiation (Entenmann and Hauner, 2006). However, similar experimental evidence has been shown in 3T3-L1 cells (Qiu *et al*., 2001) though this remains a matter of controversy as to whether MCE is prevented or merely delayed (Tang *et al*., 2003). There are also differences between murine and human adipocytes that are particularly important to the study of BAT-selective gene markers in adipose tissue; there is evidence to suggest that BAT in adult humans is more similar to murine beige adipose tissue on a molecular level (Wu *et al*., 2012). The use of primary human preadipocytes also allows for a model that more closely reflects adipose depot specific properties (Ruiz-Ojeda *et al*., 2016), which is particularly valuable in the study of obesity. Primary cultures of human preadipocytes are therefore a valuable resource for research into adipogenesis. However, they are considerably more difficult to work with than 3T3-L1 cells, with a far longer population doubling time, and far lower rates of adipogenesis compared to 3T3-L1 cells (Draman *et al*., 2013). However, as Lab4 and Lab4b are fundamentally bacterial products for use in humans, the effects of Lab4 and Lab4b CFS were investigated in primary human preadipocytes to assess potential effects on *in vitro* adipogenesis.

6.2 – Materials and methods

Human primary preadipocyte cells were a generous gift from Dr. Lei Zhang. A list of reagents used, and their suppliers is given in Appendix 1, Table 1. Media was prepared as in chapter 3.2

Cell culture

All samples were obtained with written informed consent and the approval of Wales REC 1 (formerly South East Wales) research ethics committee, REC reference 12/WA/0285. Cryopreserved subcutaneous preadipocytes from 3 patients without metabolic disease at passage 3 were seeded in T75 flasks and maintained in CM until approximately 70% confluent. Cells were trypsinised and seeded in 6-well plates and maintained in 0.5ml CM per well until approximately 90% confluent. Media was replaced in post-confluent cells in triplicate wells in treatment conditions listed in Table 6.1. Experiments were performed at passage 4-5.

Patient characteristics

Table 6.1 – Composition of treatment conditions used for human primary preadipocytes

Condition	Composition
CM	Complete media diluted 1:1 with DMEM:F12
DM	Differentiation media diluted 1:1 with DMEM:F12
DM + Lab4	Differentiation media diluted 1:1 with Lab4 CFS
DM + Lab4b	Differentiation media diluted 1:1 with Lab4b CFS

CFS was prepared as previously. Initiation of treatment was designated as day 0, media was changed every 72 hours or sooner if subjective assessment of phenol red indicator was deemed acidic. ORO staining and adipogenic foci counting was performed at 15 days.

Oil Red O staining

ORO staining was performed as in chapter 4.2.

Adipogenic foci counting

At day 15, cells were imaged (Nikon Diaphot Microscope, Nikon) at 10x magnification by light microscopy using ViewFinder software (version 3.0.1, Better Light Inc., California, USA) and images of 10 representative visual fields (determined subjectively) per well were saved. As in prior work in our laboratory (Rice *et al*., 2010; Draman *et al.,* 2017) groups of cells displaying accumulation of lipid droplets were manually counted by a single researcher in each of the 10 visual fields per well and totals recorded (i.e. totals of 10 visual fields were taken as one observation).

6.3 – Results

Adipogenic foci counting

Anticipating that ORO staining may not detect significant differences between CM and DM conditions in cells with low adipogenic potential (previous work in our laboratory suggests at maximum 10% of primary preadipocytes will differentiate (Draman *et al*., 2013)), another technique to quantify adipogenesis was employed. Images of 10 visual fields per well were saved prior to ORO staining. Adipogenic foci in these 10 visual fields were counted, data presented in Figure 6.1.

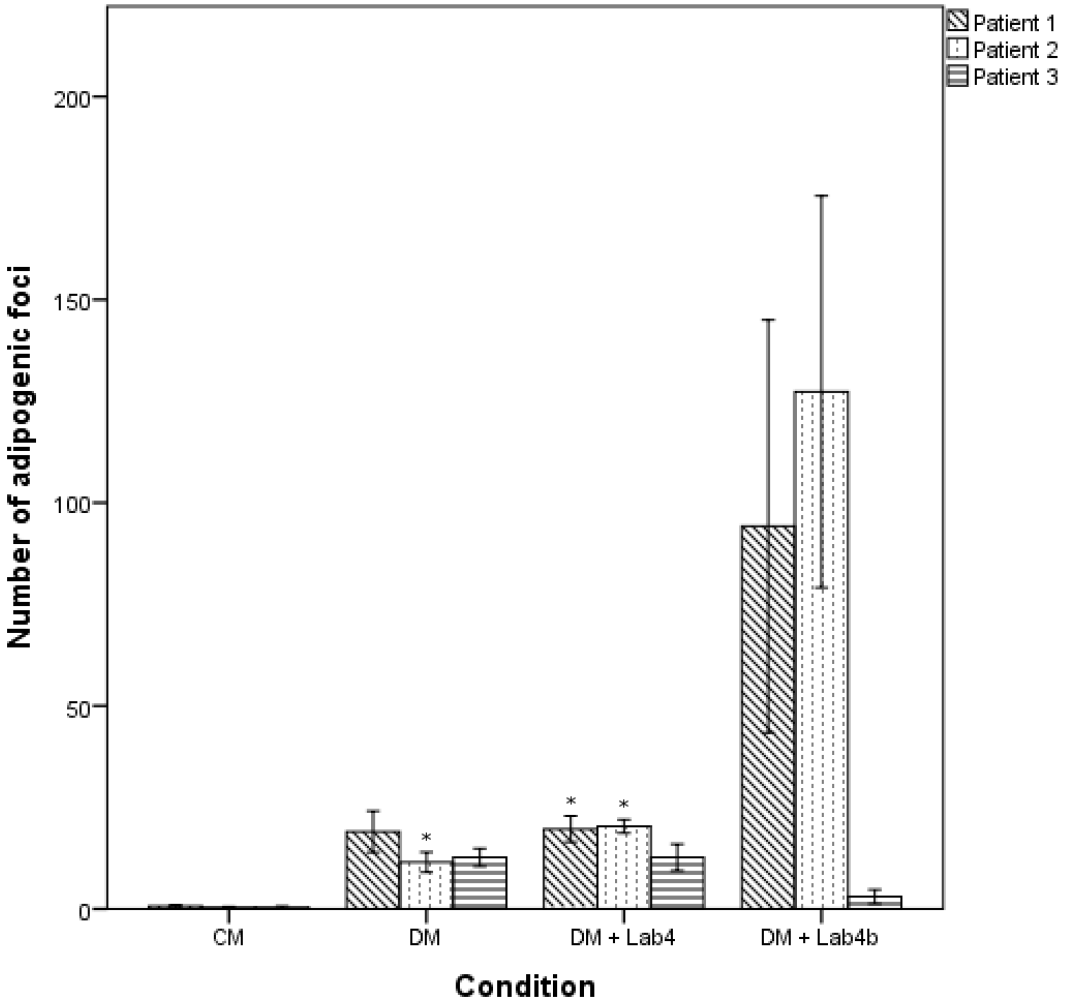

Figure 6.1. – Adipogenic foci counts of primary human preadipocyte cells at day 15 after treatment with cell free supernatant. Post-confluent human primary preadipocyte cells were maintained in either CM/DM diluted 1:1 with DMEM:F12 (CM and DM respectively), or DM diluted 1:1 with CFS of Lab4 or Lab4b (DM + Lab4/Lab4b). Adipogenic foci counting was performed at day 15. Diagonally striped bars represent results from patient 1, stippled bars represent results from patient 2, horizontally striped bars represent results from patient 3. No significant differences were found between DM conditions, though in two patients significant differences were indicated between CM and DM + Lab4. In one experiment, DM + Lab4b treatment appeared to result in a large increase in number of lipid accumulating cells, though statistical significance was not achieved. Experiments were performed in triplicate wells, bars for patients 1 and 2 represent the mean of 2 individual

experiments, bars for patient 3 represent the mean of a single experiment, error bars represent SEM. Asterisk denotes significant difference at $p = <0.05$ from CM only

Foci counting was able to distinguish between CM and DM conditions, however the co-appearance of lipid droplets extracellular bodies (speculated to be apoptotic bodies) and unusual patterns of lipid accumulation in treatment conditions coupled with inexperience with the technique and low-resolution images made suitably accurate quantification extremely difficult. Further, there appeared to be far greater cytotoxic effects of DM + Lab4b CFS in the first experiment compared to the second. Though aliquots of CFS from the same batch were used, the second experiment took place approximately 2 weeks after the first, during which time the prepared CFS + appropriate culture media was stored at 4˚C and not freshly thawed and mixed. The initial experiment was performed at passage 4, the second at passage 5. In the second experiment, DM + Lab4b CFS treated cells displayed an extreme increase in the number of cells accumulating lipids, to the extent that nearly every cell in a given visual field displayed evidence of lipid accumulation. The distribution of these vacuoles within cells appeared different to the pattern seen in differentiating cells treated with DM alone. In DM, a small number of cells appear to differentiate, displaying numerous multilocular lipid droplets that form a distinct cluster in close proximity (Figure 6.2A), whereas in DM + Lab4b CFS, a large number of cells appear to accumulate small amounts of lipid, which are often distributed throughout the cell rather than in a single cluster (Figure 6.2B). Figure 6.3 shows cells differentiating at a low level as expected in DM (Figure 6.3A) and the relative difficulty of properly classifying regions of still images due to soluble bodies (Figure 6.3B)

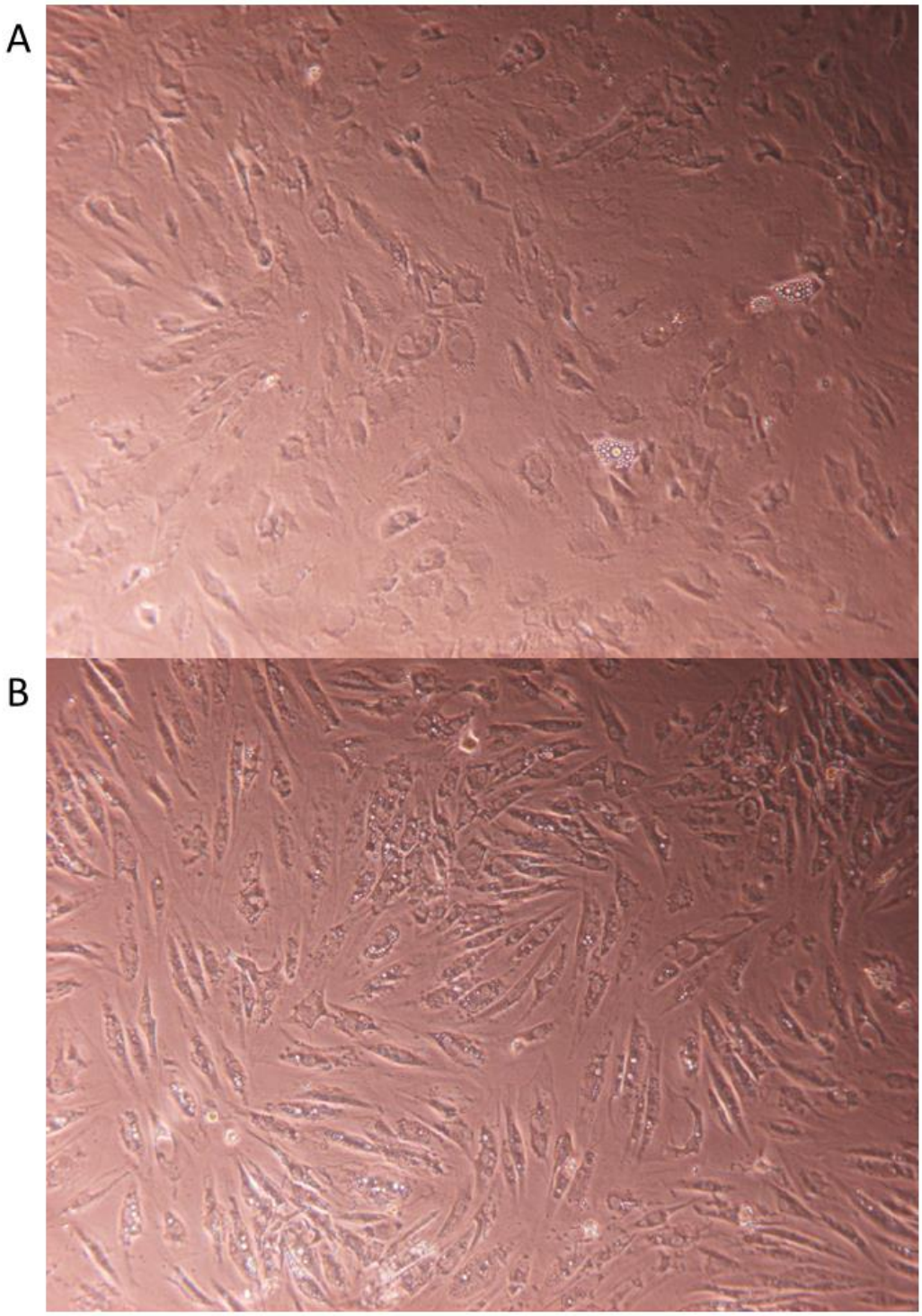

Figure. 6.2 – Images of human primary preadipocytes at day 15. Representative image of cells cultured in DM diluted 1:1 with DMEM:F12 (A) and DM + Lab4b CFS (B). In cells maintained in DM diluted 1:1 with DMEM:F12, a small number of cells differentiate, accumulating a relatively large amount of lipid. In cells that survive DM + Lab4b treatment, a large number of cells appear to accumulate a small amount of lipid, which is distributed differently within cells.

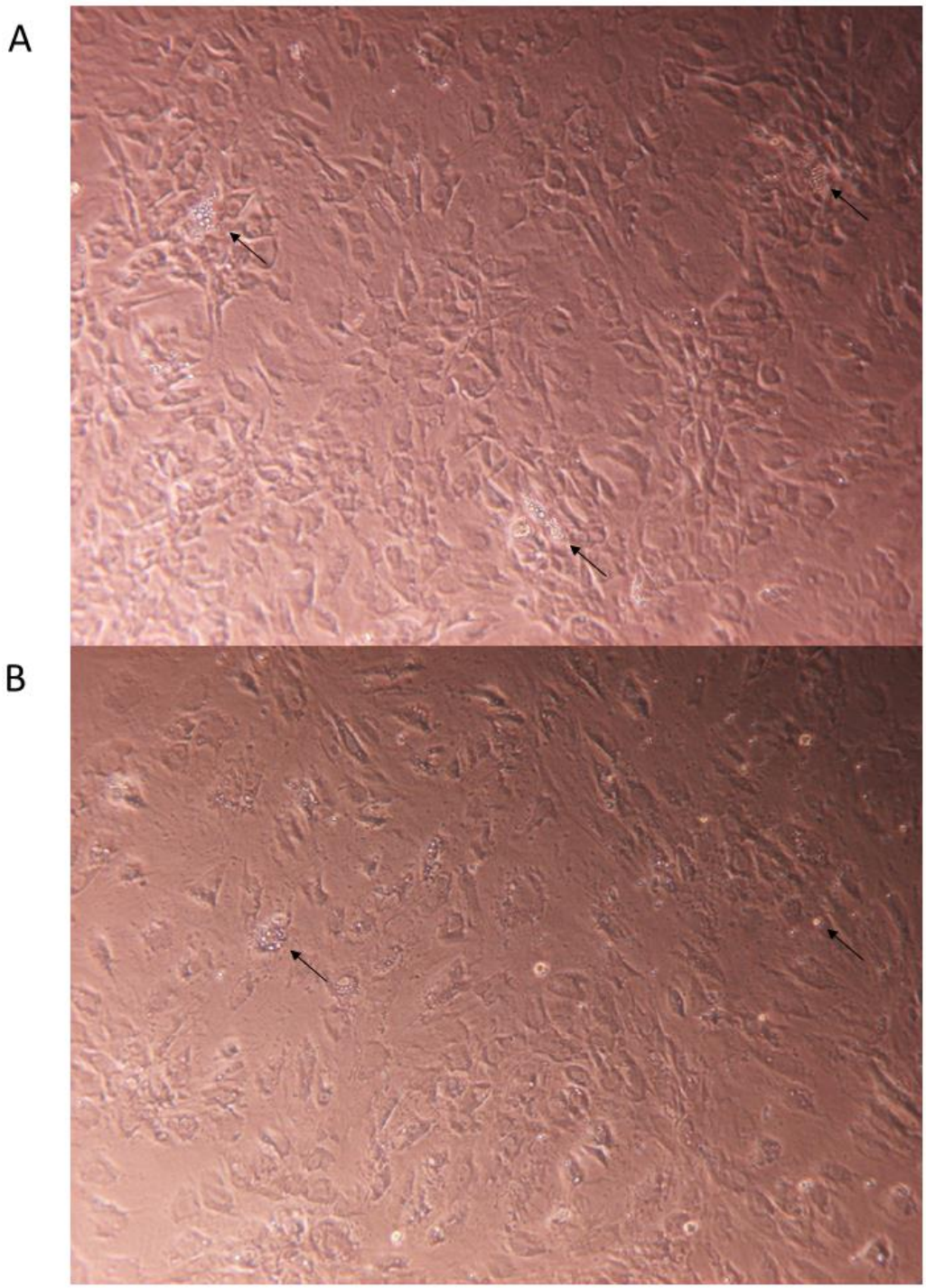

Figure. 6.3 – Images of human primary preadipocytes at day 15. (A) Cells maintained in DM diluted 1:1 with DMEM:F12 shows distinct adipogenic foci (arrows) and cell morphology (B) cells maintained in DM + Lab4 CFS show some distinct regions of adipogenesis, but the upper right hand of the field is difficult to interpret due to visual elements that may be lipid droplets or extracellular soluble bodies. Cells are from the same patient as those in Figure 6.2.

One way between subjects ANOVA was performed in data on a per-patient basis, as profound cytotoxicity in cells from patient 3 suggested data between patients may not be comparable. In patient 1 data violated the assumption of homogeneity of variances, necessitating a Welch F test; significant differences were observed between groups at p=<0.05 (F (3,7.736) = 14.566, p=0.001). A post-hoc Dunnett's T3 test was performed for pairwise comparisons, differences in foci counts between CM (0.7 ± 0.8) and DM (19 ± 12.4) were perhaps trending towards significance (p=0.067), though when compared to CM, DM + Lab4 CFS (19.7 ± 7.8) did significantly increase foci counts (p=0.009) whereas DM + Lab4b (94.2 ± 113.6) did not (p=0.465) likely due to large variance in data. However, when DM treatment conditions were compared to DM control, there were no significant differences observed in foci counts for DM + Lab4 (p=1) or Lab4b (p=0.639) .

In patient 2 data violated the assumption of homogeneity of variances, necessitating a Welch F test; significant differences were observed between groups at p=<0.05 (F (3,8.461) = 49.281, p=<0.001). A post-hoc Dunnett's T3 test was performed for pairwise comparisons, a significant difference was found in foci counts between CM (0.3 ± 0.5) and DM (11.5 ± 6.1) (p=0.029), as well as DM + Lab4 CFS (20.3 ± 4.0) (p=<0.001) but not DM + Lab4b (127.3 ± 118.1) (p=0.191) again likely due to large variance in data. However, compared to DM control, there were no significant differences observed in foci counts for DM + Lab4 (p=0.081) or Lab4b (p=0.246).

In patient 3 data violated the assumption of homogeneity of variances, necessitating a Welch F test; significant differences were observed between groups at p=<0.05 (F (3,3.479) = 11.112, p=<0.029). A post-hoc Dunnett's T3 test was performed for pairwise comparisons, however no significant differences were observed using the Dunnett's T3 test between pairs, likely as a result of the conservative nature of the test, the large variance in data, and the small number of observations. Non-significant differences were found in foci counts between CM (0.3 ± 0.6) and DM (12.7 ± 3.8) (p=0.084). Compared to DM control, no significant differences were found between either DM + Lab4 (12.7 ± 5.7) (p=1) or DM + Lab4b CFS (3 ± 3) (p=0.110) again likely due to large variance in data. Almost no adipogenic foci were observed in DM + Lab4b CFS treated cells due to profound cytotoxicity.

ORO staining

Post-confluent human primary preadipocytes from 3 patients were maintained for 15 days in CM or DM diluted 1:1 with DMEM:F12, or DM diluted 1:1 with CFS of Lab4 or Lab4b. ORO staining was performed on day 15, dye extracted, and optical density measured at 490nm. In all three patients, ORO staining did not appear to detect adipogenesis, with no observable differences seen between CM and DM, though mean optical density at 490nm actually appeared very slightly *lower* in DM compared to CM. DM + Lab4b showed what may have been a very slight increase in optical density at 490nm compared to DM control in patients 1 and 2.. One-way between subjects ANOVA tests were conducted on spectrophotometric data (corrected by subtracting the value of blank wells). In patient 1 no significant differences were observed in any condition at p=<0.05 ($F(3,20) = 1.689$, p=0.201). In patient 2 a significant effect of the use of CFS was observed at p=<0.05 ($F(3,21) = 4.833$, p=0.011). However, post-hoc comparisons using the Tukey HSD test indicated that the only significant differences were between DM + Lab4 (0.638 ± 0.010 AU) and Lab4b conditions (0.977 ± 0.010 AU, p=0.007), with no significant differences observed between DM + DMEM:F12 control (0.0753 ± 0.019 AU) and DM + Lab4 (p=0.639) or DM + Lab4b (p=0.085). In patient 3, no significant differences observed at p=<0.05 ($F(3,8) = 3.979$, p=0.053). Statistically this appeared to be trending towards significance, however results in samples from patient 3 are taken from a single experiment, as widespread cell death was apparent when treated with bacterial conditions and was not repeated. Data for all 3 patients is shown in Figure 6.4.

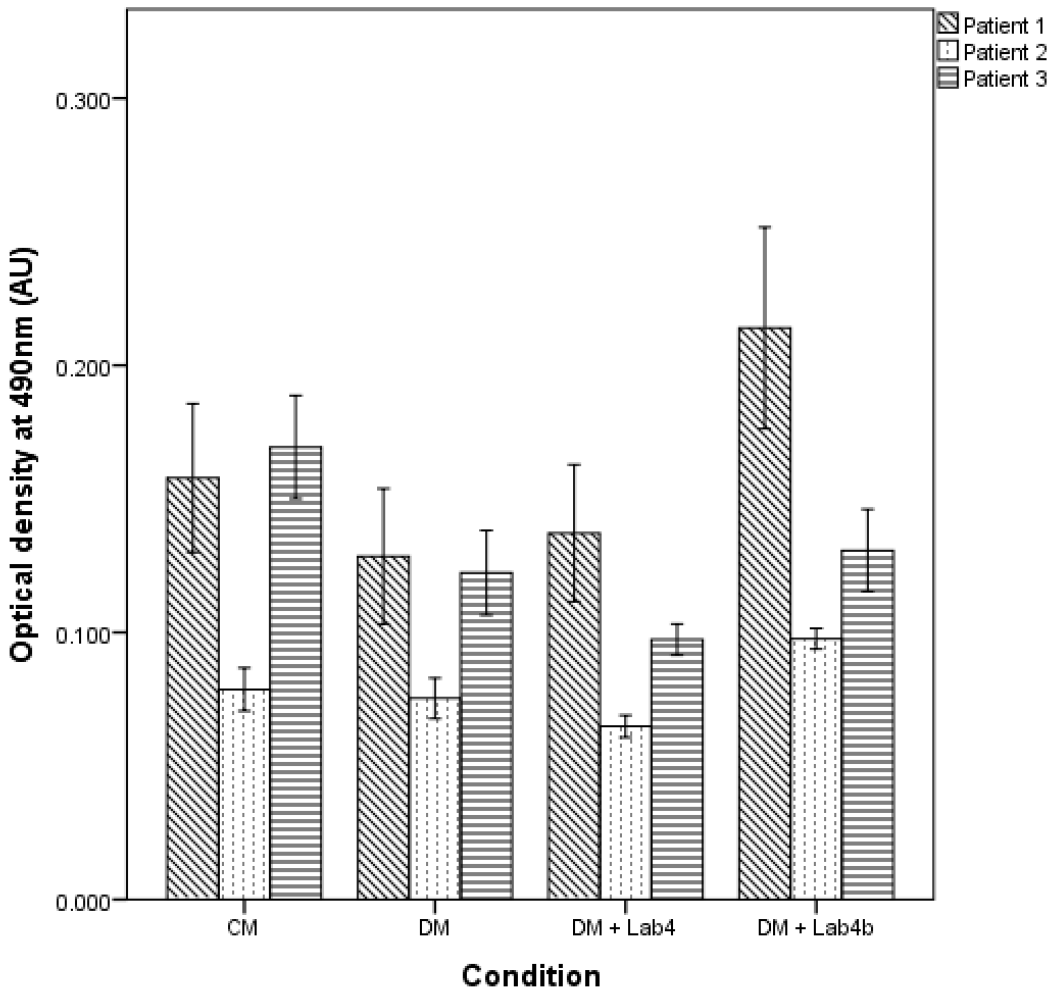

Figure. 6.4 – Oil Red O staining of human primary preadipocyte cells at day 15 after treatment with cell free supernatant. Post-confluent human primary preadipocyte cells were maintained in either CM/DM diluted 1:1 with DMEM:F12 (CM and DM respectively), or DM diluted 1:1 with CFS of Lab4 or Lab4b (DM + Lab4/Lab4b). ORO staining was performed, and dye extracted at day 15. Diagonally striped bars represent results from patient 1, stippled bars represent results from patient 2, horizontally striped bars represent results from patient 3. No significant differences were observed between experimental conditions and control. Experiments were performed in triplicate wells, bars for patients 1 and 2 represent the mean of 2 individual experiments, bars for patient 3 represent the mean of a single experiment, error bars represent SEM.

6.4 – Discussion

No significant differences were observed in any of the three patients between CM + DMEM:F12 and DM + DMEM:F12 conditions when measured by ORO staining. Under standard conditions, cultured primary preadipocytes exhibit relatively low adipogenic potential (Lee *et al*., 2012). Compounding this, in human primary preadipocytes, FCS can inhibit adipogenesis in a dose-dependent fashion (Lee *et al*., 2012). Experiments in the present study were conducted with 5% FCS after dilution of media with CFS, and FCS used in our laboratory is tested to minimise any effect on adipogenesis, so is unlikely to cause this. However, subculturing of human primary preadipocytes is known to be associated with increased population doubling time and decreased capacity to differentiate (Skurk *et al*., 2007). As cells were ultimately at passage 4 for experiments, it is likely that this had an impact on the ability of cells to differentiate. Further, though patients were known not to have metabolic disease, factors such as BMI can impact adipogenic potential (van Harmelen *et al*., 2003), and thus a number of unknown patient factors may have affected adipogenic capacity of primary preadipocytes.

Though ORO staining was inconclusive, perhaps the most intriguing results came from visual analysis. Quantitative visual analysis is heavily compounded by methodological problems which must be considered when assessing data. Concomitant appearance of what appeared to be enhanced lipid accumulation alongside large amounts of apoptosis, which appeared to vary in a subject-dependent manner, also hampered this analysis. In those samples which appeared to survive and undergo enhanced adipogenesis, counting adipogenic foci in low resolution images was an extremely difficult task, as lipid droplets were numerous, cell boundaries often difficult to distinguish, and what appeared to be apoptotic bodies presented similarly to lipid droplets in still images. Despite this, a distinct morphological difference is seen in surviving human primary preadipocyte cells treated with DM + Lab4b CFS. Due to extreme variation in the data caused by more pronounced cytotoxic effects in the first experiment than the second, Lab4b CFS treated conditions were not found to be statistically significantly different from any other,

but the magnitude of the effect observed is striking compared to the minimal amounts of lipid accumulation seen under normal conditions. It is unclear why the effects of the same aliquots of CFS had such markedly different results, and may be a result of the longer storage period a 4˚C, or may be related to the incremental passaging of cells.

To date, no study appears to have addressed the reproducibility of the adipogenic foci counting method between researchers. Though this kind of analysis is often used in conjunction with other data such as qPCR quantification of relevant gene transcripts and ORO staining, there is a need to address this issue. One suggestion is to have images assessed by multiple observers. Another issue of this method is that it provides a broad measure of the number of cells accumulating lipid, but does not account for features of those lipid droplets. This kind of analysis is already time and labour intensive, and the kinds of computer aided image analysis of lipid droplet features such as diameter previously reported use an extremely small number of cells (Rizzatti *et al*., 2013). Quantification of these observations therefore encounters many issues; however, it is reasonable to assert that treatment of human primary preadipocytes with DM + Lab4b CFS can have a profound morphological effect on surviving cells. Further work is needed to investigate the precise nature of these morphological effects and any potential effects on adipogenesis, and investigation of gene markers via qPCR is a suggested first step.

The large number of intracellular vacuoles shown in the lower image in Figure 6.2 presents unanswered questions. Most importantly, are these visual features actually lipid vacuoles? ORO staining was not able to distinguish between any condition, and accurate visual analysis was confounded by soluble bodies that were visually similar to lipid droplets in still images, but not during live light microscopy. The distribution of these vacuoles is different to traditional lipid accumulation, which may be a result of some functional cellular change or may reflect that they are not lipid droplets. Visual analysis of ORO stains showed faint staining of these vacuoles, however there was a large amount of background staining and unfortunately, images of stained cells have been lost to a storage failure. Prior usage of the foci counting technique has been used alongside qPCR quantification of LPL transcripts, which was not possible

in the present study due to time constraints. Further work should seek first to determine optimal culture conditions, particularly a dosage of CFS to ensure both survival and adipogenesis in human primary preadipocytes, and then if effects on morphology seen in the present study can be recapitulated utilise a qPCR based approach as visual determination becomes difficult. Unlike 3T3-L1 cells, human primary preadipocytes are comprised of a heterogeneous and pluripotent population of cells. Given the typically low adipogenic potential of human primary preadipocyte cells and a time course of differentiation consistent with control cells, it may be that some factor of the Lab4b CFS influences these cells towards adipogenic commitment. The induction of reactive oxygen species as a result of lactate administration has been shown in cultured rat myocytes (Brooks, 2009), and there is evidence to suggest that non-pathogenic levels of reactive oxygen species are involved in adipose commitment (Liu *et al*., 2012). As CFS composition remains unknown, this is a speculative hypothesis, however there is a strong rationale for the presence of lactate in CFS as discussed in chapter 5.4 which warrants further investigation.

Chapter 7: Discussion

The link between the gut microbiota and obesity in humans is incompletely understood. There is good evidence to support the basic rationale that bacteria in the gastrointestinal tract metabolise undigested material from the host diet and synthesise substrates which can be utilised by the host (McNeil, 1984). However, the intricacies of such a system are exceedingly difficult to model *in vitro*. The nutritional milieu of the colon is affected by both host diet and the energy salvage capacity of the resident microbiota (Ríos-Covián *et al*., 2016). The substrates available to mesenteric adipose depots are likely affected by the status of butyrate as the preferred substrate of colonocytes (Clausen and Mortensen, 1994); conversely, adipose depots elsewhere in the body are likely affected by hepatic uptake of SCFAs and peripheral SCFA concentrations are far lower than in the colon (Cummings *et al*., 1987). As such it is difficult to draw conclusions about the potential of probiotic bacteria to impact adipogenesis *in vivo* from *in vitro* data, as it is extremely difficult to both identify and represent myriad environmental variables of a given adipose depot in an *in vitro* model. The model used in the present study therefore is quite broad and represents early steps in investigating the effects of bacterial metabolites upon adipose tissue. The issue of how to model either subcutaneous or mesenteric fat requires an understanding of the relative concentrations of colonic metabolic products both within the colon and within systemic circulation, as well as an understanding of the composition of the CFS used. This would appear to be a distant goal in modelling effects of bacteria on adipogenesis *in vitro*, but would potentially aid greatly in the applicability of any results. Other suggestions to improve physiological representativeness are to use serum from probiotic treated mice, though yields would likely be very small and may necessitate much smaller numbers of cells be used. Though not performed in the same research context as the present study, coculture of Caco-2 cells (a model of the mature enterocyte often used as a general model of intestinal epithelium) with human primary preadipocytes stimulates leptin secretion and expression (Ishihara *et al*., 2015). The low levels of leptin transcription seen in 3T3-L1 cells is an interesting phenomenon, and if the

intestinal epithelium plays a stimulatory role, it is an intriguing avenue of research given that it is the primary interface with probiotic bacteria.

There is a notable gap in the literature regarding viability testing in cell models of *in vitro* adipogenesis investigating the effects of bacteria. The present study shows that Lab4 and Lab4b both reduce lipid accumulation when measured by ORO staining, however it is uncertain to what degree that is a reflection of a reduction in cell viability. A 1:1 dilution of CFS and culture media was used to maintain consistency with preliminary data. In the course of generating preliminary data, varying concentrations were trialled to assess cytotoxicity and it was believed that a 1:1 dilution did not affect viability. However, data shown herein displayed a clear effect on viability in Lab4 and Lab4b treated cells at 10 days. Unfortunately, reliable viability data was not able to be generated for all strains used. Effects of CFS for these strains remains an important question to be answered in future work, however culture conditions may also need to be optimised. MTS assay does not appear to be valid for the assessment of cell viability in 3T3-L1 cells treated with bacterial CFS, however the overestimation of viability seen in this data may be indicative of an altered redox state compared to control, which may in turn influence adipose phenotype (Carrière *et al.,* 2014). Further research is needed to determine both the cause of this overestimation and whether it has any relation to adipose phenotype. Unpublished data recently generated at Cultech suggests that CFS of certain probiotic strains may have antioxidant effects. However, as the methods employed for MTS assay in the present study required aspirating media containing CFS, washing cells, and replacing with standard culture media, it would seem to suggest a cellular effect.

Quantitative measurements of GPDH transcripts did not show any significant reductions in adipogenesis in any condition, however due to time constraints these results were obtained from only two experiments. Though not significant, differentiating 3T3-L1 cells treated with CFS of L. *acidophilus* showed the lowest level of GPDH transcription alongside the highest levels of UCP1 and PGC1-α transcription, despite bacteria growing to only half the CFU/ml of other conditions. This suggests that L. *acidophilus* CUL21 and CUL60 may influence 3T3-L1 cells towards a thermogenic phenotype, and that it is comparatively more effective than other

bacterial strains. However, an alternative explanation for the lower levels of adipogenesis in these cells is that due to the lower CFU/ml, fewer carbon sources (i.e. lactate) are secreted into the culture media to drive adipogenesis. Further evidence suggesting CFS of L. *acidophilus* may impact adipose phenotype was seen in 3T3-L1 cells in CM conditions. Treatment of 3T3-L1 cells with CM + L. *acidophilus* resulted in a significant increase of UCP1 transcripts compared to control. This was mirrored by a non-significant reduction in leptin transcripts. However, while there was a non-significant increase in UCP1 transcripts in DM + L. *acidophilus* treated 3T3-L1 cells, evidence of a reciprocal relationship with leptin was lacking.

However, oversights in the application of qPCR technique may distort data presented in this work. Though all primers developed and used specifically for this study were designed to span exon junctions, pre-existing primers for ARP and GPDH target sequences within the same exon. This introduces the possibility that results may be distorted by genomic DNA contamination of extracted RNA. Unfortunately, due to inexperience neither DNAse digests were performed on isolated RNA, nor no reverse transcriptase controls included on qPCR plates. Data presented herein therefore comes with the caveat that quantification of the housekeeping gene may potentially be affected by genomic DNA contamination, and as such affect data relating to any of the genes investigated.

Further compounding interpretation of data on effects on adipose phenotype is the uncertain role or relevance of markers in 3T3-L1 cells. Leptin has been used as a marker of classical WAT for many years, and yet its abundance in 3T3-L1 cells is drastically lower than murine adipocytes *in vivo*. 3T3-L1 cells have long been used as a model of WAT, and yet data in the present study indicates that UCP1 and PGC1-α are present in greater quantities than one of the hallmark genes of the adipogenic programme. The capacity of 3T3-L1 cells to display thermogenic capacity has been shown in a number of studies in recent years, however it is less clear to what extent beige or BAT selective genes are involved, with discordant results in the literature. Though the only significant difference observed in any of the BAT-associated genes following treatment was an increase of UCP1 transcription in cells maintained in CM + L. *acidophilus*, there were other notable potential trends. Treatment with DM + L.

salivarius non-significantly increased leptin transcription. Leptin and UCP1 are reciprocally regulated in murine BAT (Cancello *et al*., 1998), thus with an increase in leptin transcription there may be a concomitant decrease in transcription of BAT-associated genes. Indeed, L. *salivarius* did show non-significant reductions compared to control of UCP1, PGC1-α, and CITED1. However, patterns were less clear in other conditions, and the degree to which this reciprocal relationship exists in 3T3-L1 cells is an area for future research.

A major weakness of the present work is the lack of a positive control for assessment of a thermogenic phenotype in 3T3-L1 cells. Reports of the ability to induce a "beige like" phenotype in 3T3-L1 cells via treatment with the β-adrenergic agonist isoproterenol have featured in the literature in recent years (Miller *et al*., 2015). However, it remains unclear which of the putative beige phenotype markers are enriched under this protocol, and much work is still needed to investigate the extent to which adipose thermogenic gene networks are present or active in 3T3-L1 cells. Further, due to developmental methods it remains unclear which tissue or tissues the NIH-3T3 cell line is derived from (Dastagir *et al*., 2014), and thus what adipose depots and phenotypes the 3T3-L1 cell line may be most physiologically reflective of. Future work should incorporate a positive control for these purposes.

Performing robust statistical testing on much of the data in the present study has been a particularly challenging issue. Almost all of the data generated violates the assumption of homogeneity for ANOVA, further, removal of outliers or loss of wells due to infection results in different sample numbers between groups. These features of the data required different post-hoc tests to data sets with homogeneous variances. However, there are a limited number of post-hoc strategies for pairwise comparison in data with heterogeneous variances. One of the traditional post-hoc tests under these conditions, the Games-Howell test, requires at least 6 observations per group and can return results considered too liberal with small sample sizes (Shingala *et al*., 2015). Thus, the Dunnett's T3 test, which is relatively conservative, was used. As conservative statistical methods were used, and data showed wide variability, it is particularly important to emphasise the need for further data generation in order to interpret any findings from the present study.

Though the difficulties encountered in this study may be a reflection of attempting to generate a broad range of experimental data in a short period of study, it would be advantageous to try and more tightly control variables in any future work. In the present study, individual 10ml aliquots of CFS were thawed when needed, diluted in culture medium, and stored at 4˚C for use in single experiments to prevent any potential effect of freeze-thaw cycles. However, it was clear upon storing CFS at -20˚C that not all aliquots were equal. Unusually, some aliquots within a batch would remain liquid at -20˚C, while others froze. The cause for this is unclear, and so aliquots which remained liquid at -20˚C were not used, however this may be a reflection of some unaccounted for variable which could affect data generated herein. It was decided not to pool aliquots of CFS as one potentially cytotoxic aliquot could potentially prevent a whole batch from being used. However, homogenisation of CFS may yield more consistent results. Additionally, evidence in 3T3-F442a cells that shows a capacity *in vitro* to sense temperature and induce UCP1 transcription means that any handling of cells outside of an incubator may have an impact on adipose phenotype (Ye *et al*., 2013). Future work should seek to tightly regulate and normalise time spent at room temperature between conditions.

Though some work was done in assessing adipogenesis in 3T3-L1 cells throughout the time course of adipogenesis through ORO staining, it is clear that time is an important factor to consider. As fully mature 3T3-L1 cells are non-adherent in culture, it is possible for enhanced adipogenesis to present as a reduction in lipid accumulation or expression of genes used as markers of differentiation. Gene expression data in the present study was collected at a single timepoint reflective of late adipogenesis. Given the small number of repetitions and the apparent variability of GPDH expression, it is difficult to determine changes in adipogenesis based on a single timepoint. Also, the visual features of cells treated with CFS of Lab4 and Lab4b are suggestive of enhanced adipogenesis, thus when measuring a single timepoint it may not be possible to delineate between enhancement or inhibition of gene expression data. More granular data on both lipid accumulation and gene expression is needed throughout the time course of adipogenesis, and any further work should include

such longitudinal experiments in order to give a proper account of the effect of time on these features of 3T3-L1 cells cultured in CFS.

Despite these issues, there are interesting avenues for further study indicated by results in the present study. The two strains that have showed the most striking differences to control are L. *salivarius* and L. *acidophilus*. Interestingly, these strains display potential opposing effects as L. *salivarius* was shown to non-significantly increase leptin transcription, whereas L. *acidophilus* was shown to significantly increase UCP1 transcription depending on culture conditions. Each are constituent strains exclusive to either Lab4 or Lab4b and represent a good opportunity for further research. Preliminary data reported in the introductory chapter raised the possibility that Lab4b but not Lab4 increased spontaneous adipogenesis when adipogenesis was assessed in cells treated with CM + Lab4/Lab4b. Data in the present study indicates that these strains may be involved, as treatment of human primary preadipocytes (which have a typically low adipogenic potential) appeared to robustly accumulate lipids when treated with DM + Lab4b. However, this must be interpreted with caution as data from human primary preadipocytes was not able to determine adipogenesis by ORO staining, nor was qPCR able to be employed due to time constraints. It is uncertain therefore whether the presumed lipid vacuoles seen in human primary preadipocytes contained lipids, or were morphological signs of other cellular processes such as autophagy. The most striking morphological changes seen in the present study were in 3T3-L1 cells treated with DM + L. *salivarius*, and human primary preadipocytes treated with DM + Lab4b. L. *salivarius* is a constituent strain of Lab4b, which raises the possibility that the unusual morphological effects seen in human primary preadipocytes may be related to the enlargement of 3T3-L1 cells. Unfortunately, ORO data from experiments in human primary preadipocytes did not appear to be able to signify adipogenesis in DM treated conditions. As qPCR experiments were unable to be performed in these cells due to time constraints, it is not certain what the vacuoles that appeared to be induced by treatment with Lab4b CFS actually are. On the assumption that these are indeed lipid vacuoles, the hypothesis posited that these cells are influenced to commit to an adipogenic fate

through the influence of lactate is an attractive one, but remains highly speculative and requires further investigation.

One of the major themes of the present study was investigating potential effects of treatment of 3T3-L1 cells with CFS on markers of adipose phenotype. It is not possible to extrapolate this data beyond this model as it is uncertain how relevant these markers are in 3T3-L1 cells, and there is evidence to show that murine BAT appears to be more enriched with genes considered beige-selective in humans (Wu *et al*., 2012). Investigating potential effects of bacterial CFS on markers of adipose phenotype in human primary preadipocytes is a logical further step, however the variable cytotoxicity between patient samples, and the variable cytotoxicity *within* patient samples when exposed to CFS that had been stored longer suggests that culture conditions need to be optimised. As human primary preadipocytes are a valuable resource which can be difficult to culture, determining conditions to maximise viability of CFS treated cells would be extremely useful data.

Though the focus of this work was on adipogenesis, there is a suggestion from prior work on *in vitro* adipogenesis with regards to probiotic bacteria that there may be effects on lipolysis (Lee *et al*., 2015). Supplementation of HFD in rats with an L. *plantarum* strain has been shown to impact transcription of genes related to lipolysis and lipid metabolism in the liver (Li *et al*., 2014). It is plausible that similar effects may have occurred in a recent study of mice fed HFD supplemented with Lab4 plus an L. *plantarum* strain which appeared to ameliorate weight gain (Michael *et al*., 2017). Differences observed between human cohorts in lipolytic capacity using radiolabelled glycerol have been implicated in relative susceptibility to obesity (Danadian *et al*., 2001). Any potential impact of probiotic bacteria on lipolysis would therefore be of great interest in relation to obesity, and assessing lipolysis in 3T3-L1 cells treated with probiotic CFS may be a useful avenue for further research.

In summation, while firm conclusions about the effects of probiotic bacteria on *in vitro* adipogenesis cannot be drawn from the present data, there are signs that treatment of 3T3-L1 cells with CFS may impact transcription of genes associated with adipose phenotype in mice. It is uncertain whether the same is true in human cells,

but Lab4b CFS appeared to induce vacuole formation which may have been indicative of greater commitment of preadipocytes towards an adipocyte lineage. More work is needed to properly determine CFS doses which do not adversely impact cell viability, and CFS treatment may interfere with some viability assays. Further data generation and further optimised culture conditions will hopefully more definitively illuminate the cellular and molecular effects of probiotic bacteria on *in vitro* adipogenesis.

References

Ailhaud, G., Dani, C., Amri, E. Z., Djian, P., Vannier, C., Doglio, A., Forest, C. *et al.* (1989). Coupling growth arrest and adipocyte differentiation. *Environmental Health Perspectives* **80:**17-23.

Al Maskari, M. Y. and Alnaqdy, A. A. (2006). Correlation between Serum Leptin Levels, Body Mass Index and Obesity in Omanis. *Sultan Qaboos University Medical Journal* **6:**27-31.

Alang, N. and Kelly, C. R. (2015). Weight Gain After Fecal Microbiota Transplantation. *Open Forum Infectious Diseases* **2:**ofv004.

Aprile, M., Ambrosio, M. R., D'Esposito, V., Beguinot, F., Formisano, P., Costa, V. and Ciccodicola, A. (2014). PPARG in Human Adipogenesis: Differential Contribution of Canonical Transcripts and Dominant Negative Isoforms. *PPAR Research* **2014:**11.

Asano, H., Kanamori, Y., Higurashi, S., Nara, T., Kato, K., Matsui, T. and Funaba, M. (2014). Induction of Beige-Like Adipocytes in 3T3-L1 Cells. *The Journal of Veterinary Medical Science* **76:**57-64.

Ashkar, A. and Rosenthal, K. L. (2002). Toll-like Receptor 9, CpG DNA and Innate Immunity. *Current Molecular Medicine* **2:**545-556.

Bach, J.-F. (2002). The Effect of Infections on Susceptibility to Autoimmune and Allergic Diseases. *New England Journal of Medicine* **347:**911-920.

Bae, J., Ricciardi, C. J., Esposito, D., Komarnytsky, S., Hu, P., Curry, B. J., Brown, P. L. *et al.* (2014). Activation of pattern recognition receptors in brown adipocytes induces inflammation and suppresses uncoupling protein 1 expression and mitochondrial respiration. *American Journal of Physiology - Cell Physiology* **306:**C918.

Banerjee, S. S., Feinberg, M. W., Watanabe, M., Gray, S., Haspel, R. L., Denkinger, D. J., Kawahara, R. *et al.* (2003). The Krüppel-like Factor KLF2 Inhibits Peroxisome Proliferator-activated Receptor-γ Expression and Adipogenesis. *Journal of Biological Chemistry* **278:**2581-2584.

Basak, V., Bahar, T. E., Emine, K., Yelda, K., Mine, K., Figen, S. and Rustem, N. (2016). Evaluation of cytotoxicity and gelatinases activity in 3T3 fibroblast cell by root repair materials. *Biotechnology & Biotechnological Equipment* **30:**984-990.

Bastien, M., Poirier, P., Lemieux, I. and Després, J.-P. (2014). Overview of Epidemiology and Contribution of Obesity to Cardiovascular Disease. *Progress in Cardiovascular Diseases* **56:**369-381.

Batra, A., Pietsch, J., Fedke, I., Glauben, R., Okur, B., Stroh, T., Zeitz, M. *et al.* (2007). Leptin-Dependent Toll-Like Receptor Expression and Responsiveness in Preadipocytes and Adipocytes. *The American Journal of Pathology* **170:**1931-1941.

Berridge, M. V., Herst, P. M. and Tan, A. S. (2005). Tetrazolium dyes as tools in cell biology: New insights into their cellular reduction.*Biotechnology Annual Review*. Vol. 11. Elsevier, pp. 127-152.

Bloemen, J. G., Venema, K., van de Poll, M. C., Olde Damink, S. W., Buurman, W. A. and Dejong, C. H. (2009). Short chain fatty acids exchange across the gut and liver in humans measured at surgery. *Clinical Nutrition* **28:**657-661.

Borgeraas, H., Johnson, L. K., Skattebu, J., Hertel, J. K. and Hjelmesæth, J. Effects of probiotics on body weight, body mass index, fat mass and fat percentage in subjects with overweight or obesity: a systematic review and meta-analysis of randomized controlled trials. *Obesity Reviews* n/a-n/a.

Bourriaud, C., Robins, R. J., Martin, L., Kozlowski, F., Tenailleau, E., Cherbut, C. and Michel, C. (2005). Lactate is mainly fermented to butyrate by human intestinal microfloras but inter-individual variation is evident. *Journal of Applied Microbiology* **99:**201-212.

Brooks, G. A. (2009). Cell–cell and intracellular lactate shuttles. *The Journal of Physiology* **587:**5591-5600.

Buffie, C. G. and Pamer, E. G. (2013). Microbiota-mediated colonization resistance against intestinal pathogens. *Nature reviews. Immunology* **13:**790-801.

Bäckhed, F., Ding, H., Wang, T., Hooper, L. V., Koh, G. Y., Nagy, A., Semenkovich, C. F. *et al.* (2004). The gut microbiota as an environmental factor that regulates fat storage. *Proceedings of the National Academy of Sciences of the United States of America* **101:**15718-15723.

Bäckhed, F., Ley, R. E., Sonnenburg, J. L., Peterson, D. A. and Gordon, J. I. (2005). Host-Bacterial Mutualism in the Human Intestine. *Science* **307:**1915.

Bäckhed, F., Roswall, J. and Peng, Y. (2015). Dynamics and stabilization of the human gut microbiome during the first year of life. *Cell Host Microbe* **17**.

Cancello, R., Zingaretti, M. C., Sarzani, R., Ricquier, D. and Cinti, S. (1998). Leptin and UCP1 Genes are Reciprocally Regulated in Brown Adipose Tissue. *Endocrinology* **139:**4747-4750.

Cani, P. D., Amar, J., Iglesias, M. A., Poggi, M., Knauf, C., Bastelica, D., Neyrinck, A. M. *et al.* (2007). Metabolic Endotoxemia Initiates Obesity and Insulin Resistance. *Diabetes* **56:**1761.

Cannon, B. and Nedergaard, J. A. N. (2004). Brown Adipose Tissue: Function and Physiological Significance. *Physiological Reviews* **84:**277.

Carnicero, H. H. (1984). Changes in the metabolism of long chain fatty acids during adipose differentiation of 3T3 L1 cells. *Journal of Biological Chemistry* **259:**3844-3850.

Carrière, A., Jeanson, Y., Berger-Müller, S., André, M., Chenouard, V., Arnaud, E., Barreau, C. *et al.* (2014). Browning of White Adipose Cells by Intermediate Metabolites: An Adaptive Mechanism to Alleviate Redox Pressure. *Diabetes* **63:**3253.

Cawthorn, W. P., Scheller, E. L. and MacDougald, O. A. (2012). Adipose tissue stem cells meet preadipocyte commitment: going back to the future. *Journal of Lipid Research* **53:**227-246.

Chang, S.-H., Stoll, C. R. T., Song, J., Varela, J. E., Eagon, C. J. and Colditz, G. A. (2014). Bariatric surgery: an updated systematic review and meta-analysis, 2003–2012. *JAMA surgery* **149:**275-287.

Chawla, A., Repa, J. J., Evans, R. M. and Mangelsdorf, D. J. (2001). Nuclear Receptors and Lipid Physiology: Opening the X-Files. *Science* **294:**1866.

Chon, H., Choi, B., Lee, E., Lee, S. and Jeong, G. (2009). Immunomodulatory effects of specific bacterial components of Lactobacillus plantarum KFCC11389P on the murine macrophage cell line RAW 264·7. *Journal of Applied Microbiology* **107:**1588-1597.

Chondronikola, M., Volpi, E., Børsheim, E., Porter, C., Annamalai, P., Enerbäck, S., Lidell, M. E. *et al.* (2014). Brown Adipose Tissue Improves Whole-Body Glucose Homeostasis and Insulin Sensitivity in Humans. *Diabetes* **63:**4089-4099.

Clarridge III, J. E. (2004). Impact of 16S rRNA Gene Sequence Analysis for Identification of Bacteria on Clinical Microbiology and Infectious Diseases. *Clinical Microbiology Reviews* **17:**840-862.

Clausen, M. R. and Mortensen, P. B. Kinetic studies on the metabolism of short-chain fatty acids and glucose by isolated rat colonocytes. *Gastroenterology* **106:**423-432.

Coe, P. O., O'Reilly, D. A. and Renehan, A. G. (2014). Excess adiposity and gastrointestinal cancer. *British Journal of Surgery* **101:**1518-1531.

Coelho, M., Oliveira, T. and Fernandes, R. (2013). Biochemistry of adipose tissue: an endocrine organ. *Archives of Medical Science : AMS* **9:**191-200.

Collado, M. C., Rautava, S., Aakko, J., Isolauri, E. and Salminen, S. (2016). Human gut colonisation may be initiated in utero by distinct microbial communities in the placenta and amniotic fluid. *Scientific Reports* **6:**23129.

Cook, R. and Kozak, L.P. (1982). sn-glycerol-3-phosphate dehydrogenase gene expression during mouse adipocyte development in vivo. *Developmental Biology* **92**:440-448

Coombes, R. C., Rothwell, N. J., Shah, P. and Stock, M. J. (1987). Changes in thermogenesis and brown fat activity in response to tumour necrosis factor in the rat. *Bioscience Reports* **7:**791-799.

Cristancho, A. G. and Lazar, M. A. (2011). Forming functional fat: a growing understanding of adipocyte differentiation. **12:**722.

Crow, J. R., Davis, S. L., Chaykosky, D. M., Smith, T. T. and Smith, J. M. (2015). Probiotics and Fecal Microbiota Transplant for Primary and Secondary Prevention of Clostridium difficile Infection. *Pharmacotherapy: The Journal of Human Pharmacology and Drug Therapy* **35:**1016-1025.

Cummings, J. H., Pomare, E. W., Branch, W. J., Naylor, C. P. and Macfarlane, G. T. (1987). Short chain fatty acids in human large intestine, portal, hepatic and venous blood. *Gut* **28:**1221-1227.

Cypess, A. M., Lehman, S., Williams, G., Tal, I., Rodman, D., Goldfine, A. B., Kuo, F. C. *et al.* (2009). Identification and Importance of Brown Adipose Tissue in Adult Humans. *The New England journal of medicine* **360:**1509-1517.

Dalpke, A., Frank, J., Peter, M. and Heeg, K. (2006). Activation of Toll-Like Receptor 9 by DNA from Different Bacterial Species. *Infection and Immunity* **74:**940-946.

Danadian, K., Lewy, V., Janosky, J. J. and Arslanian, S. (2001). Lipolysis in African-American Children: Is It a Metabolic Risk Factor Predisposing to Obesity?1. *The Journal of Clinical Endocrinology & Metabolism* **86:**3022-3026.

Darimont, C., Gaillard, D., Ailhaud, G. and Negrel, R. (1993). Terminal differentiation of mouse preadipocyte cells: adipogenic and antimitogenic role of triiodothyronine. *Molecular and cellular endocrinology* **98:**67-73.

Darlington, G. J., Ross, S. E. and MacDougald, O. A. (1998). The Role of C/EBP Genes in Adipocyte Differentiation. *Journal of Biological Chemistry* **273:**30057-30060.

Dastagir, K., Reimers, K., Lazaridis, A., Jahn, S., Maurer, V., Strauß, S., … Vogt, P. M. (2014). Murine Embryonic Fibroblast Cell Lines Differentiate into Three Mesenchymal Lineages to Different Extents: New Models to Investigate Differentiation Processes. *Cellular Reprogramming*, **16**, 241–252.

Day, C. and Bailey, C. J. (2011). Obesity in the pathogenesis of type 2 diabetes. *The British Journal of Diabetes & Vascular Disease* **11:**55-61.

de Jong, J. M. A., Larsson, O., Cannon, B. and Nedergaard, J. (2015). A stringent validation of mouse adipose tissue identity markers. *American Journal of Physiology-Endocrinology and Metabolism* **308:**E1085-E1105.

de Oliveira, M., Síbio, M. T. D., Olimpio, R. M. C., Moretto, F. C. F., Luvizotto, R. d. A. M. and Nogueira, C. R. (2015). Triiodothyronine modulates the expression of leptin and adiponectin in 3T3-L1 adipocytes. *Einstein* **13:**72-78.

Dempersmier, J., Sambeat, A., Gulyaeva, O., Paul, S. M., Hudak, C. S. S., Raposo, H. F., Kwan, H.-Y. *et al.* (2015). Cold–inducible Zfp516 Activates UCP1 Transcription to Promote Browning of White Fat and Development of Brown Fat. *Molecular cell* **57:**235-246.

den Besten, G., van Eunen, K., Groen, A. K., Venema, K., Reijngoud, D.-J. and Bakker, B. M. (2013). The role of short-chain fatty acids in the interplay between diet, gut microbiota, and host energy metabolism. *Journal of Lipid Research* **54:**2325-2340.

Department of Health (2011). Obesity General Information [Online]. Department of Health. Available at: http://webarchive.nationalarchives.gov.uk/+/http://www.dh.gov.uk/en/Publichealth/Obesity/DH_078098 [Accessed: 12/11/2016].

Draman, M. S., Grennan-Jones, F., Zhang, L., Taylor, P. N., Tun, T. K., McDermott, J., Moriarty, P. *et al.* (2013). Effects of Prostaglandin F(2α) on Adipocyte Biology Relevant to Graves' Orbitopathy. *Thyroid* **23:**1600-1608.

Draman, M. S., Stechman, M., Scott-Coombes, D., Dayan, C. M., Rees, D. A., Ludgate, M. and Zhang, L. (2017). The Role of Thyrotropin Receptor Activation in Adipogenesis and Modulation of Fat Phenotype. *Frontiers in Endocrinology* **8:**83.

Dunigan, D. D., Waters, S. B. and Owen, T. C. (1995). Aqueous soluble tetrazolium/formazan MTS as an indicator of NADH-and NADPH-dependent dehydrogenase activity. *Biotechniques* **19:**640-649.

Eloe-Fadrosh, E. A., Brady, A., Crabtree, J., Drabek, E. F., Ma, B., Mahurkar, A., Ravel, J. *et al.* (2015). Functional Dynamics of the Gut Microbiome in Elderly People during Probiotic Consumption. *mBio* **6**.

Entenmann, G. and Hauner, H. (1996). Relationship between replication and differentiation in cultured human adipocyte precursor cells. *American Journal of Physiology-Cell Physiology* **270:**C1011-C1016.

European Medicines Agency. 2010. *Questions and answers on the suspension of medicines containing sibutramine*. London: European Medicines Agency. Available at: https://www.nhs.uk/news/2010/01January/Documents/Sibutramine-QA.pdf [Accessed: 2/11/2017].

Fajas, L., Auboeuf, D., Raspé, E., Schoonjans, K., Lefebvre, A.-M., Saladin, R., Najib, J. *et al.* (1997). The Organization, Promoter Analysis, and Expression of the Human PPARγ Gene. *Journal of Biological Chemistry* **272:**18779-18789.

Fajas, L., Fruchart, J.-C. and Auwerx, J. (1998). PPARγ3 mRNA: a distinct PPARγ mRNA subtype transcribed from an independent promoter. *FEBS Letters* **438:**55-60.

Farmer, S. R. (2006). Transcriptional control of adipocyte formation. *Cell metabolism* **4:**263-273.

Farmer, S. R., Hamm, J. K. and Park, B.-H. (2002). PPARγ in Adipogenesis and Insulin Resistance. In: Fruchart, J.C. and Gotto, A.M. and Paoletti, R. and Staels, B. and Catapano, A.L. (eds.) *Peroxisome Proliferator Activated Receptors: From Basic Science to Clinical Applications*. Boston, MA: Springer US, pp. 123-130.

Fernandez-Marcos, P. J. and Auwerx, J. (2011). Regulation of PGC-1α, a nodal regulator of mitochondrial biogenesis. *The American Journal of Clinical Nutrition* **93:**884S-890S.

Fischbach, C., Spruß, T., Weiser, B., Neubauer, M., Becker, C., Hacker, M., Göpferich, A. *et al.* (2004). Generation of mature fat pads in vitro and in vivo utilizing 3-D long-term culture of 3T3-L1 preadipocytes. *Experimental Cell Research* **300:**54-64.

Food and Agriculture Organization and World Health Organization. (2001). Evaluation of health and nutritional properties of powder milk and live lactic acid bacteria. Córdoba, Argentina

Gaillard, D., Négrel, R., Lagarde, M., & Ailhaud, G. (1989). Requirement and role of arachidonic acid in the differentiation of pre-adipose cells. *Biochemical Journal*, **257**, 389–397.

Gao, Z., Hwang, D., Bataille, F., Lefevre, M., York, D., Quon, M. J. and Ye, J. (2002). Serine Phosphorylation of Insulin Receptor Substrate 1 by Inhibitor κB Kinase Complex. *Journal of Biological Chemistry* **277:**48115-48121.

Gao, Z., Yin, J., Zhang, J., Ward, R. E., Martin, R. J., Lefevre, M., Cefalu, W. T. *et al.* (2009). Butyrate Improves Insulin Sensitivity and Increases Energy Expenditure in Mice. *Diabetes* **58:**1509-1517.

Garaiova, I., Muchová, J., Nagyová, Z., Wang, D., Li, J. V., Országhová, Z., Michael, D. R. *et al.* (2015). Probiotics and vitamin C for the prevention of respiratory tract infections in children attending preschool: a randomised controlled pilot study.

European Journal of Clinical Nutrition **69:**373-379.

Gill, S. R., Pop, M., DeBoy, R. T., Eckburg, P. B., Turnbaugh, P. J., Samuel, B. S., Gordon, J. I. *et al.* (2006). Metagenomic Analysis of the Human Distal Gut Microbiome. *Science (New York, N.Y.)* **312:**1355-1359.

Gilsanz, V., Hu, H. H. and Kajimura, S. (2013). Relevance of brown adipose tissue in infancy and adolescence. *Pediatric research* **73:**3-9.

Gregoire, F. M., Smas, C. M. and Sul, H. S. (1998). Understanding Adipocyte Differentiation. *Physiological Reviews* **78:**783.

Grygiel-Górniak, B. (2014). Peroxisome proliferator-activated receptors and their ligands: nutritional and clinical implications - a review. *Nutrition Journal* **13:**17.

Guo, K.-Y., Halo, P., Leibel, R. L. and Zhang, Y. (2004). Effects of obesity on the relationship of leptin mRNA expression and adipocyte size in anatomically distinct fat depots in mice. *American Journal of Physiology - Regulatory, Integrative and Comparative Physiology* **287:**R112.

Haberland, M., Carrer, M., Mokalled, M. H., Montgomery, R. L. and Olson, E. N. (2010). Redundant Control of Adipogenesis by Histone Deacetylases 1 and 2. *The Journal of Biological Chemistry* **285:**14663-14670.

Hafekost, K., Lawrence, D., Mitrou, F., O'Sullivan, T. A. and Zubrick, S. R. (2013). Tackling overweight and obesity: does the public health message match the science? *BMC Medicine* **11:**41-41.

Hardin, G. (1960). The Competitive Exclusion Principle. *Science* **131:**1292.

Harms, M. and Seale, P. (2013). Brown and beige fat: development, function and therapeutic potential. **19:**1252.

Harms, M. J., Ishibashi, J., Wang, W., Lim, H.-W., Goyama, S., Sato, T., Kurokawa, M. *et al.* (2014). Prdm16 is required for the maintenance of brown adipocyte identity and function in adult mice. *Cell metabolism* **19:**593-604.

Hartmann, D., Hussain, Y., Güzelhan, C. and Odink, J. (1993). Effect on dietary fat absorption of orlistat, administered at different times relative to meal intake. *British Journal of Clinical Pharmacology* **36:**266-270.

Hartstra, A. V., Bouter, K. E. C., Bäckhed, F. and Nieuwdorp, M. (2015). Insights Into the Role of the Microbiome in Obesity and Type 2 Diabetes. *Diabetes Care* **38:**159.

Hill, C. J., Lynch, D. B., Murphy, K., Ulaszewska, M., Jeffery, I. B., O'Shea, C. A., Watkins, C. *et al.* (2017). Evolution of gut microbiota composition from birth to 24

weeks in the INFANTMET Cohort. *Microbiome* **5:**4.

Hirsch, J. and Batchelor, B. (1976). Adipose tissue cellularity in human obesity. *Clinics in Endocrinology and Metabolism* **5:**299-311.

Hong, Y.-H., Nishimura, Y., Hishikawa, D., Tsuzuki, H., Miyahara, H., Gotoh, C., Choi, K.-C. *et al.* (2005). Acetate and Propionate Short Chain Fatty Acids Stimulate Adipogenesis via GPCR43. *Endocrinology* **146:**5092-5099.

Hu, F. B., Chen, C., Wang, B., Stampfer, M. J. and Xu, X. (2001). Leptin concentrations in relation to overall adiposity, fat distribution, and blood pressure in a rural Chinese population. *International Journal Of Obesity* **25:**121.

Hu, J., Kyrou, I., Tan, B. K., Dimitriadis, G. K., Ramanjaneya, M., Tripathi, G., Patel, V. *et al.* (2016). Short-Chain Fatty Acid Acetate Stimulates Adipogenesis and Mitochondrial Biogenesis via GPR43 in Brown Adipocytes. *Endocrinology* **157:**1881-1894.

Ilavenil, S., Kim, D. H., Valan Arasu, M., Srigopalram, S., Sivanesan, R. and Choi, K. C. (2015). Phenyllactic Acid from Lactobacillus plantarum PromotesAdipogenic Activity in 3T3-L1 Adipocyte via Up-Regulationof PPAR-γ2. *Molecules* **20:**15359-15373.

Ishihara, R., Mizuno, Y., Miwa, A., Hamada, A., Tsuruta, T., Wabitsch, M. and Sonoyama, K. (2015). Intestinal epithelial cells promote secretion of leptin and adiponectin in adipocytes. *Biochemical and Biophysical Research Communications* **458:**362-368.

Jacobsson, A., Cannon, B. and Nedergaard, J. (1987). Physiological activation of brown adipose tissue destabilizes thermogenin mRNA. *FEBS Letters* **224:**353-356.

Jain, S. S., Ramanand, S. J., Ramanand, J. B., Akat, P. B., Patwardhan, M. H. and Joshi, S. R. (2011). Evaluation of efficacy and safety of orlistat in obese patients. *Indian Journal of Endocrinology and Metabolism* **15:**99-104.

Jammah, A. A. (2015). Endocrine and Metabolic Complications After Bariatric Surgery. *Saudi Journal of Gastroenterology : Official Journal of the Saudi Gastroenterology Association* **21:**269-277.

Jandhyala, S. M., Talukdar, R., Subramanyam, C., Vuyyuru, H., Sasikala, M. and Reddy, D. N. (2015). Role of the normal gut microbiota. *World Journal of Gastroenterology : WJG* **21:**8787-8803.

Jeanson, Y., Carrière, A. and Casteilla, L. (2015). A New Role for Browning as a Redox and Stress Adaptive Mechanism? *Frontiers in Endocrinology* **6:**158.

Jo, J., Gavrilova, O., Pack, S., Jou, W., Mullen, S., Sumner, A. E., Cushman, S. W. *et al.* (2009). Hypertrophy and/or Hyperplasia: Dynamics of Adipose Tissue Growth. *PLOS*

Computational Biology **5:**e1000324.

Juárez Tomás, M. S., Ocaña, V. S., Wiese, B. and Nader-Macías, M. E. (2003). Growth and lactic acid production by vaginal Lactobacillus acidophilus CRL 1259, and inhibition of uropathogenic Escherichia coli. *Journal of Medical Microbiology* **52:**1117.

Karamanlidis, G., Karamitri, A., Docherty, K., Hazlerigg, D. G. and Lomax, M. A. (2007). C/EBPβ Reprograms White 3T3-L1 Preadipocytes to a Brown Adipocyte Pattern of Gene Expression. *Journal of Biological Chemistry* **282:**24660-24669.

Kaur, J. (2014). A Comprehensive Review on Metabolic Syndrome. *Cardiology Research and Practice* **2014:**943162.

Kazantzis, M., Takahashi, V., Hinkle, J., Kota, S., Zilberfarb, V., Issad, T., Abdelkarim, M. *et al.* (2012). PAZ6 Cells Constitute a Representative Model for Human Brown Pre-Adipocytes. *Frontiers in Endocrinology* **3:**13.

Keller, P., Petrie, J. T., De Rose, P., Gerin, I., Wright, W. S., Chiang, S.-H., Nielsen, A. R. *et al.* (2008). Fat-specific Protein 27 Regulates Storage of Triacylglycerol. *Journal of Biological Chemistry* **283:**14355-14365.

Kim, J. B., Sarraf, P., Wright, M., Yao, K. M., Mueller, E., Solanes, G., Lowell, B. B. *et al.* (1998a). Nutritional and insulin regulation of fatty acid synthetase and leptin gene expression through ADD1/SREBP1. *Journal of Clinical Investigation* **101:**1-9.

Kim, J. B., Wright, H. M., Wright, M. and Spiegelman, B. M. (1998b). ADD1/SREBP1 activates PPARγ through the production of endogenous ligand. *Proceedings of the National Academy of Sciences of the United States of America* **95:**4333-4337.

Kim, J. D. and Lee, H. W. (2012). Hibernoma: Intense Uptake on F18-FDG PET/CT. *Nuclear Medicine and Molecular Imaging* **46:**218-222.

Kim, S.-N., Choi, H.-Y. and Kim, Y. K. (2009). Regulation of adipocyte differentiation by histone deacetylase inhibitors. *Archives of Pharmacal Research* **32:**535-541.

Kinkel, A. D., Fernyhough, M. E., Helterline, D. L., Vierck, J. L., Oberg, K. S., Vance, T. J., Hausman, G. J. *et al.* (2004). Oil red-O stains non-adipogenic cells: a precautionary note. *Cytotechnology* **46:**49-56.

Koenig, J. E., Spor, A., Scalfone, N., Fricker, A. D., Stombaugh, J., Knight, R., Angenent, L. T. *et al.* (2011). Succession of microbial consortia in the developing infant gut microbiome. *Proc Natl Acad Sci U S A* **108**.

Kokkinosa, A., Fasseas, C., Eliopoulos, E. and Kalantzopoulos, G. (1998). Cell size of various lactic acid bacteria as determined by scanning electron microscope and image analysis. *Lait* **78:**491-500.

Kotala, J. E. (2015). Influence of Lactobacillus rhamnosus Isolated from “Amabere Amaruranu” Cultured Milk on Adipogenesis. *Electronic Theses and Dissertations* **Paper 2608**.

Kristensen, N. B., Bryrup, T., Allin, K. H., Nielsen, T., Hansen, T. H. and Pedersen, O. (2016). Alterations in fecal microbiota composition by probiotic supplementation in healthy adults: a systematic review of randomized controlled trials. *Genome Medicine* **8:**52.

Krook, A. (1981). Effect of Metronidazole and Sulfasalazine on the Normal Human Faecal Flora. *Scandinavian Journal of Gastroenterology* **16:**587-592.

Kruis, T., Batra, A. and Siegmund, B. (2014). Bacterial Translocation – Impact on the Adipocyte Compartment. *Frontiers in Immunology* **4:**510.

Kuroda, M., Tominaga, A., Nakagawa, K., Nishiguchi, M., Sebe, M., Miyatake, Y., Kitamura, T. *et al.* (2016). DNA Methylation Suppresses Leptin Gene in 3T3-L1 Adipocytes. *PLOS ONE* **11:**e0160532.

Kwon, H. and Pessin, J. E. (2013). Adipokines Mediate Inflammation and Insulin Resistance. *Frontiers in Endocrinology* **4:**71.

Ladda, B., Theparee, T., Chimchang, J., Tanasupawat, S. and Taweechotipatr, M. (2015). In vitro modulation of tumor necrosis factor α production in THP-1 cells by lactic acid bacteria isolated from healthy human infants. *Anaerobe* **33:**109-116.

Lagace, D. C. and Nachtigal, M. W. (2004). Inhibition of Histone Deacetylase Activity by Valproic Acid Blocks Adipogenesis. *Journal of Biological Chemistry* **279:**18851-18860.

Lagier, J.-C., Khelaifia, S., Alou, M. T., Ndongo, S., Dione, N., Hugon, P., Caputo, A. *et al.* (2016). Culture of previously uncultured members of the human gut microbiota by culturomics. *Nature Microbiology* **1:**16203.

Lampe, K. J., Namba, R. M., Silverman, T. R., Bjugstad, K. B. and Mahoney, M. J. (2009). Impact of Lactic Acid on Cell Proliferation and Free Radical Induced Cell Death in Monolayer Cultures of Neural Precursor Cells. *Biotechnology and bioengineering* **103:**1214-1223.

Latham, T., Mackay, L., Sproul, D., Karim, M., Culley, J., Harrison, D. J., Hayward, L. *et al.* (2012). Lactate, a product of glycolytic metabolism, inhibits histone deacetylase activity and promotes changes in gene expression. *Nucleic Acids Research* **40:**4794-4803.

Lau, C. S. M. and Chamberlain, R. S. Probiotic administration can prevent necrotizing enterocolitis in preterm infants: A meta-analysis. *Journal of Pediatric Surgery*

50:1405-1412.

Lee, K.-H., Song, J.-L., Park, E.-S., Ju, J., Kim, H.-Y. and Park, K.-Y. (2015). Anti-Obesity Effects of Starter Fermented Kimchi on 3T3-L1 Adipocytes. *Preventive Nutrition and Food Science* **20:**298-302.

Lee, M.-J., Wu, Y. and Fried, S. K. (2012). A modified protocol to maximize differentiation of human preadipocytes and improve metabolic phenotypes. *Obesity (Silver Spring, Md.)* **20:**2334-2340.

Leibowitz, U., Antonovsky, A., Medalie, J. M., Smith, H. A., Halpern, L. and Alter, M. (1966). Epidemiological study of multiple sclerosis in Israel. II. Multiple sclerosis and level of sanitation. *Journal of Neurology, Neurosurgery, and Psychiatry* **29:**60-68.
Levene, A. P., Kudo, H., Armstrong, M. J., Thursz, M. R., Gedroyc, W. M., Anstee, Q. M. and Goldin, R. D. (2012). Quantifying hepatic steatosis – more than meets the eye. *Histopathology* **60:**971-981.

Li, C., Nie, S.-P., Zhu, K.-X., Ding, Q., Li, C., Xiong, T. and Xie, M.-Y. (2014). Lactobacillus plantarum NCU116 improves liver function, oxidative stress and lipid metabolism in rats with high fat diet induced non-alcoholic fatty liver disease. *Food & Function* **5:**3216-3223.

Liguori, R., Soccol, C. R., Vandenberghe, L. P. d. S., Woiciechowski, A. L., Ionata, E., Marcolongo, L. and Faraco, V. (2015). Selection of the Strain Lactobacillus acidophilus ATCC 43121 and Its Application to Brewers' Spent Grain Conversion into Lactic Acid. *BioMed Research International* **2015:**240231.

Lim, S.-W., Loh, H.-S., Ting, K.-N., Bradshaw, T. D. and Allaudin, Z. N. (2015). Reduction of MTT to Purple Formazan by Vitamin E Isomers in the Absence of Cells. *Tropical Life Sciences Research* **26:**111-120.

Liu, G.-S., Chan, C. E., Higuchi, M., Dusting, J. G. and Jiang, F. (2012). Redox Mechanisms in Regulation of Adipocyte Differentiation: Beyond a General Stress Response. *Cells* **1**.

Lodhi, Irfan J. and Semenkovich, Clay F. (2014). Peroxisomes: A Nexus for Lipid Metabolism and Cellular Signaling. *Cell Metabolism* **19:**380-392.

Long, E. M., Millen, B., Kubes, P. and Robbins, S. M. (2009). Lipoteichoic Acid Induces Unique Inflammatory Responses when Compared to Other Toll-Like Receptor 2 Ligands. *PLOS ONE* **4:**e5601.

Loveman, E., Frampton, G. K., Shepherd, J., Picot, J., Cooper, K., Bryant, J., Welch, K. *et al.* (2011). The clinical effectiveness and cost-effectiveness of long-term weight management schemes for adults: a systematic review.

Lowe, C. E., Rahilly, S. and Rochford, J. J. (2011). Adipogenesis at a glance. *Journal of*

Cell Science **124:**2681.

MacDougald, O. A. and Lane, M. D. (1995). Transcriptional Regulation of Gene Expression During Adipocyte Differentiation. *Annual Review of Biochemistry* **64:**345-373.

MacDougald, O. A. and Mandrup, S. (2002). Adipogenesis: forces that tip the scales. *Trends in Endocrinology & Metabolism* **13:**5-11.

Magoč, T. and Salzberg, S. L. (2011). FLASH: fast length adjustment of short reads to improve genome assemblies. *Bioinformatics* **27**.

Mann, S. E., Nijland, M. J. M. and Ross, M. G. (1996). Mathematic modeling of human amniotic fluid dynamics. *American journal of obstetrics and gynecology* **175:**937-944.

Marchesi, J. R. and Ravel, J. (2015). The vocabulary of microbiome research: a proposal. *Microbiome* **3:**31.

Martínez-Redondo, V., Pettersson, A. T. and Ruas, J. L. (2015). The hitchhiker's guide to PGC-1α isoform structure and biological functions. *Diabetologia* **58:**1969-1977.

Masaki, T., Yoshimatsu, H., Chiba, S., Hidaka, S., Tajima, D., Kakuma, T., Kurokawa, M. *et al.* (1999). Tumor necrosis factor-α regulates in vivo expression of the rat UCP family differentially. *Biochimica et Biophysica Acta (BBA) - Molecular and Cell Biology of Lipids* **1436:**585-592.

Maynard, C. L., Elson, C. O., Hatton, R. D. and Weaver, C. T. (2012). Reciprocal Interactions of the Intestinal Microbiota and Immune System. *Nature* **489:**231-241.

Mazidi, M., Rezaie, P., Ferns, G. A. and Vatanparast, H. (2017). Impact of Probiotic Administration on Serum C-Reactive Protein Concentrations: Systematic Review and Meta-Analysis of Randomized Control Trials. *Nutrients* **9:**20.

McConnell, B. B. and Yang, V. W. (2010). Mammalian Krüppel-Like Factors in Health and Diseases. *Physiological reviews* **90:**1337-1381.

McNeil, N. I. (1984). The contribution of the large intestine to energy supplies in man. *The American Journal of Clinical Nutrition* **39:**338-342.

McNulty, N. P., Yatsunenko, T., Hsiao, A., Faith, J. J., Muegge, B. D., Goodman, A. L., Henrissat, B. *et al.* (2011). The impact of a consortium of fermented milk strains on the gut microbiome of gnotobiotic mice and monozygotic twins. *Science Translational Medicine* **3:**106ra106-106ra106.

Medina-Gomez, G., Virtue, S., Lelliott, C., Boiani, R., Campbell, M., Christodoulides,

C., Perrin, C. *et al.* (2005). The Link Between Nutritional Status and Insulin Sensitivity Is Dependent on the Adipocyte-Specific Peroxisome Proliferator–Activated Receptor-γ2 Isoform. *Diabetes* **54:**1706-1716.

Metchnikoff, E. (1907). Essais Optimistes in: The Prolongation of Life: Optimistic Studies. London: Heinemann.

Michael, D. R., Davies, T. S., Moss, J. W. E., Calvente, D. L., Ramji, D. P., Marchesi, J. R., Pechlivanis, A. *et al.* (2017). The anti-cholesterolaemic effect of a consortium of probiotics: An acute study in C57BL/6J mice. *Scientific Reports* **7:**2883.

Miles, A. A., Misra, S. S. and Irwin, J. O. (1938). The estimation of the bactericidal power of the blood. *The Journal of Hygiene* **38:**732-749.
Miller, C. N., Yang, J.-Y., England, E., Yin, A., Baile, C. A. and Rayalam, S. (2015). Isoproterenol Increases Uncoupling, Glycolysis, and Markers of Beiging in Mature 3T3-L1 Adipocytes. *PLOS ONE* **10:**e0138344.

Morrison, S. and McGee, S. L. (2015). 3T3-L1 adipocytes display phenotypic characteristics of multiple adipocyte lineages. *Adipocyte* **4:**295-302.

Mullish, B. H., McDonald, J. A. K., Kao, D. H., Allegretti, J. R., Petrof, E. O., Pechlivanis, A., Barker, G. F. *et al.* (2017). OC-063 Gut microbiota-host bile acid metabolism interactions in clostridium difficile infection: the explanation for the efficacy of faecal microbiota transplantation? *Gut* **66:**A33.

Murakami, Y., Tanabe, S. and Suzuki, T. (2016). High-fat Diet-induced Intestinal Hyperpermeability is Associated with Increased Bile Acids in the Large Intestine of Mice. *Journal of Food Science* **81:**H216-H222.

Naghili, H., Tajik, H., Mardani, K., Razavi Rouhani, S. M., Ehsani, A. and Zare, P. (2013). Validation of drop plate technique for bacterial enumeration by parametric and nonparametric tests. *Veterinary Research Forum* **4:**179-183.

National Center for Biotechnology Information (2017). Basic Local Alignment Search Tool [Online]. Available at: https://blast.ncbi.nlm.nih.gov/Blast.cgi [Accessed: 19/1/2017].

Navarro Llorens, J. M., Tormo, A. and Martínez-García, E. (2010). Stationary phase in gram-negative bacteria. *FEMS Microbiology Reviews* **34:**476-495.

Nebra, Y., Jofre, J. and Blanch, A. R. (2002). The effect of reducing agents on the recovery of injured Bifidobacterium cells. *Journal of Microbiological Methods* **49:**247-254.

Nedergaard, J., Golozoubova, V., Matthias, A., Asadi, A., Jacobsson, A. and Cannon, B. (2001). UCP1: the only protein able to mediate adaptive non-shivering thermogenesis and metabolic inefficiency. *Biochimica et Biophysica Acta (BBA)* -

Bioenergetics **1504:**82-106.

Newell, F. S., Su, H., Tornqvist, H., Whitehead, J. P., Prins, J. B. and Hutley, L. J. (2006). Characterization of the transcriptional and functional effects of fibroblast growth factor-1 on human preadipocyte differentiation. *The FASEB Journal* **20:**2615-2617.

Nguyen, T. L. A., Vieira-Silva, S., Liston, A. and Raes, J. (2015). How informative is the mouse for human gut microbiota research? *Disease Models & Mechanisms* **8:**1.

NHS England. 2014. *Report of the working group into: Joined up clinical pathways for obesity*. England: Publications, N.E. Available at: https://www.england.nhs.uk/wp-content/uploads/2014/03/owg-join-clinc-path.pdf [Accessed: 2/11/2017].

Nicholson, J. K., Holmes, E., Kinross, J., Burcelin, R., Gibson, G., Jia, W. and Pettersson, S. (2012). Host-gut microbiota metabolic interactions. *Science* **336**.

Nieto-Vazquez, I., Fernández-Veledo, S., Krämer, D. K., Vila-Bedmar, R., Garcia-Guerra, L. and Lorenzo, M. (2008). Insulin resistance associated to obesity: the link TNF-alpha. *Archives of Physiology and Biochemistry* **114:**183-194.

Ntambi, J. M. and Young-Cheul, K. (2000). Adipocyte Differentiation and Gene Expression. *The Journal of Nutrition* **130:**3122S-3126S.

Oishi, Y., Manabe, I., Tobe, K., Tsushima, K., Shindo, T., Fujiu, K., Nishimura, G. *et al.* *Cell Metabolism* **1:**27-39.

Pairault, J. and Green, H. (1979). A study of the adipose conversion of suspended 3T3 cells by using glycerophosphate dehydrogenase as differentiation marker. *Proceedings of the National Academy of Sciences of the United States of America* **76:**5138-5142.

Palmer, C., Bik, E. M., DiGiulio, D. B., Relman, D. A. and Brown, P. O. (2007). Development of the Human Infant Intestinal Microbiota. *PLOS Biology* **5:**e177.

Park, D.-Y., Ahn, Y.-T., Huh, C.-S., Jeon, S.-M. and Choi, M.-S. (2011). The inhibitory effect of Lactobacillus plantarum KY1032 cell extract on the adipogenesis of 3T3-L1 Cells. *Journal of medicinal food* **14:**670-675.

Park, J.-E., Oh, S.-H. and Cha, Y.-S. (2013). Lactobacillus plantarum LG42 Isolated from Gajami Sik-Hae Inhibits Adipogenesis in 3T3-L1 Adipocyte. *BioMed Research International* **2013:**460927.

Park, S. and Bae, J.-H. (2015). Probiotics for weight loss: a systematic review and meta-analysis. *Nutrition Research* **35:**566-575.

Park, S., Ji, Y., Jung, H.-Y., Park, H., Kang, J., Choi, S.-H., Shin, H. *et al.* (2017). Lactobacillus plantarum HAC01 regulates gut microbiota and adipose tissue accumulation in a diet-induced obesity murine model. *Applied Microbiology and Biotechnology* **101:**1605-1614.

Payne, V. A., Au, W.-S., Lowe, C. E., Rahman, S. M., Friedman, J. E., O'Rahilly, S. and Rochford, J. J. (2009). C/EBP transcription factors regulate SREBP1c gene expression during adipogenesis. *The Biochemical journal* **425:**215-223.

Pepper, J. W. and Rosenfeld, S. The emerging medical ecology of the human gut microbiome. *Trends in Ecology & Evolution* **27:**381-384.

Petrovic, N., Walden, T. B., Shabalina, I. G., Timmons, J. A., Cannon, B. and Nedergaard, J. (2010). Chronic Peroxisome Proliferator-activated Receptor γ (PPARγ) Activation of Epididymally Derived White Adipocyte Cultures Reveals a Population of Thermogenically Competent, UCP1-containing Adipocytes Molecularly Distinct from Classic Brown Adipocytes. *The Journal of Biological Chemistry* **285:**7153-7164.

Piątek, J., Gibas-Dorna, M., Olejnik, A., Krauss, H., Wierzbicki, K., Żukiewicz-Sobczak, W. and Głowacki, M. (2012). The viability and intestinal epithelial cell adhesion of probiotic strain combination - in vitro study. *Annals of Agricultural and Environmental Medicine* **19:**99-102.

Plummer, S., Weaver, M. A., Harris, J. C., Dee, P. and Hunter, J. (2004). Clostridium difficile pilot study: effects of probiotic supplementation on the incidence of C. difficile diarrhoea. *International Microbiology* **7:**59-62.

Ponsonby, A., van der Mei, I., Dwyer, T. and et al. (2005). Exposure to infant siblings during early life and risk of multiple sclerosis. *JAMA* **293:**463-469.

Prosberg, M., Bendtsen, F., Vind, I., Petersen, A. M. and Gluud, L. L. (2016). The association between the gut microbiota and the inflammatory bowel disease activity: a systematic review and meta-analysis. *Scandinavian Journal of Gastroenterology* **51:**1407-1415.

Puigserver, P., Wu, Z., Park, C. W., Graves, R., Wright, M. and Spiegelman, B. M. A Cold-Inducible Coactivator of Nuclear Receptors Linked to Adaptive Thermogenesis. *Cell* **92:**829-839.

Qian, S.-W., Tang, Y., Li, X., Liu, Y., Zhang, Y.-Y., Huang, H.-Y., Xue, R.-D. *et al.* (2013). BMP4-mediated brown fat-like changes in white adipose tissue alter glucose and energy homeostasis. *Proceedings of the National Academy of Sciences of the United*

States of America **110:**E798-E807.

Qiu, Z., Wei, Y., Chen, N., Jiang, M., Wu, J. and Liao, K. (2001). DNA Synthesis and Mitotic Clonal Expansion Is Not a Required Step for 3T3-L1 Preadipocyte Differentiation into Adipocytes. *Journal of Biological Chemistry* **276:**11988-11995.

Rajakumari, S., Wu, J., Ishibashi, J., Hee-Woong, L., Giang, A.-H., Won, K.-J., Reed, R. R. *et al.* (2013). EBF2 determines and maintains brown adipocyte identity. *Cell metabolism* **17:**562-574.

Ramji, D. P. and Foka, P. (2002). CCAAT/enhancer-binding proteins: structure, function and regulation. *Biochemical Journal* **365:**561-575.

Ramírez-Zacarías, J. L., Castro-Muñozledo, F. and Kuri-Harcuch, W. (1992). Quantitation of adipose conversion and triglycerides by staining intracytoplasmic lipids with oil red O. *Histochemistry* **97:**493-497.

Ren, D., Collingwood, T. N., Rebar, E. J., Wolffe, A. P. and Camp, H. S. (2002). PPARγ knockdown by engineered transcription factors: exogenous PPARγ2 but not PPARγ1 reactivates adipogenesis. *Genes & Development* **16:**27-32.

Renz, H., Brandtzaeg, P. and Hornef, M. (2011). The impact of perinatal immune development on mucosal homeostasis and chronic inflammation. *Nature Reviews Immunology* **12:**9.

Rice, S. P. L., Zhang, L., Grennan-Jones, F., Agarwal, N., Lewis, M. D., Rees, D. A. and Ludgate, M. (2010). Dehydroepiandrosterone (DHEA) treatment in vitro inhibits adipogenesis in human omental but not subcutaneous adipose tissue. *Molecular and Cellular Endocrinology* **320:**51-57.

Riss, T. L., Moravec R.A., Niles A.L., *et al.* (2013). Cell Viability Assays. In: Sittampalam G.S., C.N.P., Brimacombe K., *et al*. (ed.) *Assay Guidance Manual*. Bethesda, Maryland: Eli Lilly & Company and the National Center for Advancing Translational Sciences.

Rizzatti, V., Boschi, F., Pedrotti, M., Zoico, E., Sbarbati, A. and Zamboni, M. (2013). Lipid Droplets Characterization in Adipocyte Differentiated 3T3-L1 Cells: Size and Optical Density Distribution. *European Journal of Histochemistry : EJH* **57:**e24.

Roach, J. C., Glusman, G., Rowen, L., Kaur, A., Purcell, M. K., Smith, K. D., Hood, L. E. *et al.* (2005). The evolution of vertebrate Toll-like receptors. *Proceedings of the National Academy of Sciences of the United States of America* **102:**9577-9582.

Rodríguez, J. M. (2014). The Origin of Human Milk Bacteria: Is There a Bacterial Entero-Mammary Pathway during Late Pregnancy and Lactation? *Advances in Nutrition* **5:**779-784.

Rodríguez, J. M., Murphy, K. and Stanton, C. (2015). The composition of the gut microbiota throughout life, with an emphasis on early life. *Microb Ecol Health Dis* **26**.

Roediger, W. E. W. (1982). Utilization of Nutrients by Isolated Epithelial Cells of the Rat Colon. *Gastroenterology* **83:**424-429.

Rolfe, M. D., Rice, C. J., Lucchini, S., Pin, C., Thompson, A., Cameron, A. D. S., Alston, M. *et al.* (2012). Lag Phase Is a Distinct Growth Phase That Prepares Bacteria for Exponential Growth and Involves Transient Metal Accumulation. *Journal of Bacteriology* **194:**686-701.

Rook, G. A. W., Adams, V., Hunt, J., Palmer, R., Martinelli, R. and Brunet, L. R. (2004). Mycobacteria and other environmental organisms as immunomodulators for immunoregulatory disorders. *Springer Seminars in Immunopathology* **25:**237-255.

Rook, G. A. W. and Brunet, L. R. (2005). Microbes, immunoregulation, and the gut. *Gut* **54:**317-320.

Rosen, E. D. and MacDougald, O. A. (2006). Adipocyte differentiation from the inside out. **7:**885.

Rossmeislová, L., Mališová, L., Kračmerová, J. and Štich, V. (2012). Adaptation of human adipose tissue to hypocaloric diet. *International Journal Of Obesity* **37:**640.

Rowland, L. A., Bal, N. C. and Periasamy, M. (2015). The role of skeletal-muscle-based thermogenic mechanisms in vertebrate endothermy. *Biological reviews of the Cambridge Philosophical Society* **90:**1279-1297.

Ruas, J. L., White, J. P., Rao, R. R., Kleiner, S., Brannan, K. T., Harrison, B. C., Greene, N. P. *et al.* (2012). A PGC-1α isoform induced by resistance training regulates skeletal muscle hypertrophy. *Cell* **151:**1319-1331.

Ruhl, C. E., Harris, T. B., Ding, J., Goodpaster, B. H., Kanaya, A. M., Kritchevsky, S. B., Simonsick, E. M. *et al.* (2007). Body mass index and serum leptin concentration independently estimate percentage body fat in older adults. *The American Journal of Clinical Nutrition* **85:**1121-1126.

Ruiz-Ojeda, F. J., Rupérez, A. I., Gomez-Llorente, C., Gil, A. and Aguilera, C. M. (2016). Cell models and their application for studying adipogenic differentiation in relation to obesity: a review. *International journal of molecular sciences* **17:**1040.

Rutayisire, E., Huang, K., Liu, Y. and Tao, F. (2016). The mode of delivery affects the diversity and colonization pattern of the gut microbiota during the first year of infants' life: a systematic review. *BMC Gastroenterology* **16:**86.

Rutkowski, J. M., Stern, J. H. and Scherer, P. E. (2015). The cell biology of fat expansion. *The Journal of Cell Biology* **208:**501-512.

Ríos-Covián, D., Ruas-Madiedo, P., Margolles, A., Gueimonde, M., de los Reyes-Gavilán, C. G. and Salazar, N. (2016). Intestinal Short Chain Fatty Acids and their Link with Diet and Human Health. *Frontiers in Microbiology* **7:**185.

Sacks, H. and Symonds, M. E. (2013). Anatomical Locations of Human Brown Adipose Tissue. *Diabetes* **62:**1783.

Sanchez-Gurmaches, J., Hung, C.-M., Sparks, C. A., Tang, Y., Li, H. and Guertin, D. A. (2012). PTEN loss in the Myf5 lineage redistributes body fat and reveals subsets of white adipocytes that arise from Myf5 precursors. *Cell metabolism* **16:**348-362.

Schindler, C., Levy, D. E. and Decker, T. (2007). JAK-STAT Signaling: From Interferons to Cytokines. *Journal of Biological Chemistry* **282:**20059-20063.

Scott, R. E., Florine, D. L., Wille, J. J. and Yun, K. (1982). Coupling of growth arrest and differentiation at a distinct state in the G1 phase of the cell cycle: GD. *Proceedings of the National Academy of Sciences* **79:**845-849.

Seale, P. (2015). Transcriptional Regulatory Circuits Controlling Brown Fat Development and Activation. *Diabetes* **64:**2369.

Seale, P., Kajimura, S., Yang, W., Chin, S., Rohas, L., Uldry, M., Tavernier, G. *et al.* (2007). Transcriptional Control of Brown Fat Determination by PRDM16. *Cell metabolism* **6:**38-54.

Seiler, S. E., Xu, D., Ho, J.-P., Lo, K. A., Buehrer, B. M., Ludlow, Y. J. W., Kovalik, J.-P. *et al.* (2015). Characterization of a primary brown adipocyte culture system derived from human fetal interscapular fat. *Adipocyte* **4:**303-310.

Sender, R., Fuchs, S. and Milo, R. (2016). Revised Estimates for the Number of Human and Bacteria Cells in the Body. *PLOS Biology* **14:**e1002533.

Seto, E. and Yoshida, M. (2014). Erasers of Histone Acetylation: The Histone Deacetylase Enzymes. *Cold Spring Harbor Perspectives in Biology* **6:**a018713.

Shabalina, I. G., Backlund, E. C., Bar-Tana, J., Cannon, B. and Nedergaard, J. (2008). Within brown-fat cells, UCP1-mediated fatty acid-induced uncoupling is independent of fatty acid metabolism. *Biochimica et Biophysica Acta (BBA) - Bioenergetics* **1777:**642-650.

Shah, N. P. Probiotic Bacteria: Selective Enumeration and Survival in Dairy Foods.

Journal of Dairy Science **83:**894-907.

Shao, D. and Lazar, M. A. (1997). Peroxisome Proliferator Activated Receptor γ, CCAAT/ Enhancer-binding Protein α, and Cell Cycle Status Regulate the Commitment to Adipocyte Differentiation. *Journal of Biological Chemistry* **272:**21473-21478.

Sharp, L. Z., Shinoda, K., Ohno, H., Scheel, D. W., Tomoda, E., Ruiz, L., Hu, H. *et al.* (2012). Human BAT Possesses Molecular Signatures That Resemble Beige/Brite Cells. *PLOS ONE* **7:**e49452.

Shibasaki, M., Takahashi, K., Itou, T., Miyazawa, S., Ito, M., Kobayashi, J., Bujo, H. *et al.* (2002). Alterations of insulin sensitivity by the implantation of 3T3-L1 cells in nude mice. A role for TNF-α? *Diabetologia* **45:**518-526.

Shimomura, I., Hammer, R. E., Richardson, J. A., Ikemoto, S., Bashmakov, Y., Goldstein, J. L. and Brown, M. S. (1998). Insulin resistance and diabetes mellitus in transgenic mice expressing nuclear SREBP-1c in adipose tissue: model for congenital generalized lipodystrophy. *Genes & Development* **12:**3182-3194.

Shingala, M. C. and Rajyaguru, A. Comparison of post hoc tests for unequal variance.

Sinha, R., Abnet, C. C., White, O., Knight, R. and Huttenhower, C. (2015). The microbiome quality control project: baseline study design and future directions. *Genome Biology* **16:**276.

Skurk, T., Alberti-Huber, C., Herder, C. and Hauner, H. (2007). Relationship between Adipocyte Size and Adipokine Expression and Secretion. *The Journal of Clinical Endocrinology & Metabolism* **92:**1023-1033.

Smetanková, J., Hladíková, Z., Valach, F., Zimanová, M., Kohajdová, Z., Greif, G. and Greifová, M. (2012). Influence of aerobic and anaerobic conditions on the growth and metabolism of selected strains of Lactobacillus plantarum. *Acta Chimica Slovaca* **5:**204-210.

Snel, M., Jonker J.T., Schoones, J., Lamb, H., de Roos, A., Pijl, H., Smit, J. *et al.* (2012). Ectopic Fat and Insulin Resistance: Pathophysiology and Effect of Diet and Lifestyle Interventions. *International Journal of Endocrinology* **2012:**18.

Spalding, K. L., Arner, E., Westermark, P. O., Bernard, S., Buchholz, B. A., Bergmann, O., Blomqvist, L. *et al.* (2008). Dynamics of fat cell turnover in humans. *Nature* **453:**783-787.

Stevenson, K., McVey, A. F., Clark, I. B. N., Swain, P. S. and Pilizota, T. (2016). General calibration of microbial growth in microplate readers. *Scientific Reports*

6:38828.

Strachan, D. P. (1989). Hay fever, hygiene, and household size. *BMJ : British Medical Journal* **299:**1259-1260.

Student, A. K., Hsu, R. Y. and Lane, M. D. (1980). Induction of fatty acid synthetase synthesis in differentiating 3T3-L1 preadipocytes. *Journal of Biological Chemistry* **255:**4745-4750.

Sundvold, H. and Lien, S. (2001). Identification of a Novel Peroxisome Proliferator-Activated Receptor (PPAR) γ Promoter in Man and Transactivation by the Nuclear Receptor RORα1. *Biochemical and Biophysical Research Communications* **287:**383-390.

Tang, Q.-Q., Otto, T. C. and Lane, M. D. (2003). Mitotic clonal expansion: A synchronous process required for adipogenesis. *Proceedings of the National Academy of Sciences of the United States of America* **100:**44-49.

Tchoukalova, Y. D., Koutsari, C., Karpyak, M. V., Votruba, S. B., Wendland, E. and Jensen, M. D. (2008). Subcutaneous adipocyte size and body fat distribution. *The American Journal of Clinical Nutrition* **87:**56-63.

Tiraby, C., Tavernier, G., Lefort, C., Larrouy, D., Bouillaud, F., Ricquier, D. and Langin, D. (2003). Acquirement of Brown Fat Cell Features by Human White Adipocytes. *Journal of Biological Chemistry* **278:**33370-33376.

Tontonoz, P., Hu, E. and Spiegelman, B. M. (1994). Stimulation of adipogenesis in fibroblasts by PPARγ2, a lipid-activated transcription factor. *Cell* **79:**1147-1156.

Trayhurn, P. and Beattie, J. H. (2001). Physiological role of adipose tissue: white adipose tissue as an endocrine and secretory organ. *Proceedings of the Nutrition Society* **60:**329-339.

Uldry, M., Yang, W., St-Pierre, J., Lin, J., Seale, P. and Spiegelman, B. M. Complementary action of the PGC-1 coactivators in mitochondrial biogenesis and brown fat differentiation. *Cell Metabolism* **3:**333-341.

Umek, R. M., Friedman, A. D. and McKnight, S. L. (1991). CCAAT-enhancer binding protein: a component of a differentiation switch. *Science* **251:**288.

Ussar, S., Lee, K. Y., Dankel, S. N., Boucher, J., Haering, M.-F., Kleinridders, A., Thomou, T. *et al.* (2014). Asc-1, PAT2 and P2RX5 are novel cell surface markers for white, beige and brown adipocytes. *Science translational medicine* **6:**247ra103-247ra103.

Valladares, A., Roncero, C., Benito, M. and Porras, A. (2001). TNF-α inhibits UCP-1 expression in brown adipocytes via ERKs. *FEBS Letters* **493:**6-11.

van Beek, E. A., Bakker, A. H., Kruyt, P. M., Vink, C., Saris, W. H., Franssen-van Hal, N. L. W. and Keijer, J. (2008). Comparative expression analysis of isolated human adipocytes and the human adipose cell lines LiSa-2 and PAZ6. *International Journal Of Obesity* **32:**912.

van Harmelen, V., Skurk, T., Röhrig, K., Lee, Y. M., Halbleib, M., Aprath-Husmann, I. and Hauner, H. (2003). Effect of BMI and age on adipose tissue cellularity and differentiation capacity in women. *International Journal Of Obesity* **27:**889.

Vandeputte, D., Falony, G., Vieira-Silva, S., Tito, R. Y., Joossens, M. and Raes, J. (2016). Stool consistency is strongly associated with gut microbiota richness and composition, enterotypes and bacterial growth rates. *Gut* **65:**57.

Villacorta, L., Schopfer, Francisco J., Zhang, J., Freeman, Bruce A. and Chen, Y. E. (2009). PPARγ and its ligands: therapeutic implications in cardiovascular disease. *Clinical Science* **116:**205.

Vincent, C. and Manges, A. R. (2015). Antimicrobial Use, Human Gut Microbiota and Clostridium difficile Colonization and Infection. *Antibiotics* **4:**230-253.

Vrieze, A., Van Nood, E., Holleman, F., Salojärvi, J., Kootte, R. S., Bartelsman, J. F. W. M., Dallinga–Thie, G. M. *et al.* Transfer of Intestinal Microbiota From Lean Donors Increases Insulin Sensitivity in Individuals With Metabolic Syndrome. *Gastroenterology* **143:**913-916.e917.

Waldén, T. B., Hansen, I. R., Timmons, J. A., Cannon, B. and Nedergaard, J. (2012). Recruited vs. nonrecruited molecular signatures of brown, “brite,” and white adipose tissues. *American Journal of Physiology - Endocrinology And Metabolism* **302:**E19.

Walls, H. L., Peeters, A., Proietto, J. and McNeil, J. J. (2011). Public health campaigns and obesity - a critique. *BMC Public Health* **11:**136.

Wang, H. and Peng, D.-Q. (2011). New insights into the mechanism of low high-density lipoprotein cholesterol in obesity. *Lipids in Health and Disease* **10:**176.

Wang, Q. A., Tao, C., Gupta, R. K. and Scherer, P. E. (2013). Tracking adipogenesis during white adipose tissue development, expansion and regeneration. **19:**1338.

Wang, W. and Seale, P. (2016). Control of brown and beige fat development. *Nature reviews. Molecular cell biology* **17:**691-702.

Ward, J. B. J., Keely, S. J. and Keely, S. J. (2014). Oxygen in the regulation of intestinal epithelial transport. *The Journal of Physiology* **592:**2473-2489.

Welsh Government. (2016). Obesity Pathway Working Group: All Wales Obesity Pathway. Wales: Welsh Government. Available at:

http://gov.wales/docs/phhs/publications/100824obesityen.doc [Accessed: 2/11/17].

Weyer, C., Foley, J. E., Bogardus, C., Tataranni, P. A. and Pratley, R. E. (2000). Enlarged subcutaneous abdominal adipocyte size, but not obesity itself, predicts Type II diabetes independent of insulin resistance. *Diabetologia* **43:**1498-1506.

Williams, E. A., Stimpson, J., Wang, D., Plummer, S., Garaiova, I., Barker, M. E. and Corfe, B. M. (2009). Clinical trial: a multistrain probiotic preparation significantly reduces symptoms of irritable bowel syndrome in a double-blind placebo-controlled study. *Alimentary Pharmacology & Therapeutics* **29:**97-103.

World Health Organization. (2017). Obesity and overweight fact sheet [Online]. World Health Organization. Available at: http://www.who.int/mediacentre/factsheets/fs311/en/ [Accessed: 23/7/2017].

Wu, J., Boström, P., Sparks, L. M., Ye, L., Choi, J. H., Giang, A.-H., Khandekar, M. *et al.* (2012). Beige Adipocytes are a Distinct Type of Thermogenic Fat Cell in Mouse and Human. *Cell* **150:**366-376.

Wu, Z., Rosen, E. D., Brun, R., Hauser, S., Adelmant, G., Troy, A. E., McKeon, C. *et al.* (1999). Cross-Regulation of C/EBPα and PPARγ Controls the Transcriptional Pathway of Adipogenesis and Insulin Sensitivity. *Molecular Cell* **3:**151-158.

Yazdanbakhsh, M., Kremsner, P. G. and van Ree, R. (2002). Allergy, Parasites, and the Hygiene Hypothesis. *Science* **296:**490.

Ye, L., Wu, J., Cohen, P., Kazak, L., Khandekar, M. J., Jedrychowski, M. P., Zeng, X. *et al.* (2013). Fat cells directly sense temperature to activate thermogenesis. *Proceedings of the National Academy of Sciences of the United States of America* **110:**12480-12485.

Yeh, W. C., Cao, Z., Classon, M. and McKnight, S. L. (1995). Cascade regulation of terminal adipocyte differentiation by three members of the C/EBP family of leucine zipper proteins. *Genes & Development* **9:**168-181.

Yoo, E. J., Chung, J.-J., Choe, S. S., Kim, K. H. and Kim, J. B. (2006). Down-regulation of Histone Deacetylases Stimulates Adipocyte Differentiation. *Journal of Biological Chemistry* **281:**6608-6615.

Zebisch, K., Voigt, V., Wabitsch, M. and Brandsch, M. (2012). Protocol for effective differentiation of 3T3-L1 cells to adipocytes. *Analytical Biochemistry* **425:**88-90.

Zhang, J., Fu, M., Cui, T., Xiong, C., Xu, K., Zhong, W., Xiao, Y. *et al.* (2004). Selective disruption of PPARγ2 impairs the development of adipose tissue and insulin sensitivity. *Proceedings of the National Academy of Sciences of the United States of*

America **101:**10703-10708.

Zhang, J., Tang, H., Zhang, Y., Deng, R., Shao, L., Liu, Y., Li, F. *et al.* (2014). Identification of suitable reference genes for quantitative RT-PCR during 3T3-L1 adipocyte differentiation. *International journal of molecular medicine* **33:**1209-1218.

Zhang, K., Guo, W., Yang, Y. and Wu, J. (2011). JAK2/STAT3 pathway is involved in the early stage of adipogenesis through regulating C/EBPβ transcription. *Journal of Cellular Biochemistry* **112:**488-497.

Zhang, L., Paddon, C., Lewis, M. D., Grennan-Jones, F. and Ludgate, M. (2009). Gsα signalling suppresses PPARγ2 generation and inhibits 3T3L1 adipogenesis. *The Journal of Endocrinology* **202:**207-215.

Zhang, Q., Wu, Y. and Fei, X. (2016). Effect of probiotics on body weight and body-mass index: a systematic review and meta-analysis of randomized, controlled trials. *International Journal of Food Sciences and Nutrition* **67:**571-580.

Appendix

Appendix 1.

Table 1. – List of reagents and suppliers

Reagent	Supplier
Agarose	Fisher Scientific, UK
Chloroform	
DMEM (4.5g/L glucose, with L-glutamine)	
Ethanol	
Foetal Calf Serum	
Ham's F12	
Isopropanol	
Molecular Biology grade water	
Dehydrated MRS broth	Oxoid, UK
10x Buffer	Promega
5x Buffer	
dNTPs (2mM)	
$MgCl_2$	
M-MLV reverse transcriptase	
OligoDT	
RNAse inhibitor	
Bicarbonate	Sigma-Aldrich, UK
Biotin (33µM)	
Hydrocortisone (1µM)	
Insulin (500nM)	
Oil Red O	
Pantothenate (17µM)	
Penicillin/Streptomycin	
Phosphate Buffered Saline	

Pioglitazone (1µM)	
Pyruvate	
Tri reagent	
Triiodothyronine (1nM)	
Trypan Blue	
Trypsin IX	
Amplitaq Gold DNA polymerase	Thermo Fisher, UK
BigDye Terminator v1.1	
Ethidium Bromide	
Platinum SYBR Green qPCR SuperMix-UDG	
Sodium Acetate	
TAE buffer	

Appendix 2.

Sanger sequencing data for ZIC1 sample. Bolded, underlined bases represent high quality sequence data.

CTTCGCAGCCATAAAGTCAGCGAGGGCAAG**CCCTTCAAGCCAAATACAAACTGGGTCAACCACATCCGTAGTGCACACAGGCGAAAAGCCTTTTCCCTGCCCGTTTCCTGGCTGCGGCAAGGTTTTCGCGCGTTCAGAGAACCTCAAGATCCACAAAAGGACACACACAGGGG**A

Sanger sequencing data for PGC1-α sample. Bolded, underlined bases represent high quality sequence data.

TATCCTAGCGTTGGTTCGACGAATACAT**TTGTCACAGCAAAAGCCACAAAGACGTCCCTAGGCTCAGTAGCTTCTCAAGTATCTTGTACCACAAACGATGACCCTCCTCACACCAAACCCACAGAAAACAGGAACAGCAGCA**A

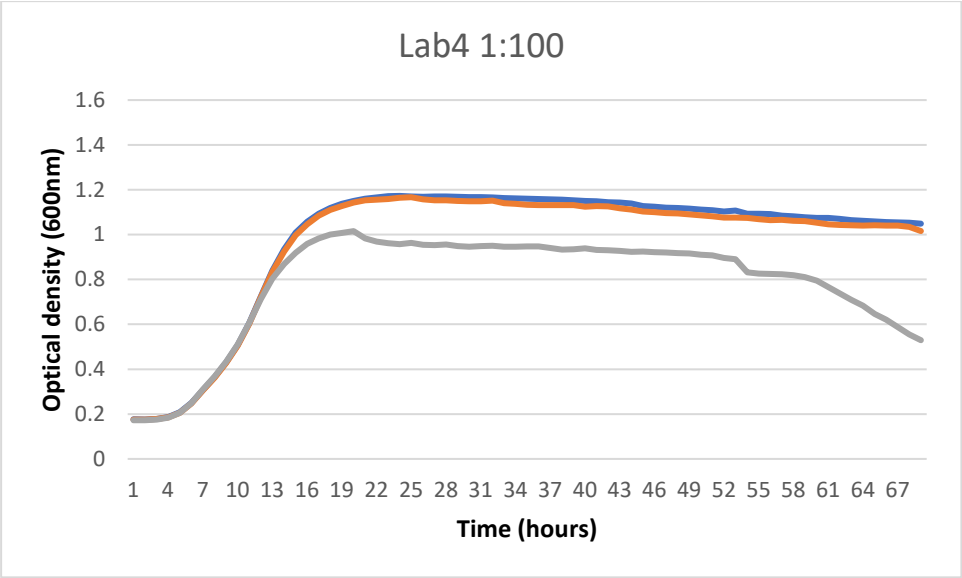

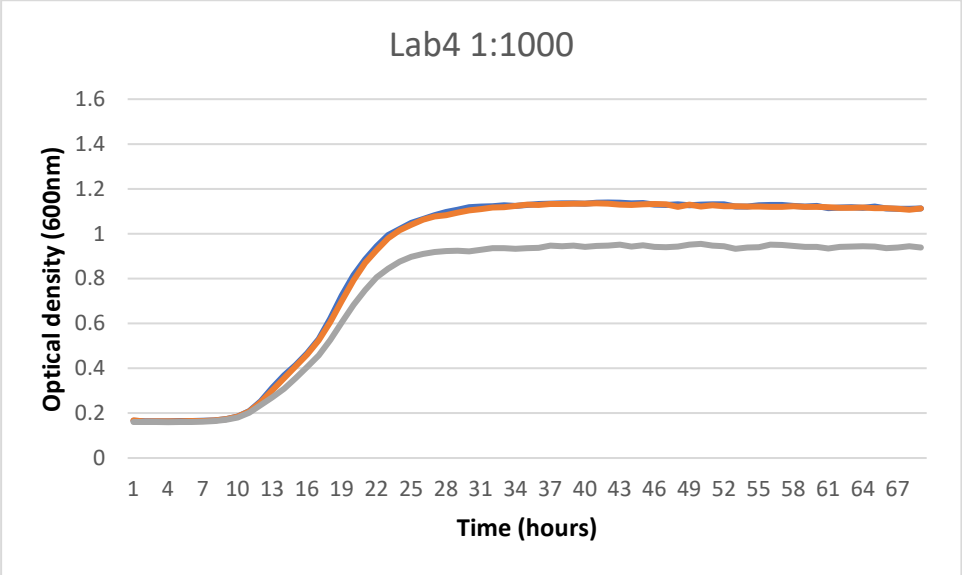

Figure A1. – 70-hour growth curve of Lab4 diluted to 1:100 (above) and 1:1000 (below) in MRS from starting inoculum. Optical density at 600nm is plotted on the Y axis in arbitrary units. Time is plotted on the X axis in hours. Each coloured line represents readings from a single well, each condition was plated in triplicate from 3 separate inocula. Linear growth of bacteria appears to cease before 24 hours. The lower plateau in the grey line in both experiments may reflect some issue with the starting inoculum or pipetting error.

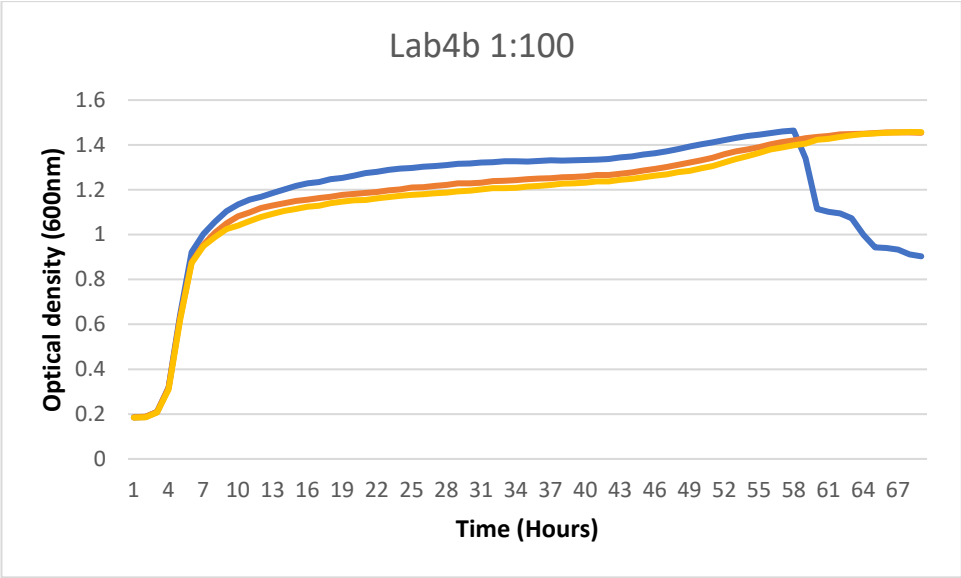

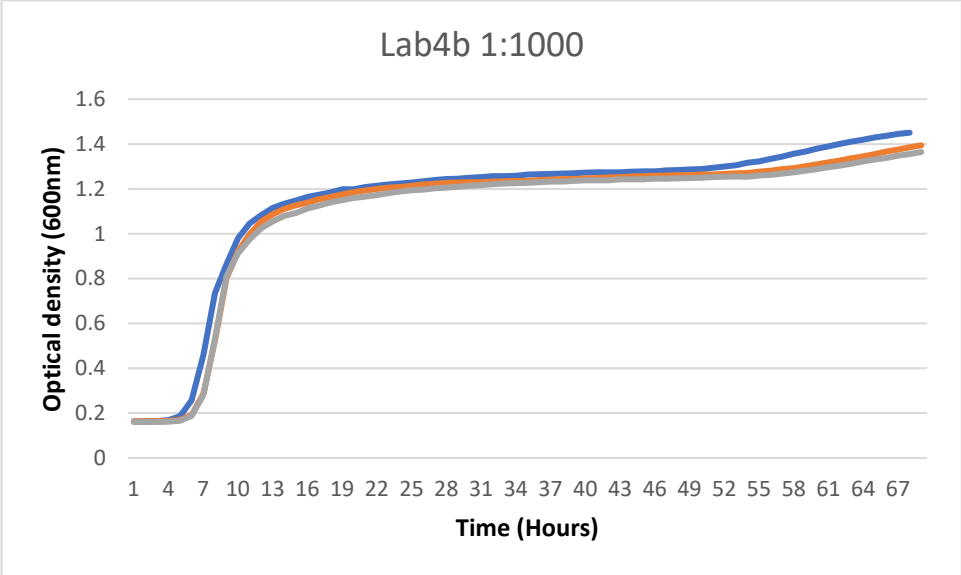

Figure A2. – 70-hour growth curve of Lab4b diluted to 1:100 (above) and 1:1000 (below) in MRS from starting inoculum. Optical density at 600nm is plotted on the Y axis in arbitrary units. Time is plotted on the X axis in hours. Each coloured line represents readings from a single well, each condition was plated in triplicate from 3 separate inocula. Linear growth of bacteria appears to cease before 24 hours. The well represented by the blue line in the 1:100 dilution appears to reach the death phase at around 60 hours.

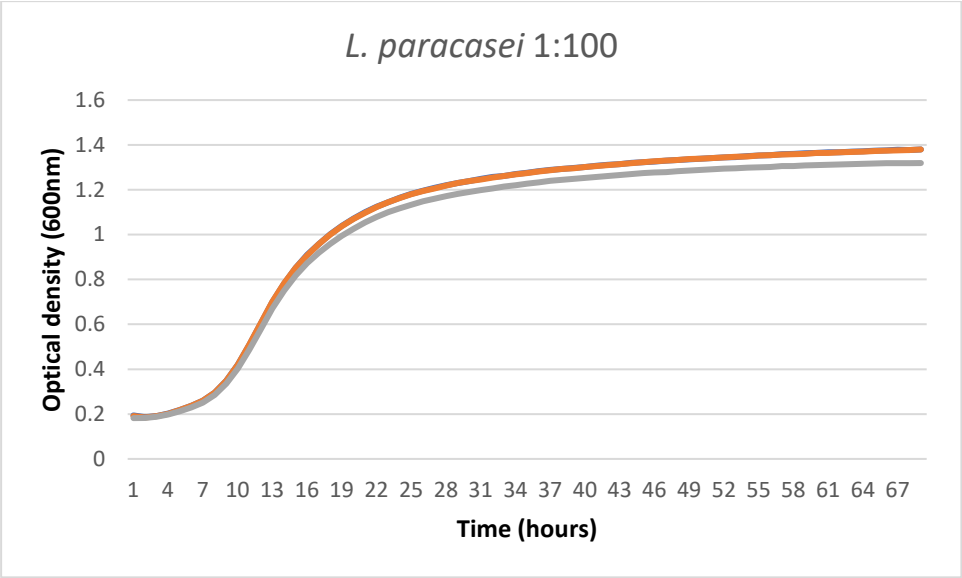

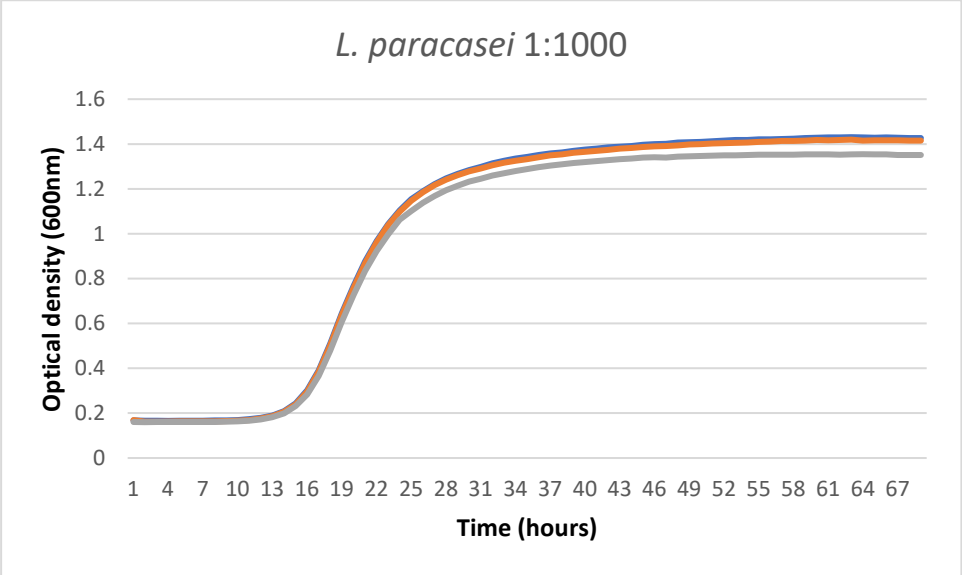

Figure A3. – 70-hour growth curve of *L. paracasei* diluted to 1:100 (above) and 1:1000 (below) in MRS from starting inoculum. Optical density at 600nm is plotted on the Y axis in arbitrary units. Time is plotted on the X axis in hours. Each coloured line represents readings from a single well, each condition was plated in triplicate from 3 separate inocula. Linear growth of bacteria appears to cease before 24 hours in the 1:100 dilution and at around 24 hours in the 1:1000 dilution.

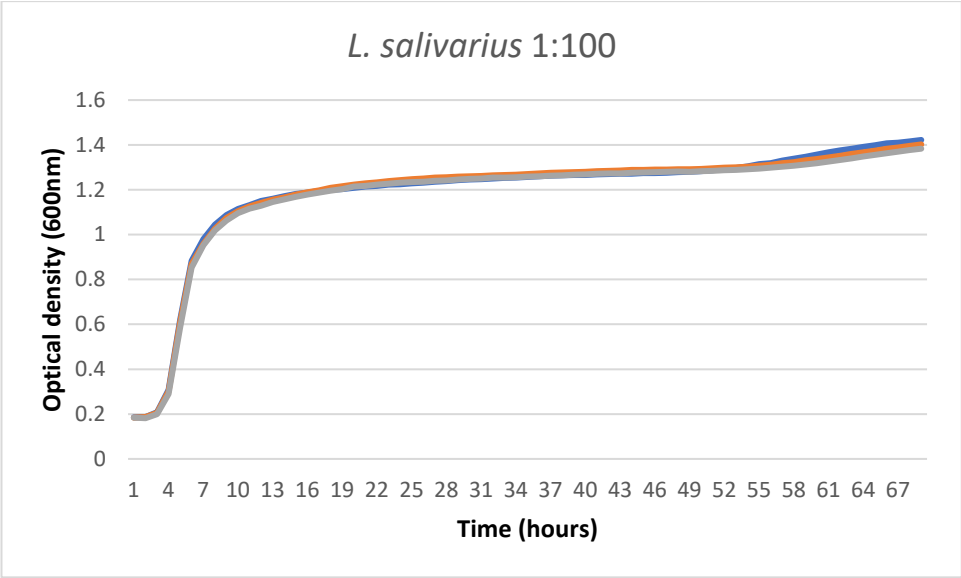

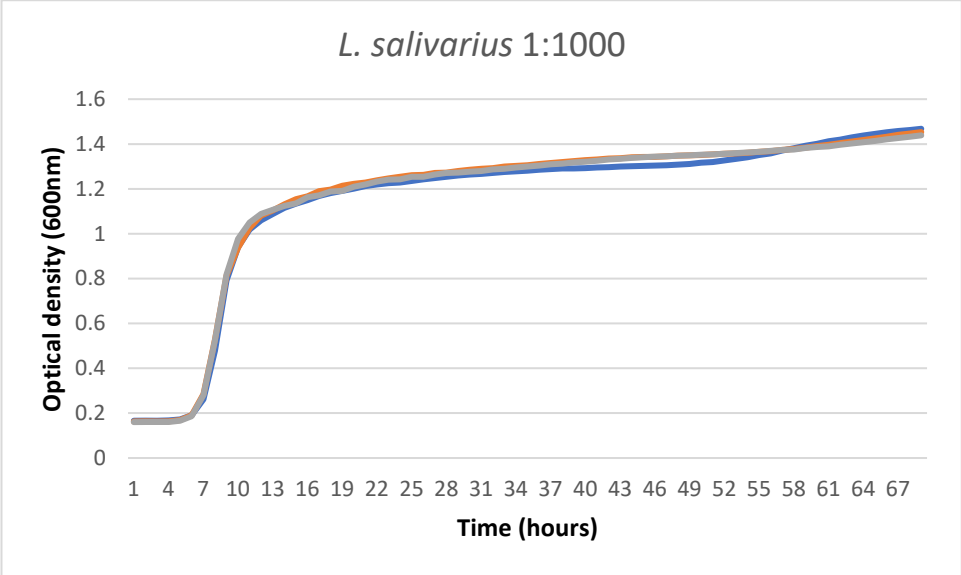

Figure A4. – 70-hour growth curve of *L. salivarius* diluted to 1:100 (above) and 1:1000 (below) in MRS from starting inoculum. Optical density at 600nm is plotted on the Y axis in arbitrary units. Time is plotted on the X axis in hours. Each coloured line represents readings from a single well, each condition was plated in triplicate from 3 separate inocula. Linear growth of bacteria appears to cease before 24 hours.

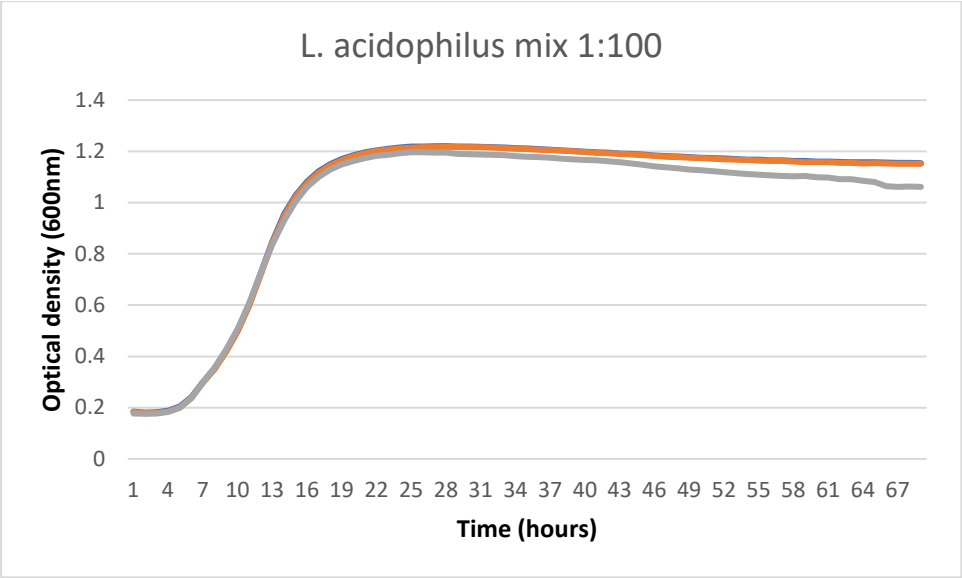

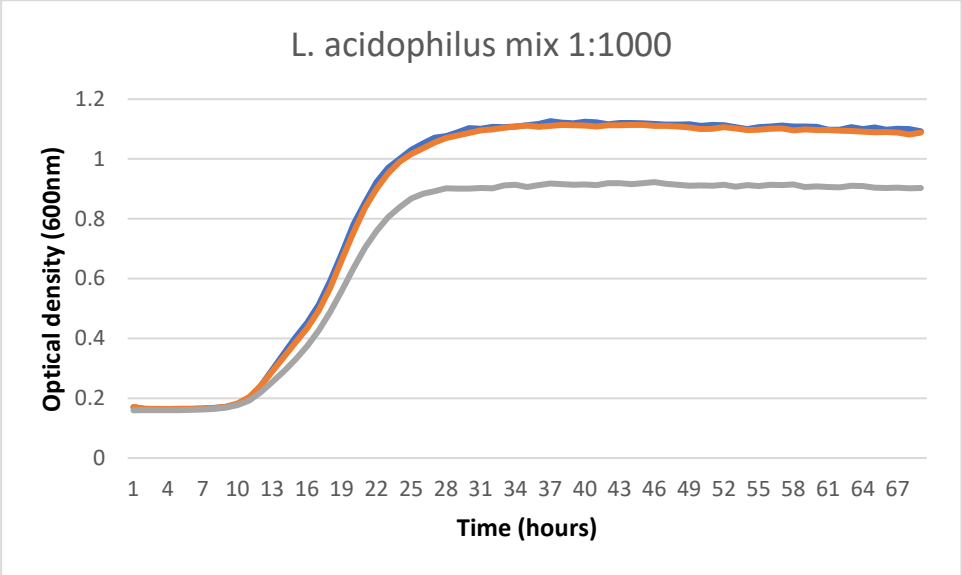

Figure A5. – 70-hour growth curve of *L. acidophilus* diluted to 1:100 (above) and 1:1000 (below) in MRS from starting inoculum. Optical density at 600nm is plotted on the Y axis in arbitrary units. Time is plotted on the X axis in hours. Each coloured line represents readings from a single well, each condition was plated in triplicate from 3 separate inocula. Linear growth of bacteria appears to cease before 24 hours. The well represented by the grey line in the 1:1000 dilution appears to grow to a lower optical density, this may reflect pipetting error.

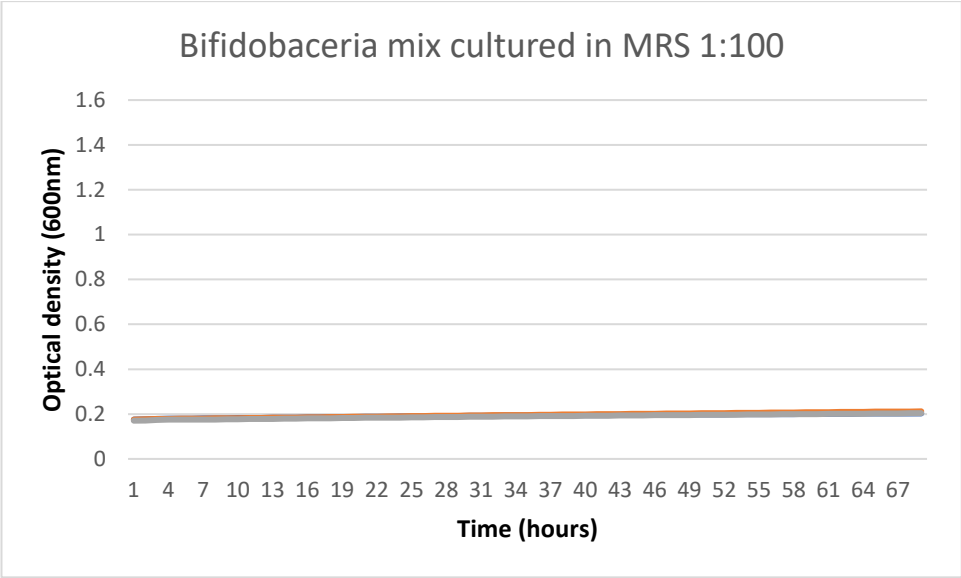

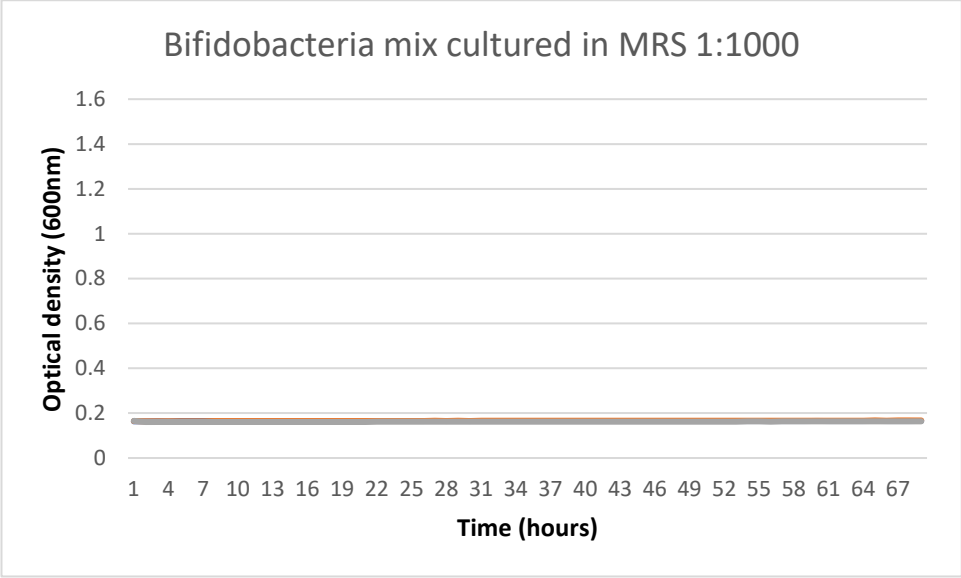

Figure A7. – 70-hour growth curve of *Bifidobacteria* diluted to 1:100 (above) and 1:1000 (below) in MRS from starting inoculum. Optical density at 600nm is plotted on the Y axis in arbitrary units. Time is plotted on the X axis in hours. Each coloured line represents readings from a single well, each condition was plated in triplicate from 3 separate inocula. A long, extremely slow period of minimal growth throughout the time course, which is relatively even between replicates is seen in the 1:100 dilution. However, there is essentially no detectable growth in the 1:1000 dilution. Neither appears to show good growth despite anaerobic conditions.

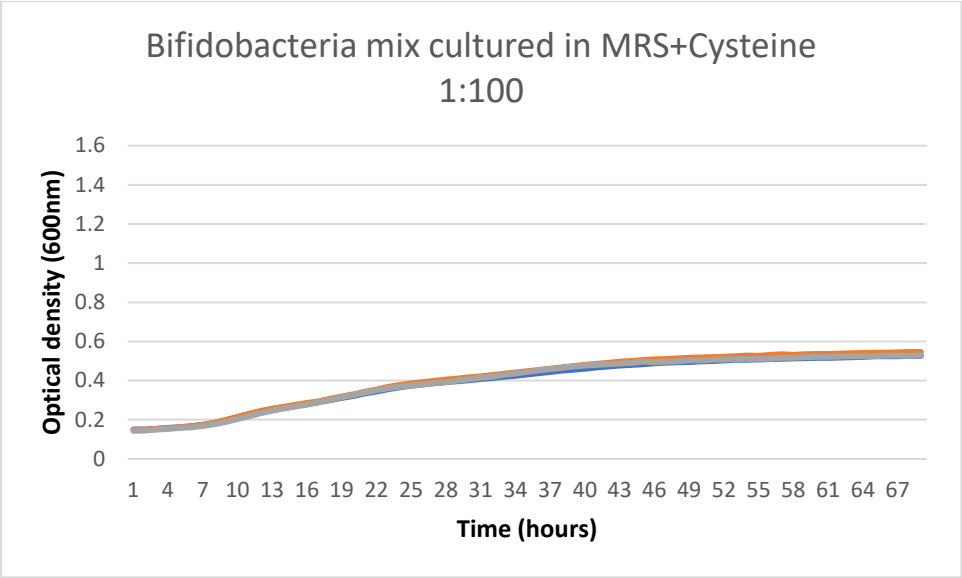

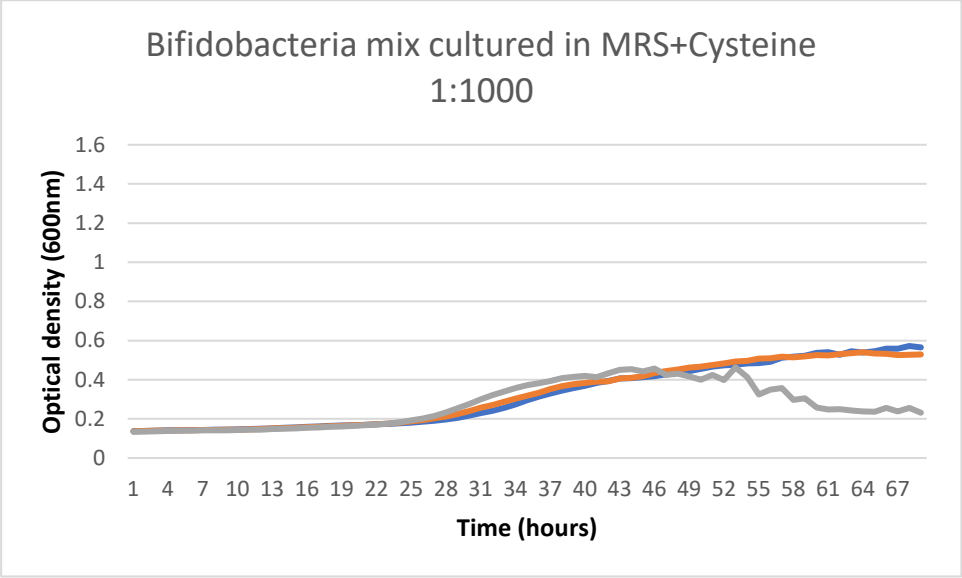

Figure A8. – 70-hour growth curve of *Bifidobacteria* diluted to 1:100 (above) and 1:1000 (below) in MRS supplemented with 0.05% cysteine from starting inoculum. Optical density at 600nm is plotted on the Y axis in arbitrary units. Time is plotted on the X axis in hours. Each coloured line represents readings from a single well, each condition was plated in triplicate from 3 separate inocula. A long, slow period of growth that is relatively even between replicates is seen in the 1:100 dilution, however there is a larger degree of variance in the 1:1000 dilution and the well represented by the grey line appears to reach the death phase. Growth appears to be improved by addition of cysteine to MRS broth, but neither dilution displays a distinct period of linear growth.

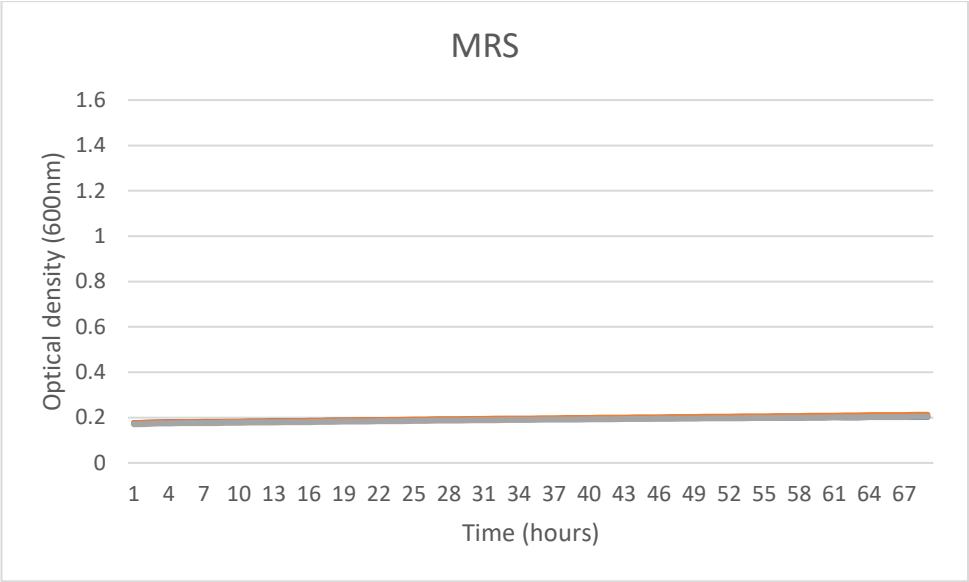

Figure A9. – 70-hour growth curve of MRS control wells. Optical density at 600nm is plotted on the Y axis in arbitrary units. Time is plotted on the X axis in hours. Each coloured line represents readings from a single well. No growth was apparent in control wells.